



ISSN 1454-9166

**ANNALS
OF THE UNIVERSITY OF PETROSANI**
MECHANICAL ENGINEERING

VOL. 19 (XLVI)

**UNIVERSITAS Publishing
PETROȘANI – ROMANIA
2017**

EDITOR OF PUBLICATION
Prof. PhD. Eng. Sorin Mihai RADU

ADVISORY BOARD:

Prof.Eng. Moise-Ioan ACHIM Ph.D. - “1 Decembrie 1918” University of Alba-Iulia, *Romania*;
Prof.Eng. Iosif ANDRAȘ Ph.D. - University of Petroșani, *Romania*;
Prof.Eng. Nicolae-Napoleon ANTONESCU Ph.D. - “Petroleum-Gas” University of Ploiești, *Romania*;
Prof.Eng. Alexandru BOROIU Ph.D. - University of Pitești, *Romania*;
Prof.Eng. Ioan CARȚIȘ Ph.D. - Politechnical University of Timișoara, *Romania*;
Prof.Eng. Ion CIUCĂ Ph.D. - “Politehnica” University of București, *Romania*;
Prof. Eng. Pascu-Mihai COLOJA Ph.D. - “Petroleum-Gas” University of Ploiești, *Romania*;
Prof.Eng. Predrag DAŠIĆ Ph.D. - High Technical Mechanical School R. Krstića, Trstenik, *Serbia*;
Prof.Eng. Sorin DIMITRIU Ph.D. - “Politehnica” University of București, *Romania*;
Prof.Eng. Valeriu DULGHERU Ph.D. – Tech.University of Moldova, Chișinău, *Republic of Moldova*;
Assoc.Prof.Eng. António GONÇALVES-COELHO Ph.D. - Universidade Nova de Lisboa, *Portugal*;
Prof.Eng. Otto GRIGOROV Ph.D. - National Technical University of Kharkov, *Ukraine*;
Prof.Eng. Anatoli GHRABCHENKO Ph.D. - National Technical University of Kharkov, *Ukraine*;
Prof.Eng. Nicolae ILIAȘ Ph.D. - University of Petroșani, *Romania*;
Prof.Eng. Ioan-Iulian IRIMIE Ph.D. - University of Petroșani, *Romania*;
Prof.Eng. Iosif KOVACS Ph.D. - University of Petroșani, *Romania*;
Assoc.Prof.Eng. Krzysztof KOTWICZA Ph.D. – AGH University of Science and Technology, *Poland*;
Assoc.Prof.Eng. Gábor LADÁNYI Ph.D. - University of Miskolc, *Hungary*;
Assoc.Prof.Eng. Traian MAZILU Ph.D. - “Politehnica” University of București, *Romania*;
Prof. Eng. Mihai MINEȘCU Ph.D. - “Petroleum-Gas” University of Ploiești, *Romania*;
Prof.Eng. Marin-Silviu NAN Ph.D. - University of Petroșani, *Romania*;
Assoc.Prof.Eng. Mircea NICOARĂ Ph.D. - Politechnical University of Timișoara, *Romania*;
Prof.Eng. Gyula PATKO Ph.D. - University of Miskolc, *Hungary*;
Prof.Eng. Eugen PAY Ph.D. – North University of Baia-Mare, *Romania*;
Assoc.Prof.Eng. Eugen PĂMÎNȚAȘ Ph.D. - Politechnical University of Timișoara, *Romania*;
Prof.Eng. Șerban RAICU Ph.D. - “Politehnica” University of București, *Romania*;
Prof.Eng. Janusz REŚ Ph.D. – AGH University of Science and Technology, *Poland*;
Prof.Eng. Alexei TOCA Ph.D. - Technical University of Moldova, Chișinău, *Republic of Moldova*;
Prof.Eng. Raul R. TURMANIDZE Ph.D. - Technical University of Tbilisi, *Georgia*;
Prof.Eng. Nicolae UNGUREANU Ph.D. – Technical University of Cluj-Napoca, *Romania*;
Prof.Eng. Ioan VIDA-SIMITI Ph.D. - Politechnical University of Cluj-Napoca, *Romania*;
Assoc.Prof.Eng. Zoltán VIRÁG Ph.D. - University of Miskolc, *Hungary*;

EDITORIAL BOARD:

Editor-in-chief: **Assoc.Prof.Eng. Sorin MIHĂILESCU Ph.D.** - University of Petroșani, *Romania*
Deputy Editor: **Lecturer Eng. Andrei ANDRAȘ Ph.D.** - University of Petroșani, *Romania*
Associate Editors: **Prof.Eng. Ioan-Lucian BOLUNDUȚ Ph.D.** - University of Petroșani, *Romania*;
Assoc.Prof. Eng. Iosif DUMITRESCU Ph.D. - University of Petroșani, *Romania*;
Assoc.Prof.Eng. Gabriel PRAPORGESCU Ph.D. - University of Petroșani, *Romania*;
Prof.Eng.Habil. Florin Dumitru POPESCU Ph.D. - University of Petroșani, *Romania*;
Assoc.Prof.Eng. Sorin VĂTAVU Ph.D. - University of Petroșani, *Romania*

Editorial office address:

University of Petroșani, 20 University Street, 332006, Petroșani, Romania,
Phone: (40) 254/54.29.94, 54.25.80, 54.25.81, 54.25.82, **Fax.** (40)254/54.34.91, 54.62.38,
<https://www.upet.ro/annals/mechanical/> E-mail: andrei.andras@gmail.com

Contents

Bădiță (Popescu), D., Țuțuianu, G., Nan, M.S., Grecea, D., Sultan, A., Plotogea, C., <i>Research on the Mechanization of Technological Processes in the Execution of Vertical Mining Works for Aeration of Secondary Pipelines at Hateg Hydroconstruction</i>	5
Cozma B.-Z., Urdea G.-B., Dumitrescu I., <i>Stand For The Rotative Boring Of Rock Salt</i>	15
Cozma B.-Z., Urdea G.-B., Dumitrescu I., <i>The Constructive Analysis Of The Borer Heads For The Rotative Boring Of Soft Rocks</i>	23
Gîlmă, I., <i>Reliability Study Of Escrc-1400 Bucket Wheel Excavator Travel System. A New Approach</i>	31
Gîlmă, I., Ilioni, C., <i>Aspects Regarding Maintainabilty Analysis Of Escrc-1400 Bucket Wheel Excavator</i>	39
Gireadă, A.L., Nan, M.S., Rad, M., Nicolescu, C., Kovacs, I., Grecea, D., <i>Results Obtained On The Optimization Of Labor Use In Work Exercises For Salvators For The Surface Industry</i>	49
Itu R.B., Dumitrescu I., Itu V., <i>The Equations Of Motion Of The Extraction Drive Wheel Cable System And The Relation Between The Tensions Between The Extreme Points Of The Wrapping Of The Cable On The Drive Wheel</i>	55
Jula, D., Gîlma, I., <i>Aspects Regarding Determination Of Reliability Characteristics For Bucket Wheel Excavator Teeth</i>	63
Kertész (Brînaș), I., Andraș, A., Popescu, F.D., <i>Improving The Functional Performances of The Bucket Wheel Excavators (BWEs) Cutting-Teeth</i>	71
Kertész (Brînaș), I., Popescu, F.D., Radu, S.M., Ilioni, C., <i>The Analysis Of The Deformations And Stresses Of The Cutting-Teeth Of Bucket-Wheel Excavators (BWEs) During Operation, Using Finite Elements Method (FEM)</i>	81
Ladányi, G., <i>Strength Assessment Of A Truss Bridge For Belt Conveyors</i>	91
Ladányi, G., <i>Vibration And Current Signature Monitoring Experiences At The Márkushegy Mine Plant</i>	97

Mareş, R., Păun, A.-P., Popescu-Stealea, M., <i>Catia V5 – Software in Modeling And Solving Engineering Applications with Finite Element Method as a Work Tool</i>	103
Mărculescu, D.O., Lazăr, G., <i>Deadly Mass Casualty Incidents - A Constant Challenge In The Cooperation Between The Forensic Pathologist And Criminal Prosecutor To Identify The Victims</i>	109
Plotogea, C., Nan, M.S., Sultan, A., Vladu, B., <i>Research Regarding The Use Of Drones In Monitoring And Controlling Mining Processes And Environment Protection</i>	113
Praporgescu, G., Mihăilescu, S., <i>Technical Solutions For Mining Tunnels Excavation Technology</i>	119
Rad, M.D., Nan, M.S., Grecea, D., Magyari, M., Sălăşan, D., <i>Improving Security And Health Through Proper Implementation Of The Inspection And Maintenance Programme Of Electric Power Ex Equipment Designed In Flameproof Enclosure "D" And Increased Safety "E" Type Of Protection</i>	127
Tomuş, O.B., Jula, D., Rada, A.C., <i>Reliability Analysis Of The Braking System Of The Industrial Loader/Transporter Machines</i>	135
Tomuş, O.B., Jula, D., Rada, A.C., <i>Study Of The Cutting Forces And Specific Cutting Resistance From The Point Of View Of The Cutting Direction Relative To Stratification Of The Coal Seam</i>	143
Țuțuianu, G., Bădiță, (Popescu) D., Nan, M.S., Grecea, D., Vladu, B., Sultan, A., <i>Researches On The Modernization Of The Execution Technologies Of Digging, Arranging And Fitting Works In Hydrotechnical Constructions</i>	149
Index of Authors	159
Instructions for Authors	160

RESEARCH ON THE MECHANIZATION OF TECHNOLOGICAL PROCESSES IN THE EXECUTION OF VERTICAL MINING WORKS FOR AERATION OF SECONDARY PIPELINES AT HATEG HYDROCONSTRUCTION

**DORINA BĂDIȚĂ (POPESCU)¹, GABRIEL ȚUȚUIANU²,
MARIN SILVIU NAN³, DĂNUȚ GRECEA⁴, CĂTĂLIN PLOTOGEA⁵**

Abstract: The purpose of this paper is , on the one hand, to set the kinematics of the mining extraction system used for the mechanization of well drilling and, on the other hand, o perform calculations to verify the metal structure of the metal tower of extraction system, both by classic analytical calculation as well as by the finite element method. The metal structure of the extraction tower is modeled as a planar frame, which is an unspecified static system loaded with the technological forces that appear in the extraction cable and the mass forces given by the weight of the tower with the Solid Edge utility by 3D modeling.

Keywords: metal structure, extraction installation, Solid Edge utility, 3D modeling

1. INTRODUCTION

The evolution of modern society cannot be conceived without the proper development of energy sector, namely the widespread use of electricity in all sectors of the economy, in the social, cultural and household use. Production and specific consumption of electricity is, in contemporary society, significant indicators of technical and social level achieved.

¹ *Ph. D. Student, Eng., University of Petroșani,*

² *Ph. D. Student, Eng., University of Petroșani*

³ *Professor, Ph.D. Eng., University of Petroșani, nan.marins@gmail.com*

⁴ *Ph. D. Student, Eng., University of Petroșani*

⁵ *Ph. D. Student, Eng., University of Petroșani*

The use of electricity involves the existence of power systems, representing large technical systems, which encompass all the installations for the production, transport, distribution and consumption of electricity.

In the hydroelectric power systems are found hydroelectric power plants, which represent about 25% of the installed power plants in Romania.

In this context, the hydro-energetic arrangement of the Râul Mare Retezat is also included, in which, in order to improve the current conditions of use and exploitation, it is necessary to execute a de-aeration well, the approach of which is the subject of this paper. It is specified that the de-aeration well is a classical mining work, similar to that used for the extraction of useful minerals, generally particularity consisting in the conditions of location in the mountain area of the extraction installation..

2. KINEMATICS OF THE EXTRACTION SYSTEM

In the extraction installations equipped with a bucket, the time-varying velocity and acceleration diagram has several phases because of the three safety bridges through which the bucket has to pass at a low speed, having a totally different aspect to the hoisting with cages or skip-charging gear.

The particularities of the kinematics, but especially the dynamics of these bucket elevator installations, derive from the fact that there is only one branch with which they ascend and descend, this type of installation combining the particularities of the cable and winch transport with the vertical transport with classic extraction installations. This is the reason why, in the literature, in the bucket elevator installations, the name of extraction winch is found instead of extraction machine.

In determining the kinematic and dynamic characteristics of the bucket elevator system, it is to be assumed that the drive of the motor drum is made with an asynchronous motor, which leads to a linear variation of the velocity in the acceleration periods.

For establishing the general dynamic equation of the bucket system, the methodology and the particularities applied to the extraction systems with non-discharging vessels are taken into account.

2.1. Establishing input data required for kinematic calculation

For the analyzed extraction installation, the solution was adopted by which the mobile working and safety bridge is also the bridge for fastening and stretching the cables of the bucket guide system.

The distance traveled by bucket from the operating front to the guiding cable (mobile bridge), H_f , must be within the range of 15 to 25 m. The $H_f = 20$ m is adopted.

The maximum displacement speed on this portion is:

- Maximum 2 m/s for the material conveyor. $V_{fm} = 1.5$ m/s is adopted;
- Maximum 1.0 m/s for passenger transport. $V_{fp} = 1.0$ m/s is adopted.

When bucket passing through the opening mobile working bridge, the upper clamp the cable binding device drives the carriage guide.

Due to the fact that on the unguided portion the bucket can plow, there is the danger of its striking when passing through the bridge by the edges of the passage. For this reason, bridge speed must drop to 0.4 ... 0.6 m/s. $V_p = 0.5$ m/s is adopted. Thus, the movement of the bucket on the non-guided portion to the mobile bridge can be considered to be carried out after a trapezoidal tachograph, the shape of the diagram on the acceleration portion being imposed by the asynchronous drive motor of the extraction machine. During t_f (unguided), the maximum speed being V_f , it decreases when passing through the bridge opening at $v_p = 0.5$ m/s. After bucket moving to the mobile bridge, the bucket movement is guided and takes place during the t_g (guided) period in the free section of the shaft after a trapezoidal tachograph.

The maximum speed on this shaft portion is adopted after the relationship:

$$v_{max} \leq \frac{2}{3} \cdot 0,8 \sqrt{H_g} = 0,53 \sqrt{H_g}, \text{ m/s}, \quad (1)$$

where H_g is the length of the route.

For the projected installation $H_g = 75$ m, such that $v_{max} \leq 4,59$ m/s. Adopt $v_{max} = 4$ m/s.

The bucket acceleration must be maintained within $a = 0.3$ to 0.5 m/s². It adopts $a = 0.4$ m/s².

The height of the positioning of the bridge discharge (emptying) of bucket to the bridge at the shaft head (the vehicular platform system) is $H_1 = 8$ m, the distance is determined from the condition for travel by self-weight of the material loading chute in the means of transport.

The bucket is overloaded with $H_2 = 1.5$ m from the unloading platform to hook the hook of the suspended chain to the ring on its bottom.

At this distance, the bucket moves on a uniform speed $v_{g0} = 0.5$ m/s at a distance, and then on the last part from the distance to stop evenly decelerated with deceleration $a = 0.5$ m/s².

The distance on which the descending bucket moves to the emptying position is carried out in three phases, a distance, h_{c1} , uniformly accelerated, the second at constant speed, h_{c2} , and the third and last phase, h_{c3} , until it stops in the position of emptying is evenly slowed down. The uniform speed is $v_{c0} = 0.5$ m/s, and acceleration and deceleration $a = 1$ m/s².

The time of emptying the bucket, t_{go} , is in the range of 10 ... 20 s. The $t_g = 20$ s is adopted. The pause time at the required front for auxiliary operations, referring to a complete transport cycle, is $t_{pf} = 40$ s.

2.2. Determination of kinematic parameters

The kinematic analysis of the extraction system involves determining the variation in time of bucket velocities and accelerations as well as of the enveloped spaces when moving it from the working front to the discharge point on the discharge bridge in

the extraction shaft tower.

Figure 1 shows the tachograph of the extraction system, specifying that the scale representation is not respected, in the desire to clearly highlight the characteristic points of the diagram.

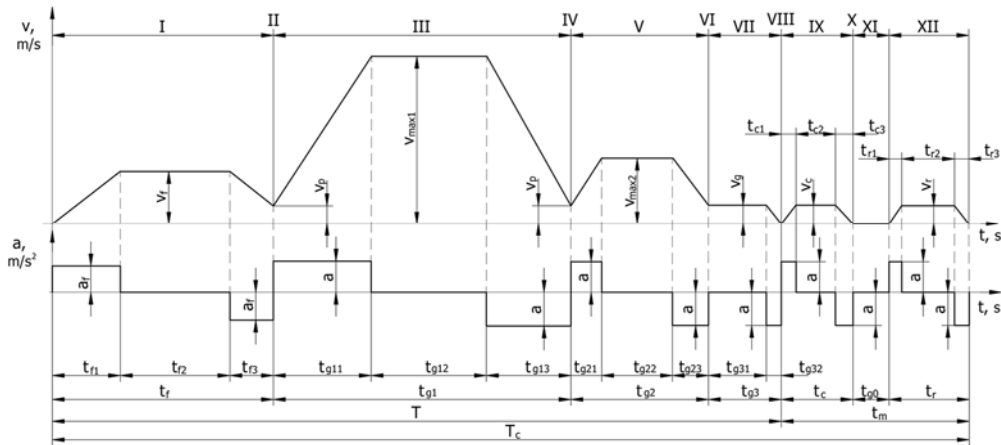


Fig. 1. Tachograph of bucket displacement

I – moving without guidance from the front to the mobile bridge; II - passage through the mobile bridge; III - guided movement between the mobile bridge and the fixed safety bridge 2; IV - passage through the fixed safety bridge 2; V - displacement between the two fixed safety bridges 1 and 2; VI - passage through the fixed bridge 1 from the mouth of the shaft; VII - tower to the unloading bridge, with cradle for coupling the discharge chain; VIII - bucket stop; IX - lowering for unloading; X - bucket stop; XI - bucket emptying; XII - maneuvers for repositioning bucket

It is specified that kinematic parameters were determined for the final stage of digging the shaft. The configuration of the tachograph is mainly influenced by the speed limitations imposed on the passage through the three working and safety bridges.

The kinematic calculation allows you to determine the number of races per hour possible to achieve with the extraction system, which allows for the assessment of the technical and economic indicators of the installation.

The data was organized as spreadsheets and processed using the Excel utility. Figure 2 shows the sequence of the spreadsheet showing the variation in time of the velocity, acceleration and space, the time base used is from 0.005 s ($1/200$), which allow tachograph representation of bucket displacement.

The screenshot also illustrates the computational elements for analyzing the dynamics of the extraction system, namely the forces, distances and powers for the entire upward course.

The iterative calculation process using the Excel utility was accomplished by 21784 lines, imposed by the time base of 0.005 s , from which it follows that each of the graphical representations are plotted by 21784 points.

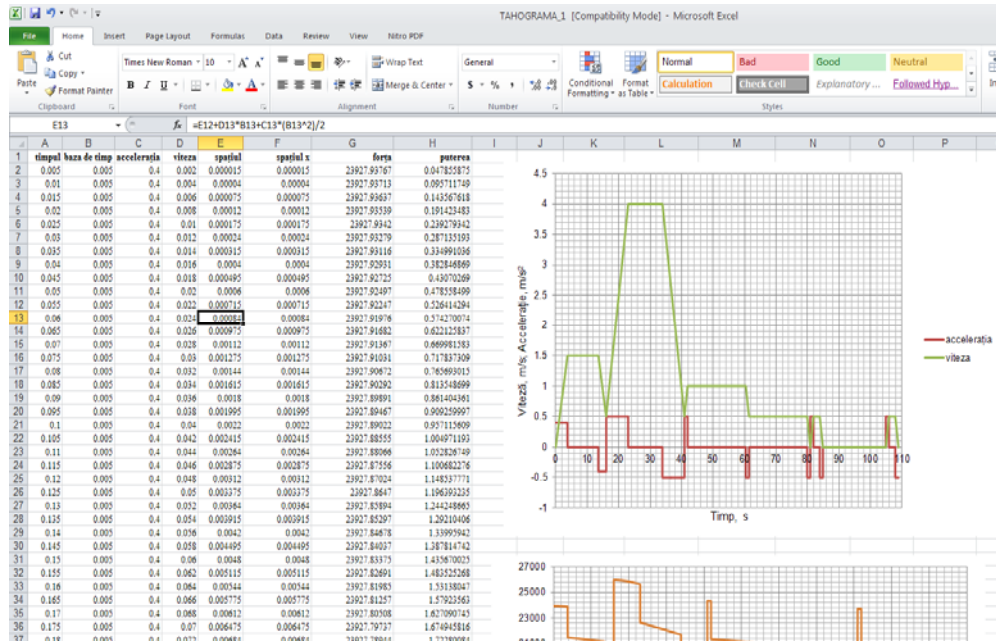


Fig. 2. Organization of the calculation base

Figure 3 shows the tachograph of the extraction system, represented during the transport course at the working front (considered at the maximum drilling depth) until the discharge and repositioning of the bucket on the unloading platform.

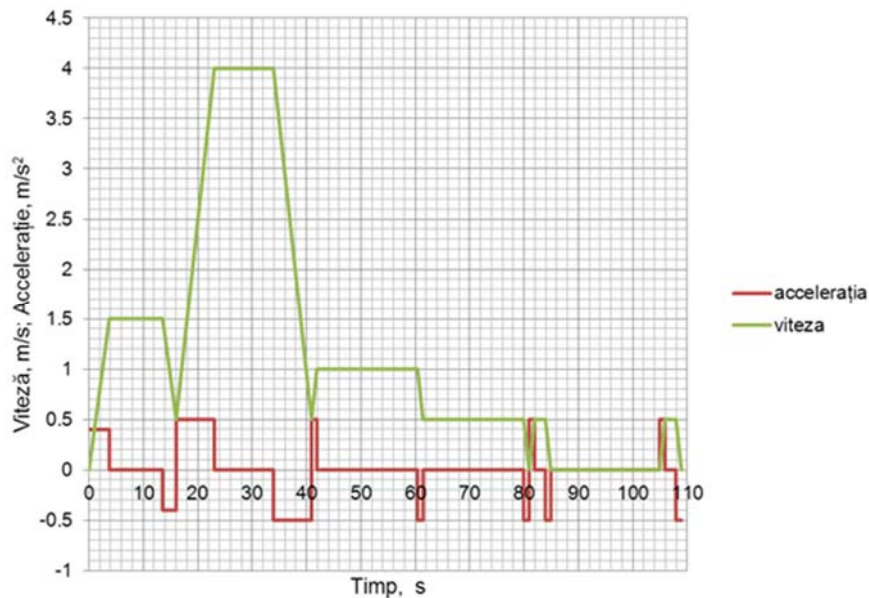


Fig. 3. Tachograph of the bucket elevator installations

It is a seven-speed tachograph whose altitude is imposed by the speed restrictions imposed on passing through the three bridges.

By overlapping this representation with the tachograph of Figure 1 and using the data in Figure 2, it is very easy to identify the temporal evolutions of the kinematic characteristics of the extraction system.

The presence of bucket in the bridging area is signaled in the extraction machine house via the electrical control and signaling system, including the level indicator.

Figure 4 shows the dependence of the gap length space on time, resulting in a rapid increase in the speed range of 4 m/s , the time interval $18\text{-}38\text{ s}$, immediately after the mobile working bridge, as well as the horizontal zone in which the bucket is stopped for discharge, corresponding to the time interval $84 \dots 104\text{ s}$.

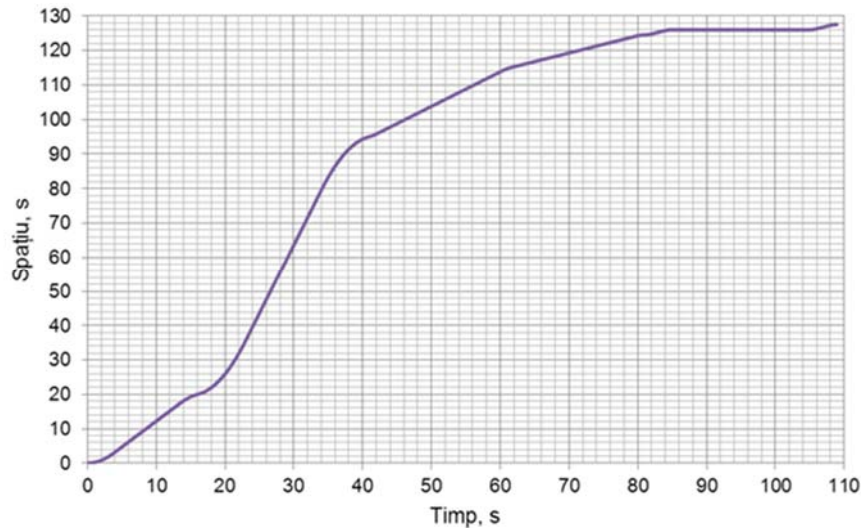


Fig. 4. The time dependence of space travel by the bucket on the transport of the work piece material

The kinematics of the mining extraction system used for the mechanization of well drilling is largely influenced by the overall construction solution of the plant, mainly by the existence of working and safety bridges through which the bucket has to pass at a low speed (0.5 m/s) by the single-drum winch, so that the upward stroke of the cable is wrapped on the drum, the downward stroke being carried out under its own weight, as well as the method of unloading the bucket, which has to be raised over the bridge 8 m above the ground level to ensure the overturning link followed by emptying and repositioning maneuvers.

The tachograph is complicated and is made up of seven steps, with low space and time, making it difficult to handle the transport route, as there are many acceleration and braking intervals. This tachograph configuration increases the importance of existing level indicators on the transport route, indicating the position of the bucket in the shaft, or even stopping the system in case of damage.

For drawing the actual tachograph, iterative tabular calculus specific to the Excel utility is used, which also allows for graphical representations of accuracy, influenced by the time base of 0.005 s.

3. REQUEST STATE DETERMINATION AND DEFORMATIONS IN TOWER OF EXTRACTION SYSTEM

The tower of the extraction system, represented by using the Solid Edge 3D model, in Figures 5 and 6, is a mixed metal structure, mainly removable, made of L160 and L100 profiles angle, of gouges and welded connecting together by welding but mainly by screws.

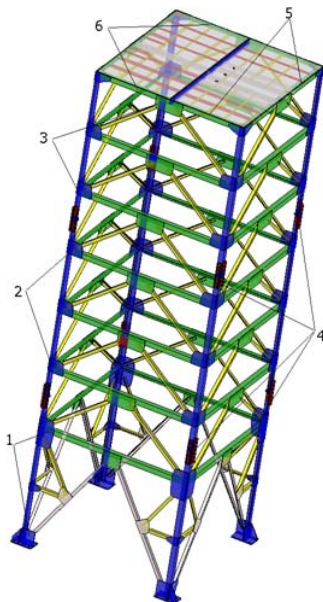


Fig. 5. The 3D model of the tower
1 – lower segment; 2 – intermediate segment;
3 – upper segment; 4 – fishplates connecting
segment; 5 – upper platform 1; 6 – upper
platform 2.

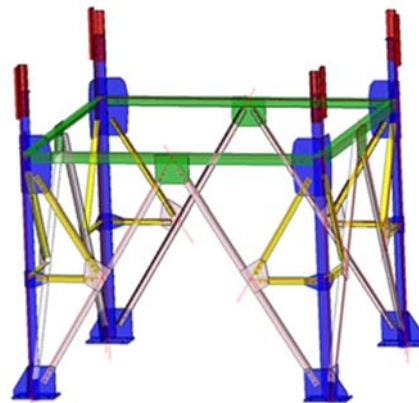


Fig. 6. The 3D model of the lower
segment with highlighting the neutral axis
(red line) of L160 and L100 profiles angle
to form lattice beams specific to metal
constructions

It is a three-sectioned metal structure with a square section with a 5 m side and a functional height up to the 16 m extraction bridge mounting bridge.

The calculation performed on this metallic structure requires the analytical determination of the solicitations, and implicitly of the safety coefficients, which constitute a verification of metal structure.

Critical sections required to perform the analytical calculation. Also, this representation is the basis of meshing necessary for the finite element calculation.

Figure 7 shows the calculation model with the geometrical dimensions of the tower, which determines the stressing loads of the metal structure.

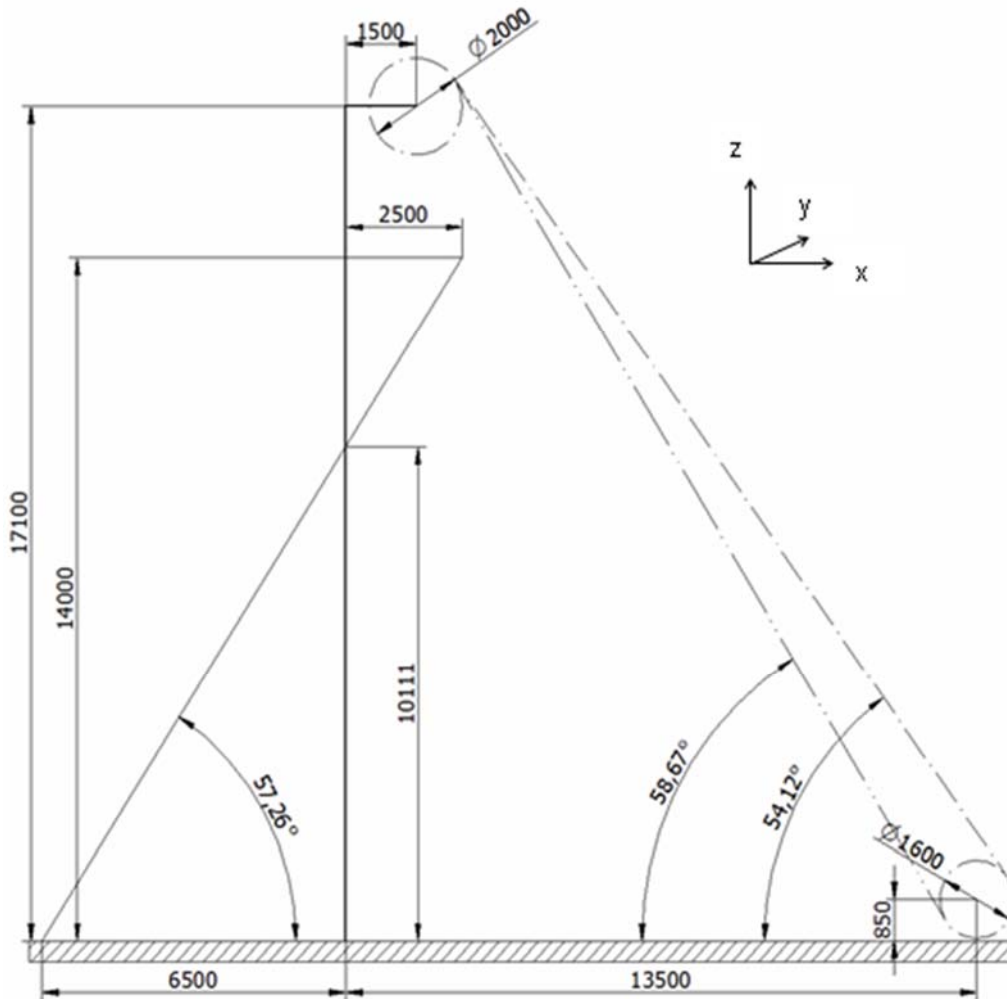


Fig. 7. The calculation model of the forces acting on the tower

The forces acting on the tower are existing technology in the wire extraction, the extraction material with bucket elevator, respectively launching and removing the mobile bridge work, and to be transmitted to the tower by bearings pulley, and the mass data of the weight of the tower and parts mounted on it.

Both technological and mass forces are considered to be concentrated forces. The technological force is reported to the center of symmetry of the $\text{Ø}2000$ extraction

shaft, and the mass forces are applied to the center of gravity of the calculated element, its position being appreciated by the designer.

The baseline for which the application points of the forces are defined is the level of the ground, the share 0,00 on which the metallurgy of the tower is mounted, and its axis of symmetry.

4. CONCLUSIONS

The purpose of this paper is , on the one hand, to set the kinematics of the mining extraction system used for the mechanization of well drilling and, on the other hand, to perform calculations to verify the metal structure of the metal tower of extraction system, both by classic analytical calculation as well as by the finite element method.

The metal structure of the extraction tower is modeled as a planar frame, which is an unspecified static system loaded with the technological forces that appear in the extraction cable and the mass forces given by the weight of the tower.

The maximum technological forces applied to the center of symmetry of the extraction pulley and which are transmitted to the tower through the two bearings of the pulley are calculated for two situations, a first case for the bucket transport of the rock or materials and the second for launching or removing the working bridge.

Considering the importance of the installation, the security rules impose a safety factor of 3, especially because personnel transport is carried out, so that a calculation coefficient is adopted in a dynamic coefficient of 1.6, multiplied by the modulus of the technological forces used in the calculation metal structure.

For the verification of the extraction tower, the components of the technological forces applied in the center of the pulley are $F_x = 19410\text{ N}$ and $F_z = 59960\text{ N}$ for the bucket material transport and $F_x = 52220\text{ N}$ and $F_z = 161300\text{ N}$ for the launching or extraction of the mobile bridge.

The tower's weight is defined by the z-axis vector having the module as the sum of the weights of the elements and the application point calculated according to the weight centers of the component elements.

By solving the unspecified static system using the Mohr-Maxwell-Veresciaghin process, axial forces, cutting forces and bending moments are determined over the entire frame contour, as well as the forces introduced into the anchor cables, all of which are calculated for the two aforementioned situations.

Determination of loadings on the contour of the frame was made for different points of attachment of the anchorages of the tower metal structure, concluding that the loads decrease with the increase of the anchorage height.

The geometric characteristics of the critical sections of the tower's metal structure are obtained by using the Solid Edge utility, which allows direct reading of inertia moments and resistors relative to x and y horizontal axes as well as the section area and maximum distances to medium fiber.

REFERENCES

- [1]. **Bădiță (Popescu), D.**, *Stadiul actual și tendințe modern în procesele tehnologice de execuție a lucrărilor miniere, Raport de cercetare științifică nr. 1*, Petroșani, decembrie 2011.
- [2]. **Bădiță (Popescu), D.**, *Cercetări teoretice și experimentale privind posibilitățile de modernizare a proceselor de execuție a lucrărilor miniere, Raport de cercetare științifică nr. 2*, Petroșani, aprilie 2012.
- [3]. **Bădiță (Popescu), D.**, *Contribuții teoretice și applicative la creșterea gradului de mecanizare în procesele de execuție a lucrărilor miniere, Raport de cercetare științifică nr. 3*, Petroșani, iulie 2012.
- [4]. **Băduț, M., Iosip, M.**, *Bazele proiectării cu Solid Edge*, Editura Albastră, Cluj-Napoca, 2003.
- [5]. **Magyari, A.**, *Instalații mecanice miniere*, Editura Tehnică, București, 1990.
- [6]. **Magyari, A., Achim, M.I.**, *Instalații de extracție miniere. Îndrumător de proiect*, Litografia Institutului de Mine Petroșani, 1990.
- [7]. **Pop, A.I., Itu, R.B., Radu, S.M.**, *Application of forces reduction in the calculation of technological mechanical loads transmitted to the tower of a winding engine through extraction pulley bearings*, 16th GeoConference on Science and Technologies in Geology, Exploration and Mining SGEM 2016, Conference Proceedings, Albena, Bulgaria, 30.06-6.07.2016, Book 1, vol. II, pp. 49 – 56, ISBN 978-619-7105-56-8, ISSN 1314-2704. DOI: 10.5593/SGEM2016/B12/S03.017
- [8]. **Popescu F, Andraș A, Kertesz I**, *The method of minimizing the calculated power of vertical transport installations*, 17th International Multidisciplinary Scientific GeoConference SGEM 2017, www.sgem.org, SGEM2017 Conference Proceedings, ISBN 978-619-7105-00-1 / ISSN 1314-2704, 29 June - 5 July, 2017, Vol. 17, Issue 13, 901-908 pp. DOI: 10.5593/sgem2017/13/S03.11
- [9]. **Popescu, F.D., Radu, S.M.**, *Vertical Hoist Systems: New Trends Optimizations*, LAP Lambert Academic Publishing, Saarbrücken Germany, 2013, ISBN 978-3-659-49895-4.
- [10]. **Popescu, F.D., Nan, M.S., Radu, S.M., Tutuianu, G.**, *Study Of Kinematics Of Multi-Rope Hoisting Machinery Statically, Balanced Using Solidworks®*, Proceedings of MultiScience - XXX. microCAD International Multidisciplinary Scientific Conference, University of Miskolc, Hungary, 21-22 April 2016, ISBN 978-963-358-113-1

STAND FOR THE ROTATIVE BORING OF ROCK SALT

**BOGDAN-ZENO COZMA ¹, GHEORGHE-BOGDAN URDEA ²,
IOSIF DUMITRESCU ³**

Abstract: This paper presents the way of making up a stand for the rotative boring of soft rocks (coal, plaster stone, rock salt, very soft limestones, compact marble) which have the boring and cutting resistance up to $f = 3$, according to prof. M.M. Protodiakonov. In order to achieve a wider range of revolutions and axial advances there was used an ordinary lathe which has a device mounted on the main body where the evidence used for boring is caught, and in the knife frog, by means of a translator the rod with borer head is fixed. The catch of the sample is made up by a biaxial pretensioning that is similar to working circumstances. By measuring the moment and the advance force, the most favourable boring running can be established (revolution, advance), as well as the most favourable geometrical shape of the borer head, according to the mechanical characteristics of the rock.

Key words: rotative boring, soft rocks, geometrical shapes, dynamometer, stand.

1. INTRODUCTION

The exploitation of useful mineral substances has been, is and will remain, at least for some more period of time, one of the main activities of human society. Economically speaking, this activity is extremely expensive, but essential nevertheless, because it is the basis of most industrial activities.

The phenomenon of rocks mechanical displacement is a very complex one and depends on a very large number of factors, connected both to the characteristics of the rock and to the displacement procedure. Among the factors that are addicted to the rock, we mention:

¹ *Lecturer Eng. PhD. at University of Petroșani, România, cbogdy@netlog.ro*

² *Lecturer Eng. PhD. at University of Petroșani, România*

³ *Assoc. Prof. Eng. PhD. at University of Petroșani, România*

- the rocks mechanical proprieties that define the forces the installation must convey to the tool in order to obtain a certain productivity;
- the boring rocks capacity to use the tool during rock displacement which determines the exchange frequency among the used tools;
- the clefts and cracks that exist within the rocks and which play an important role in their displacement;
- the tension condition of the rocks which has a very important role in the displacement process;

The first two factors of influence, i.e. the mechanical proprieties and the usage capacity, can be determined on rock sample in the lab, and the last two can only be determined in situ.

By realizing a stand for soft rocks boring (coal, plaster stone, rock salt, very soft limestones, compact marble), having the possibility to measure the moment and the advance force, one can establish the optimal conditions of boring (revolution, advance) and the geometrical shape of the borer head according to the mechanical characteristics of the rock.

2. STAND CONSTRUCTION AND RUNNING

In order to achieve a wider range of revolutions and axial advances there was used an ordinary lathe for which there have been projected and built two devices in order to realise the stand for the rotative boring of soft rocks presented in figure 1.

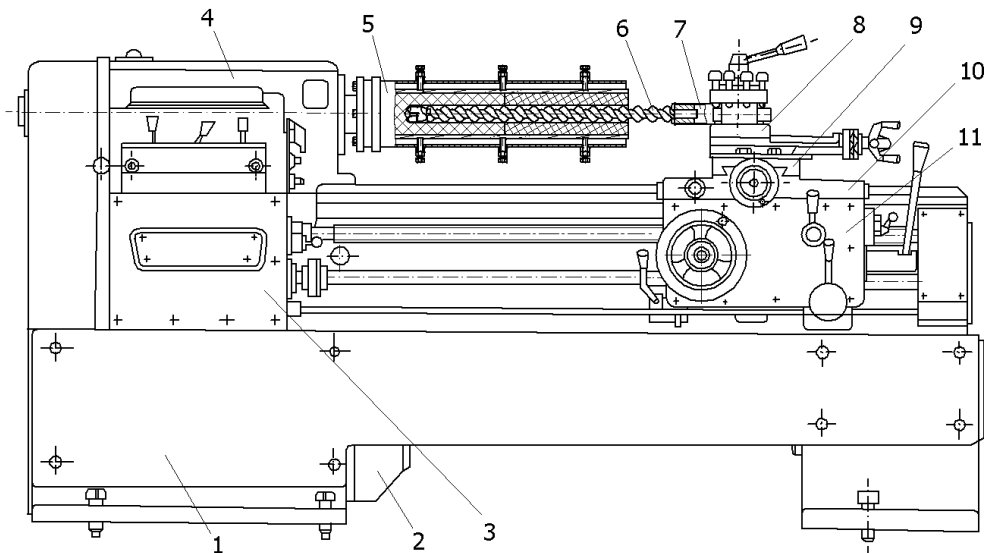


Fig. 1. Stand for the rotative boring of soft rocks

This is made up of: 1 – the lathe metal construction; 2 – electric engine; 3 – the box with advances and threads; 4 – the fixed tool and the gear box; 5 – the sample stand, fixed on the main body; 6 – the elicoid rod and the borer head type CR; 7 – the diameter with tensiometer stamps to measure the advance force and the torsion moment; 8 – the knife frog with its knife frog slide; 9 – the transversal slide; 10 – the longitudinal slide; 11 – the lathe truck.

Mounting the sample prop 5 on the main body is done, after disassembling the lathe chuck, with the help of those four screws and that of the pacer, by centering the prop flange on the cone-shaped surface of the main body, in the same way as the lathe chuck.

The dynamometer is fixed on the knife frog in such a way as the axis of the borer head should be in the area of the rotative axis of the sample, and the horizontal adjustment is done with the help of the transversal slide 9. In order to have enough space at the beginning of boring, when the borer is in the extension of the prop, the mobile clew is disassembled from the lathe.

In figure 2 is presented the constructive solution of the two devices of catching the sample and the borer, that are to be mounted on the ordinary lathe, where there have been put down: 1 – the dynamometer prop; 2 – fixing bolt of the pipe; 3 – thin wall pipe conductor, having the role of translator; 4 – the rod; 5 – parallel keys; 6 – the borer rod; 7 – detachable borer head type CR; 8 – the first sample; 9 – wooden rulers; 10 – the sample prop; 11 – M12 screws; 12 – screw nuts to block the screws; 13 – the second sample; 14 – the fixing screws of the lathe chuck on the main body; 15 – the fixing flange of the lathe chuck; 16 – shoulder screw nuts to fix the lathe chuck.

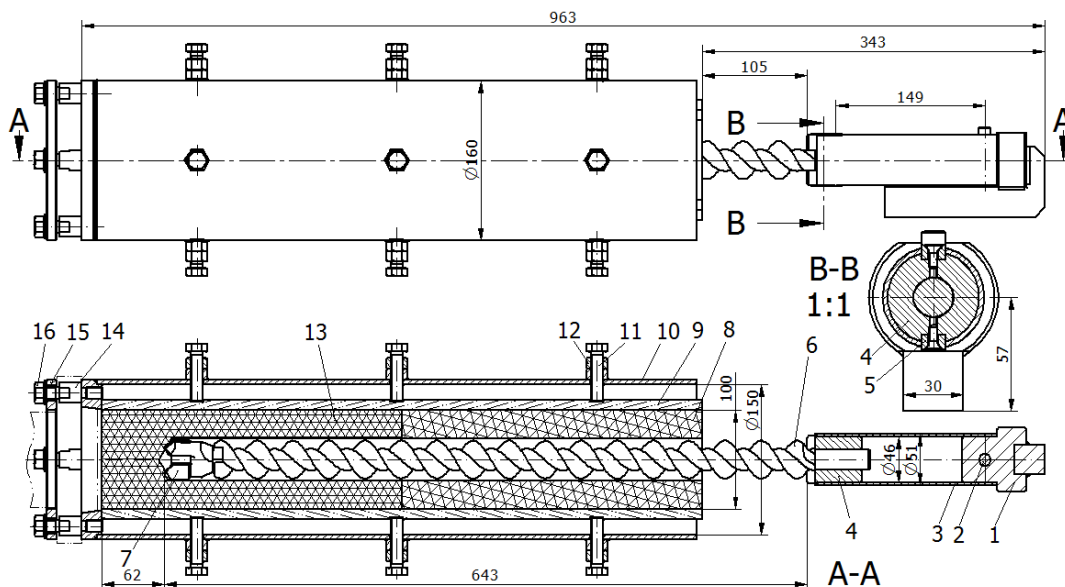


Fig. 2. The devices of the prop for fixing the sample and the borer

The pipe is the elastic element that will deform under the action of the torsion moment and of the axial force conveyed from the borer rod to the lathe knife frog and which is measured by the tensiometrical stamps. The way of pipe distortion is presented in figure 3, where the prolonging within the perpendicular plane on the pipe axis (XY) is $5,22 \cdot 10^{-5}$ mm, and within the plane of the pipe axis (YZ) is $1,25 \cdot 10^{-3}$ mm for the area for stamps fixing.

The tensiometrical stamps are fixed on pipe 3, two of them to measure the axial force, one alongside the pipe generator and the other is transversal on this one, and two of them to measure the moment, laid at 45° towards the generators.

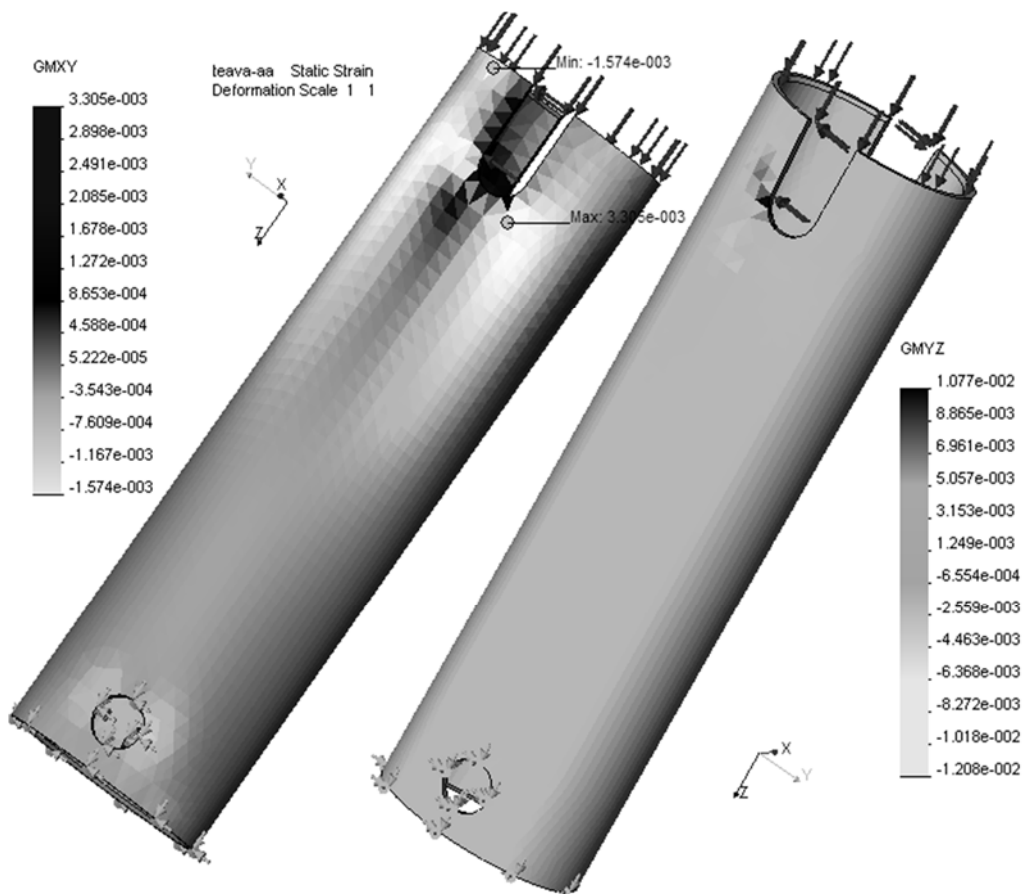


Fig. 3. The way of variation of the longings within planes XY and YZ for $F=10$ kN, $M=250$ Nm

The axial force is given by the advance longitudinal system of the lathe and conveyed from the knife frog to the borer head 7 through the dynamometer prop 1, pipe 3, rod prop 4 and the borer rod 6.

The torsion moment is produced by the main body of the lathe and conveyed to the rock samples 8 and 13 by means of prop 10 and that of the fixing system of the samples in the prop, made up of wooden rulers 9 and the screws 11 with their blocking screw nuts 12. Conveying the torsion moment from the borer head 7 to the pipe 3 of the dynamometer is realised by the key-shaped assemblings between the borer head-rod and rod prop-rod and by two keys 5 from the rod prop to the pipe.

The positioning of the three elements of the dynamometer is done throughout the two intermediate adjustments realised between the pipe and the dynamometer prop, that is the rod prop. This disassembling construction was chosen in order to have the possibility to change the compound elements and to use the dynamometer even to make a hole into the metals on the lathe.

The two samples 8 and 13, of 100x100x300 mm, are positioned among four wooden rulers 9 and introduced within the pipe prop 10. By tightening the screws 11 and by blocking them with screw nuts 12 there is realised both the samples centring and their fixing.

3. MEASUREMENTS REALISED WHEN MAKING ROTATIVE BORING OF ROCK SALT

Figure 4 presents the prop according to which the rotative boring of rock salt has been realised; this is made up of: 1 – the ordinary lathe; 2 – the device which catches the two samples out of salt; 3 – the dynamometrical device; 4 – the rod and the borer head; 5 – the computer with the acquisition plate of the measured data; 6 – constructive types of borer heads.

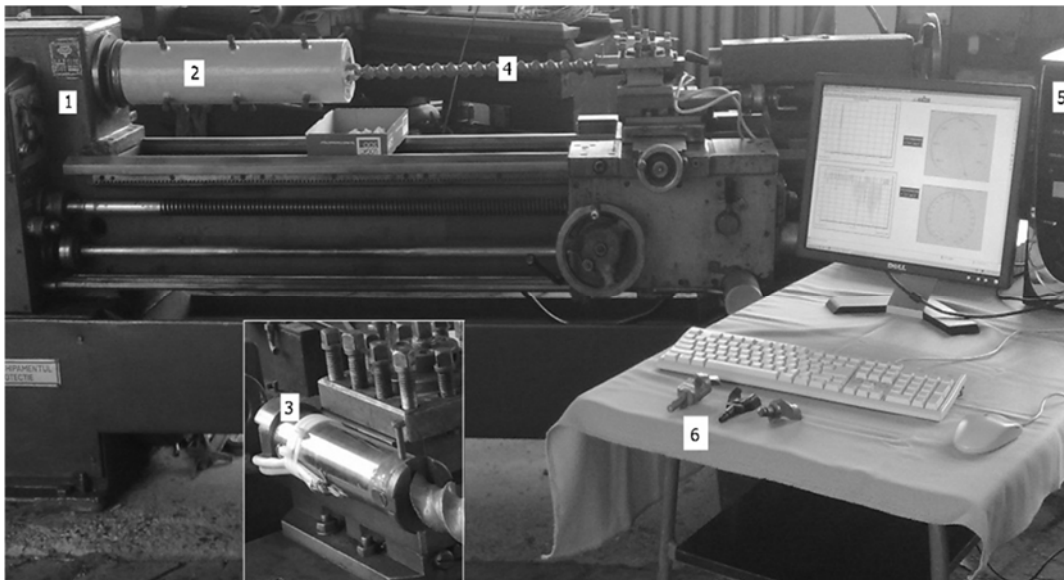


Fig. 4. The stand for rotative boring of salt and the measuring apparatus

There have been realised measurements with those three types of borer heads for 100 and 200 r.p.m and advances from 0,1 up to 3,2 mm/rot. In figure 5 there are presented the results of the measurements for the standardized borer head, the one on the right figure 4, for 100 r.p.m and an advance of 3,2 mm/rot, which means a boring speed of 0,32 m/min. The data registering frequency is 50 Hz, and this results in the fact that the moment variation M diagram and the advance force F has been realised in 3 sec, that is approximately 30 registerings a rotation.

It is noticeable that with the maximum value of the advance force $F=11770,4$ N it has been registered the maximum value of the torsion moment as well $M=269,817$ Nm, and with the minimum value $F=-14,261$ N a moment value of $M=228,194$ Nm. From the axial force diagram comes out that there is a perturbation factor of the measured data with a frequency of 45 – 47 registerings a cicle, corresponding to about 1,5 rotations.

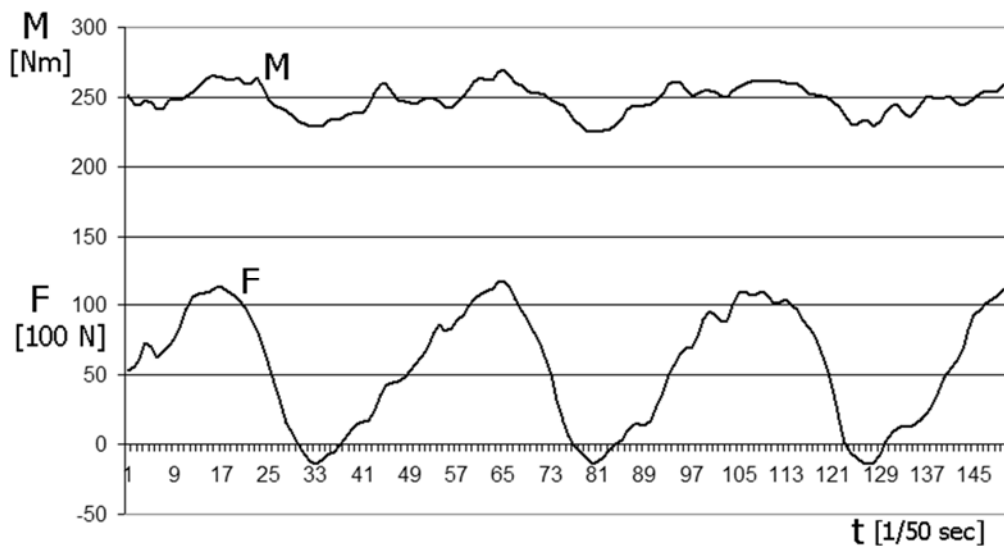


Fig. 5. The moment and force variation

After making some more measurements with different boring types on borer heads with different splitted geometry, the same perturbation frequency appeared. I have fixed a borer with the diameter of 28 mm, within the dynamometer and I've made holes both in the metal and in the salt to compare the measurements results. On grounds of these measurements I've noticed that the perturbator element is the elicoidal borer rod which has been 3D shaped and where there has been a kind of modal analysis with finite elements to determine its own vibrations, which is represented in figure 6. It is noticeable that the displacements on direction Z reach the area of the borer head, on a tooth to a maximum and the other to a minimum, which leads to losing the contact between the borer head and the foot of the hole, respectively the negative advance force.

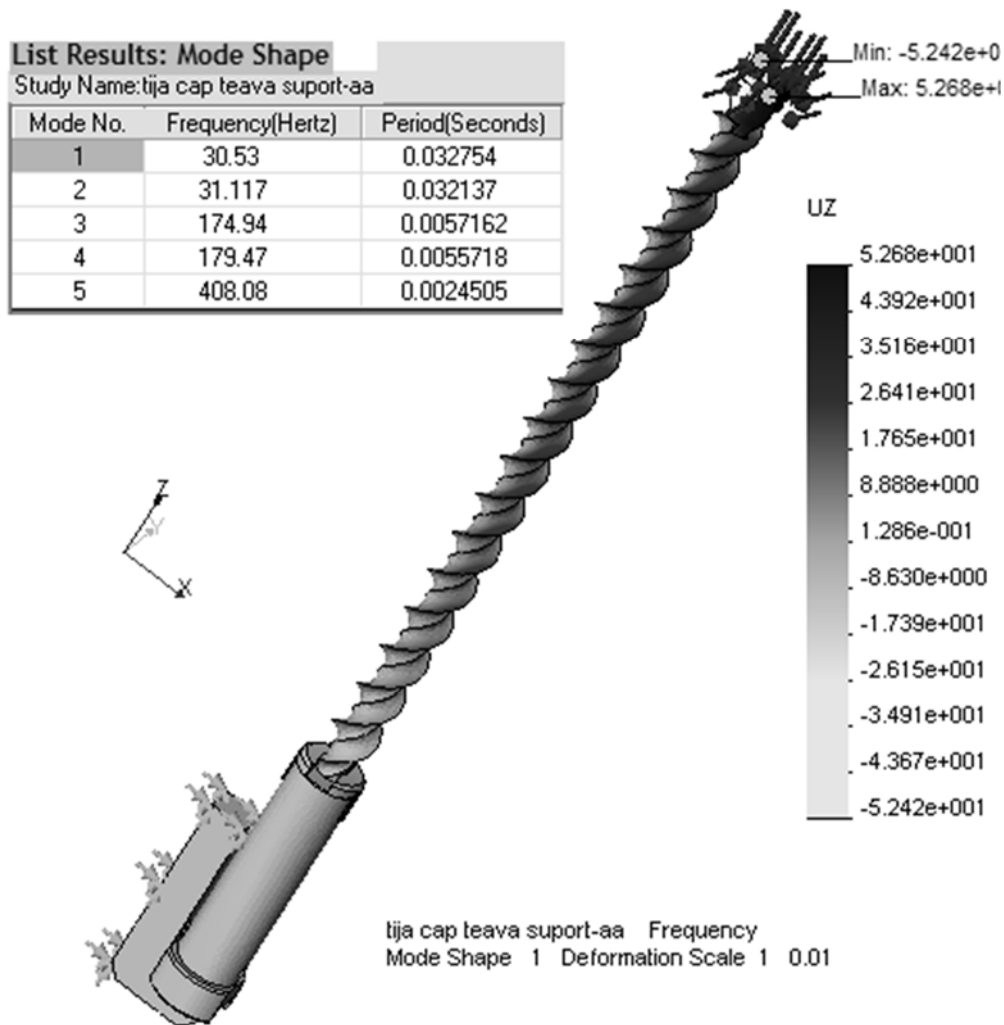


Fig. 6. The modal analysis of the borer rod

4. CONCLUSIONS

The stand for rotative boring of soft rocks has been made throughout a relatively simple construction, due to the usage of an ordinary lathe which allowed getting a wide range of rock salt boring types.

The constructive solution of the prop allows several modifications of the boring types for the same sample and with the same catching which leads to the exact settlement of the optimum boring type.

By fixing the sample on the other side with the help of wooden jaws and of the fixing screws it is realised the bidirectional pre-tensioning of the sample that is similar to working conditions.

One can use boring heads with different splinting geometries in the case of boring the same sample, resulting from this a better optimization of splinting geometry according to the characteristics of the bored rock.

Throughout the achieved measurements it has been pointed out the way in which salt displacement is produced with the rotative boring, the influence of the borer rod on rock displacement, with irregular splinters that produce a pulsatile stress of the borer head, the rod and the boring installation. These data regarding the displacement frequency, respectively the stresses that appear, allow the establishment of the optimum types of boring for some rocks and used boring installations.

In the future, we suggest the execution of a detached teeth borer head, with a different boring geometry and, on grounds of the measures taken on the stand, we could establish a theoretical correlation (calculus relations, mathematical and virtual modelling) between the geometry of the borer head and the type of the boring rock, respectively, the optimum regime of boring according to the durability of the borer head and the price of the boring operation.

REFERENCES

- [1]. **Bolunduț I.L., Dumitrescu I. & Cozma B.** (2002) *The Study Tools of Rotary Perforation a Auger Holes*, Annals of the University of Petroșani (Mechanical Engineering), vol.4 (XXXI), pp.5 ... 20, Petroșani, ISSN 1454-9166.
- [2]. **Cozma B.** (2004) *Studies and Research on Technology Drilling Auger Holes*, Referat teză de doctorat, Petroșani, (Doctorate Thesis Review).
- [3]. **Cozma B.** (2007) *The study of the Detachable Bits for Rotating Drilling*, International forum of young researches, "Topical Issues of Subsoil Usage", working group 5, St. Petersburg, Rusia.
- [4]. **Dinescu, S., Andraș, A.,** *Environmental Friendly Equipment and Technology for Underground Civil Excavations*, Annals Of The University Of Petrosani, Mechanical Engineering, Vol. 10 (XXXVII) 2008, pag. 47-52; ISSN: 1454-9166
- [5]. **Radu, S.M.,** *The mechanized face as a system*, SMO 08: Proceedings Of The 8th Wseas International Conference On Simulation, Modelling And Optimization Pages: 89-+ (2008), WOS:000262950300012
- [6]. * * * - Solid Edge Software v.19, Academic license ADA Computers București.
- [7]. * * * - Cosmos Design Star Software v.4, License S.C. INICAD DESIGN S.R.L: București.

THE CONSTRUCTIVE ANALYSIS OF THE BORER HEADS FOR THE ROTATIVE BORING OF SOFT ROCKS

**BOGDAN-ZENO COZMA ¹, GHEORGHE-BOGDAN URDEA ²,
IOSIF DUMITRESCU ³**

Abstract: In Romania there is standardized (STAS 7476-71) only one detachable head type cocked with plates made up of metallic carbides meant for the rotative boring, CR (like a spigot), having the diameter between 35 and 43 mm. Due to the complexity of the geometrical shape of the body, of the small dimensions ($L < 100$ mm), of the technological complexity of its carrying out (moulding or special moulding procedures), similar to splinting tools, to the market request, due to the mining industry recession, all this lead to the impossibility of existing a Romanian producer who could produce such borer heads. In this paper, with the help of the 3D designing softs, there is made a constructive analysis of the borer head body from the technology carrying out point of view, aiming to simplify the geometrical shape of the body in order to reduce the manufacturing price, but without modifying its functional purpose and its resistance.

Key words: borer head, constructive analysis, rotative boring.

1. INTRODUCTION

Rotative boring of mine holes is achieved with detachable heads cocked with plates made up of metallic carbides. Around the worlds there have been made several such tools types both for coal boring or other soft rocks (salt, plaster stone), and for useless rock boring. In Romania the detachable heads cocked with plates made up of metallic carbides are standardized for percussive boring and rotative boring (STAS 7476-90), being made only one detachable type for rotative boring, like a spigot, CR typed, having the nominal diameters of mine holes of 35, 38, 41 and 43 mm.

¹ *PhD, Eng. Lecturer, University of Petroșani, România, cbogdy@netlog.ro*

² *PhD, Eng. Lecturer, University of Petroșani, România*

³ *PhD, Eng. Assoc. Prof., University of Petroșani, România*

Due to the complexity of the geometrical shape of the body, similar to splinting tools and to the small dimensions ($L < 100$ mm), it requires complex achieving

technologies to assure the dimensional precision and the surface quality that are requested. The body of the detachable heads for rotative boring is made of OSC 7 or OSC 8, by moulding or special moulding procedures (in shapes made up of special mixtures, under pressure in metallic shapes etc), in order to have a very good metal usage coefficient.

The market request is relatively small, due to the mining industry recession, all this leading to the impossibility of existing a Romanian producer who could produce such borer heads, they being made up in the mining exploitation workshops under shapes that don't follow the standard type anymore; before 1989 they were made up at I.S. Râșnov.

With the help of the 3D designing softwares, there is made a constructive analysis of the borer head body from the technology carrying out point of view, aiming to simplify the geometrical shape of the body in order to reduce the manufacturing price, but without modifying its functional purpose and its resistance.

2. THE CONSTRUCTIVE ANALYSIS OF BORER HEADS

With the help of Solid Edge software, the geometric model of the detachable head for rotative boring CR 43 type has been made up – it's presented in figure 1.

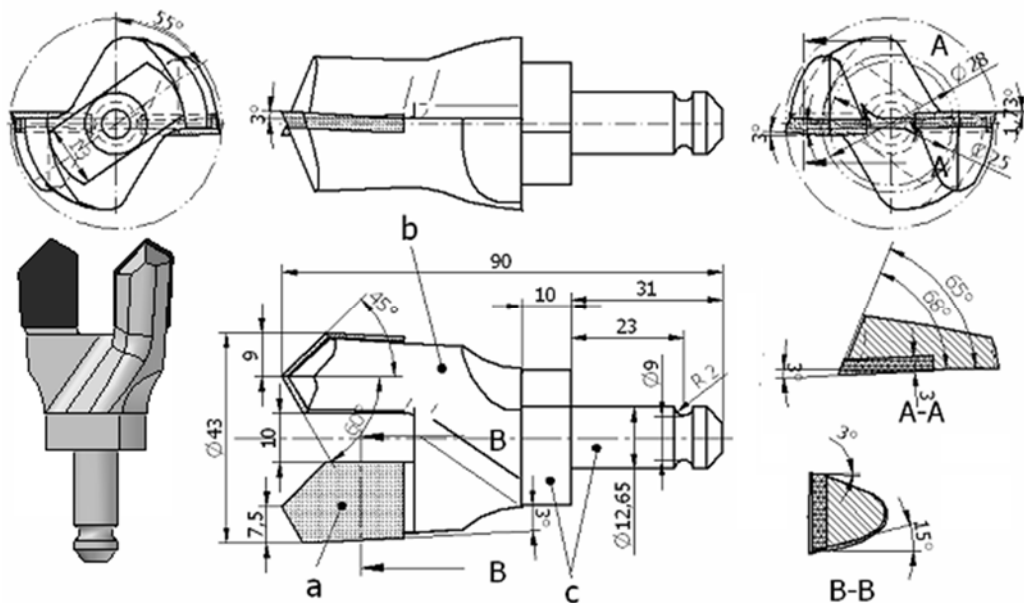


Fig. 1. The geometric model and the constructive solution of the CR 43 type borer head

On grounds of the created geometric model there has been automatically generated its achieving drawing, mentioning the number of the views and the necessary sections to compare the constructive dimensions and angles with those specified in

STAS 7471-90 (fig. 9 and tab. 3) [6]. This one is made up of the active *a* part, the borer head *b* and of the catching and fixing part *c*.

The active part is made up of four edges, two on each plate, with a central unsplintered region having the diameter of 10 mm. The two plates have the same geometrical shapes which simplify the technological achievement of the borer head, but the top of each borer head is found on an outer surface with the diameter of 28 mm, respectively 25 mm.

The 45° and 60° attack angles, respectively the angles that are secondary situated are made up on the plate shape, the main 25° positioning angle is obtained by sharpening the borer head, and the releasing 3° angle by positioning the plate on the borer head body.

The body of the detachable borer head has the aim to allow re-sharpening, hole calibration, guiding the detachable borer head in the hole and evacuating the rock.

The catching and fixing side of the detachable borer head allows fixing the detachable borer head in the borer rod through the cylindrical side Ø12,65 and through a peg of Ø3,2, and the fixing is achieved by the 13 mm key typed joining.

This model is realised by unitary moulding, by the piece by piece moulding of the parts, having a usage coefficient of the small material (below 40%), with a reduced productivity and a great energetical consumption (at least one warming for each part). This type of moulding is used in the small forging worksops belonging to the mining exploitations, simplifying the geometrical shape.

Starting from the standardized borer head, figure 1, and its classical achievement technology, I suggested the simplifying of its geometrical shape in order to have obtained, by means of a multiple moulding, from a 20 mm diameter bar, the consecutive moulding on a horizontal forging machine with four running stations, just like in figure 2.

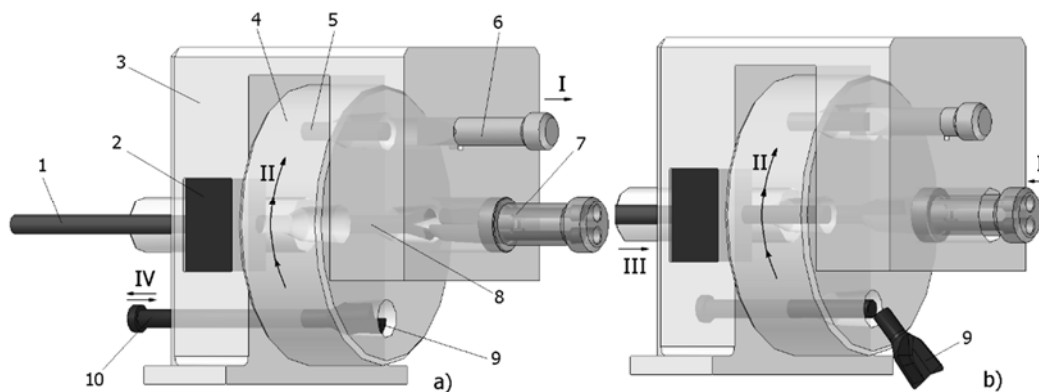


Fig. 2. The multiple moulding of the borer head body

In figure 2 there have been put down: 1 – the rolled bar Ø20mm; 2 – bar warming inducto; 3 – the steel construction installation; 4 – four working areas disk; 5 – the cut off semi-finished; 6 – chisel; 7 – stamp for moulding; 8 – split head semi-finished; 9 – the moulded semi-finished of the borer head body; 10 – extractor; I – the chisel and

stamp pressing and withdrawal movement; *II* – the disk irregular turning movement; *III* – the bar advancing movement; *IV* – the extractor linear – alternative movement.

In figure 2.a movement *II* is realised which leads to cutting off the semi-finished from the warmed bar and to bringing the other semi-finished around the chiesel and stamp working area, and in figure 2.b there is presented the splitting stage of the semi-finished and its moulding by movement *I*. At the same time, following the tracks of movement *I* movements *III* and *IV* are produced; they are the bar advancing movement and the moulded product evacuation movement.

Within the disk there are fixed the alloy steeled mouldings, in each working area, and so are the moulding stamp heads – they are made up of alloy steel having the possibility to be changed in case of worn out. Both the chiesel and the stamp head are cooled the moment the disk withdraws and spins. Both with unitary moulding and multiple moulding, there must be transformed by lathing the fang of the borer head and by cutting the fixing part. For these operations there has been suggested a simple catching device for the moulded semi-finished, that is presented in figure 3, where one finds the notes: *1* – moulded semi-finished; *2* – device; *3* – semi-finished fixing screw; *4* – the lathed surface; *5* – the cut surface.

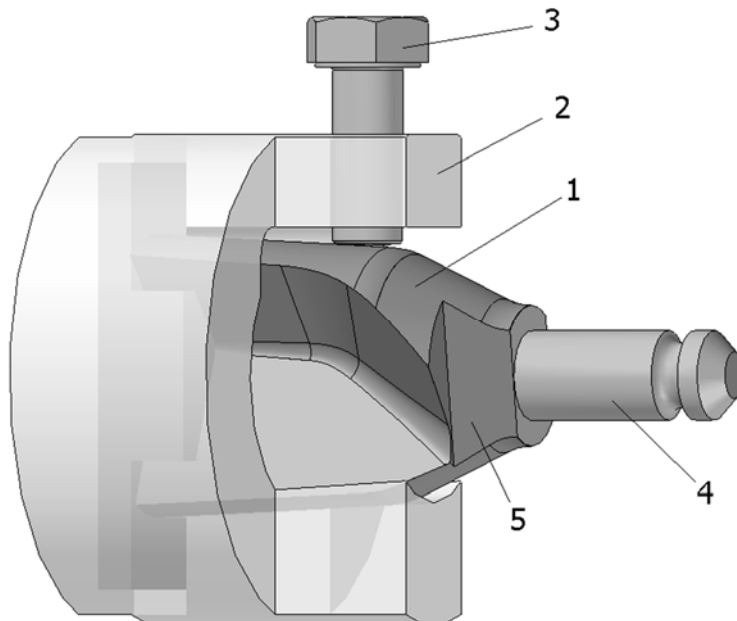


Fig. 3. Catching device for the moulded semi-finished

Blocking the moulded semi-finished spinning in the device is realised through a plate with a geometrical shape standing for the emptiness between the two fangs of the borer head.

Due to the complexity of the borer head body execution and to a small number of re-sharpening (up to 10) it's imposed finding a constructive solution of the borer head with unmounted fangs.

In figure 4 there is presented such a solution, where there have been noted: 1 – the borer head body; 2 – left fang; 3 – right fang; 4 – fangs fixing bolt; 5 – bolt fixing screw.

The handle of the fang is introduced in the cone-shaped bore hole and is positioned in such a way as the handle emission should be concentric to the bolt bore hole. Blocking the fangs both against their spinning and their disassembling is realised by bolt 4, that is assured by screw 5.

Processing the fang handle emission is made through a perforation device, by introducing the fangs handles in the cone-shaped bore holes of the device in the positions corresponding to the cutting geometry of the borer head. As well, there can be delivered fangs without processing the emission, this one is adjusted with the assembling of the fang within the borer head body.

When reaching the acceptable wearing out of the fangs, the bolt is disassembled and with the help of a fishing tap introduced through the lateral holes from the borer head body there is achieved the unblocking of the fang handle made of the cone-shaped bore hole, by hitting it in the head of the fang handle.

Due to the borer head cutting geometry, according to standard, there are necessary two fangs (on the left and on the right). If the same cutting geometry is used for both fangs, the construction and their way of exploitation is simplified.

In order to see the way of behaving of the borer head and of the detachable fang there has been made a finite elements analysis (Cosmos Design Star) of these having an advance force of 10000 N and a torsion moment of 200 Nm.

The results of this analysis are presented in figure 5.a for the borer head where one can notice that the most stressed areas are the metallic plates edges and tops, there where the stress is the greatest and the fang body in the area between the two fangs and the fixing area.

In figure 5.b is presented the analysis for the disassembling fang, where one can notice that the most stressed areas are the cutting edges, and that there is a stress of 294,8 MPa at the fixed joining between the handle and the fang body.

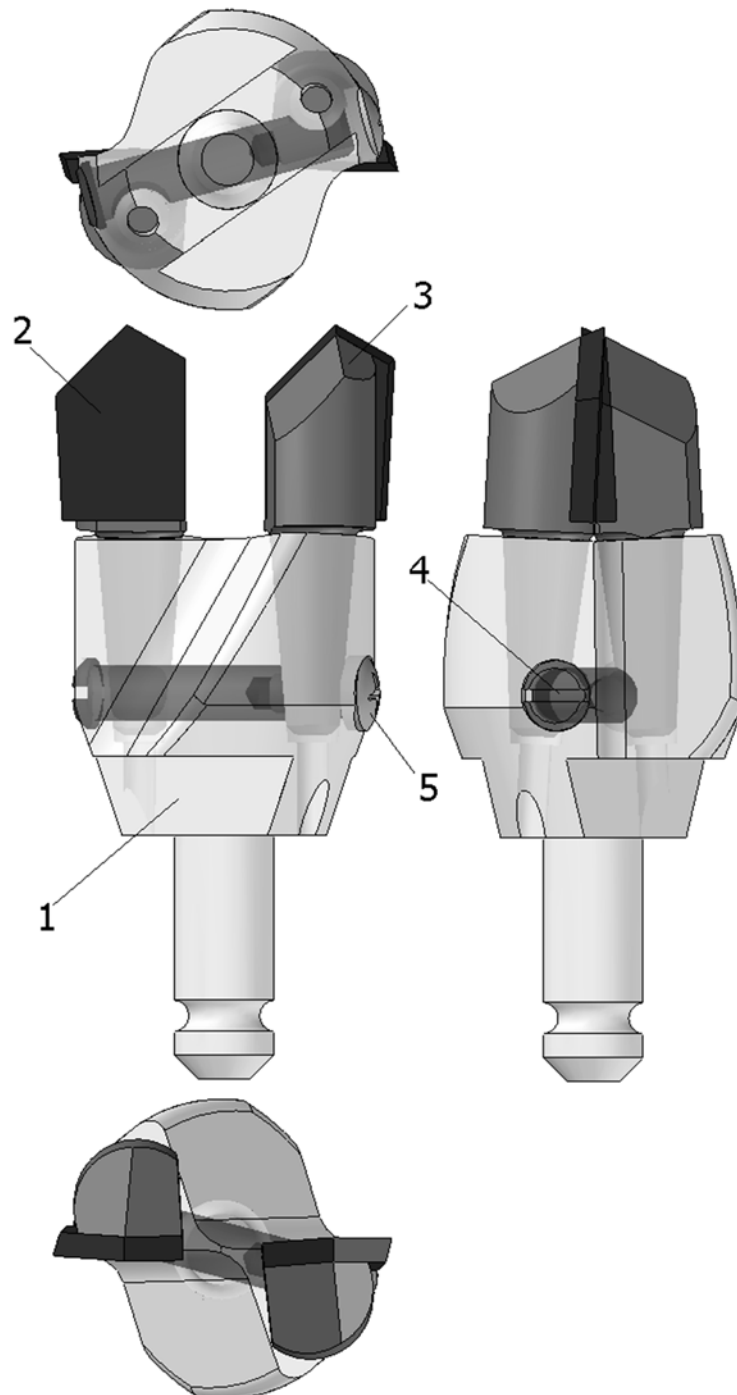


Fig. 4. The detachable fangs borer head

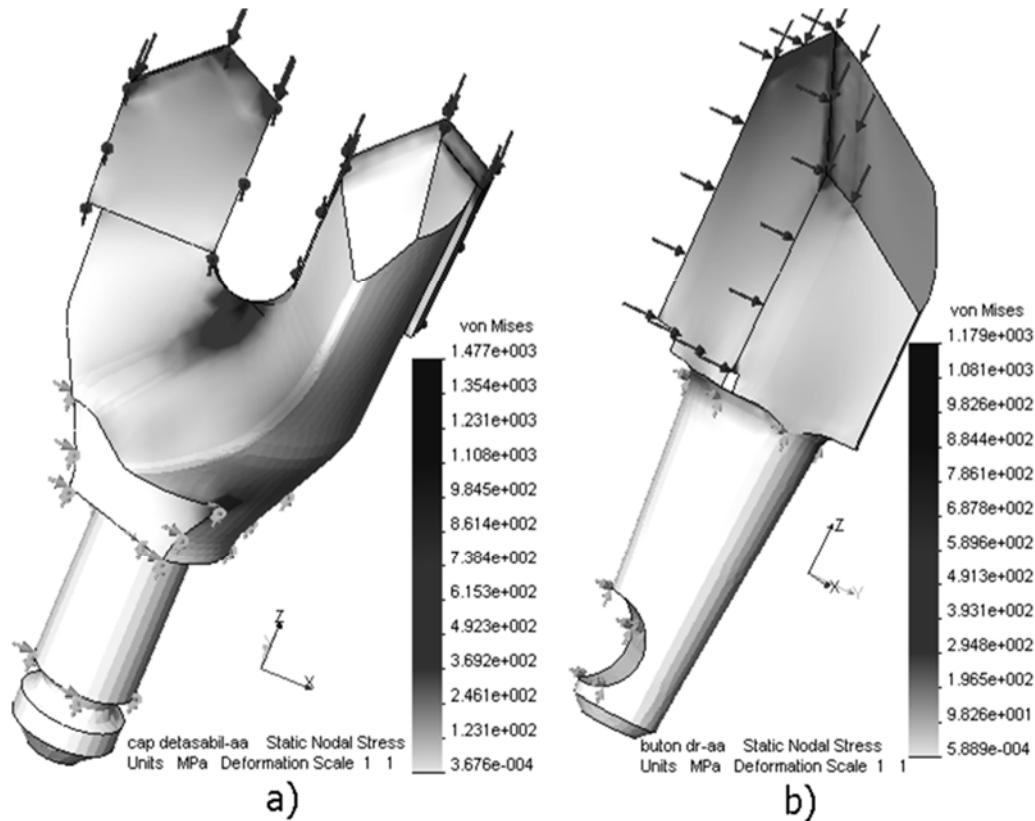


Fig. 5. Checking the borer head and the fang

3. CONCLUSIONS

Due to the usage of the 3D (Solid Edge) modelling software it was possible the achievement of a constructive analysis of the standardized borer head, from the execution technology of the borer head body, and the results were the following:

- simplifying the constructive body shape, by using simple geometrical shapes (cone, cylinder) regarding the elicoidal surface from the inferior part of the standardized borer head body;
- increasing the usage coefficient of the OSC 7 or OSC 8 material (there are no more grinding removals), reducing energy consumption to increase productivity, by using multiple moulding;
- reducing manufacturing and exploitation costs by using the detachable fangs borer head, due to reducing OSC tools carbon steel (only for the fang), using the same borer head body for 10 ... 15 pairs of fangs (according to rock abrasion) and reducing the exploitation cost due to rapid change of worn out fangs.

- pointing out the strongly stressed areas of the borer head and of the fang with the help of the finite elements analysis allows the elimination of tension concentrators and achieving a borer head body shape with very low tensions, respectively using a cheaper steel and a lower cost of the borer head.

REFERENCES

- [1]. **Bolunduț I.L., Dumitrescu I. & Cozma B.** (2002) *The Study Tools of Rotary Perforation a Auger Holes*, Annals of the University of Petroșani (Mechanical Engineering), vol.4 (XXXI), pp.5 ... 20, Petroșani, ISSN 1454-9166.
- [2]. **Cozma B.** (2004) *Improving Construction Tools for the Perforation Auger Holes*, Referat teză de doctorat, Petroșani, (Doctorate Thesis Review).
- [3]. **Cozma B.** (2007) *The study of the Detachable Bits for Rotating Drilling*, International forum of young researches, "Topical Issues of Subsoil Usage", working group 5, St. Petersburg, Rusia.
- [4]. * * * - Solid Edge Software v.19, Academic license ADA Computers București.
- [5]. * * * - Cosmos Design Star Software v.4, License S.C. INICAD DESIGN S.R.L: București.
- [6]. * * * - STAS 7476-90 Detachable head armed with plates of metal carbides for perforation percussive and rotary perforation.

RELIABILITY STUDY OF EsRc-1400 BUCKET WHEEL EXCAVATOR TRAVEL SYSTEM. A NEW APPROACH

ION GÎLMA¹

ABSTRACT: The paper presents the results obtained in determining the reliability of EsRc-1400 bucket wheel excavator travel system. The main reliability indicators are determined that quantify the operating ability of the travel system and, implicitly, of the excavator. A special attention is given to the interpretation of the reliability indicators that are at the basis of establishing the quality level of the excavator.

Key Words: bucket wheel excavator, travel system, reliability, failure rate, probability, law of distribution, mathematical statistics.

1. GENERAL CONSIDERATIONS

The EsRc-1400 type bucket wheel excavator is mostly used in Oltenia open pit mines. An important subassembly of the excavator is the travel system, which ensures its mobility in the work face. The studies performed on the excavators show that the travel system is a significant source of failures, decisively influencing its operating capacity.

In general, a reliability study performed on a product involves seven stages.

Stage 1. Establishing a data basis on the functioning capacity of the product

Stage 2. Determination of the empirical repartition functions

Stage 3. Estimation of the theoretical distribution functions

Stage 4. Calculation of the punctual values of the theoretical distribution functions

Stage 5. Testing concordance between empirical and theoretical distributions

Stage 6. Calculation and graphical representation of reliability indicators by validated distribution

Stage 7. Interpretation of results and decision making.

¹ *Eng. Ph. D. Student, at University of Petroșani*

2. QUANTIFICATION OF RELIABILITY INDICATORS

The synthesis of the seven stages to be followed for the determination of the reliability indicators are further presented for EsRc-1400 bucket wheel excavator travel system.

In order to establish the failure moments of the travel mechanisms, two data bases have been used:

- files regarding the situation of failures, by which the day and hour of the occurrence of the failure is pointed out, as well as the time required for the failure to be remedied and for the product to be functioning again;

- files regarding the effective operating times, per days, of each excavator, which takes into account only the duration of the effective work of the excavator in coal or sterile, and which take into account the nature of all causes leading to the down-time of the excavators.

The analysis and interpretation of the two data bases for the 76 recorded failures, resulted in the series of $n = 76$ values, in increasing order, representing the number of *hours* of effecting operating of the travel mechanisms until failure occurred, for the eight excavators, for a year of operation: 10; 12; 13; 14; 15; 15; 16; 17; 17; 17; 18; 18; 25; 26; 28; 28; 29; 32; 33; 33; 35; 42; 43; 45; 50; 51; 54; 61; 64; 66; 69; 73; 80; 92; 98; 100; 101; 105; 109; 113; 133; 137; 140; 146; 151; 152; 156; 157; 162; 163; 170; 186; 194; 202; 229; 320; 339; 341; 354; 370; 386; 406; 411; 540; 540; 582; 612; 622; 638; 698; 749; 773; 801; 836; 904; 1044.

Table 1 shows the values of the empirical repartition function, $\hat{F}(t_i)$, calculated with formula

$$\hat{F}(t_i) = \frac{i - 0,3}{n + 0,4} , \quad (1)$$

where i is the order number of operating times, and n the number of total times noticed.

Table 1. Empirical (experimental) repartition function values $\hat{F}(t_i)$

1	0.009162	14	0.179319	27	0.349476	40	0.519634	53	0.689791	66	0.859948
2	0.022251	15	0.192408	28	0.362565	41	0.532723	54	0.702880	67	0.873037
3	0.035340	16	0.205497	29	0.375654	42	0.545812	55	0.715969	68	0.886126
4	0.048429	17	0.218586	30	0.388743	43	0.558901	56	0.729058	69	0.899215
5	0.061518	18	0.231675	31	0.401832	44	0.571990	57	0.742147	70	0.912304
6	0.074607	19	0.244764	32	0.414921	45	0.585079	58	0.755236	71	0.925393
7	0.087696	20	0.257853	33	0.428010	46	0.598168	59	0.768325	72	0.938482
8	0.100785	21	0.270942	34	0.441099	47	0.611257	60	0.781414	73	0.951571
9	0.113874	22	0.284031	35	0.454188	48	0.624346	61	0.794503	74	0.964660
10	0.126963	23	0.297120	36	0.467277	49	0.637435	62	0.807592	75	0.977749
11	0.140052	24	0.310209	37	0.480366	50	0.650524	63	0.820681	76	0.990838
12	0.153141	25	0.323298	38	0.493455	51	0.663613	64	0.833770		
13	0.166230	26	0.336387	39	0.506545	52	0.676702	65	0.846859		

In the study of the system reliability, exponential negative, normal and bi and tri-parameter Weibull distribution laws are taken into consideration.

The negative exponential distribution law, having the symbol ep , is characterized by λ parameter, representing the failure intensity or rate in *failure/hour*. Parameter λ is estimated by the Least Squares Method.

The normal distribution law (Gauss-Laplace), having the symbol nv , is defined by parameters m_n , mean operating time, in *hours*, and σ_n , the mean square deviation or standard deviation, in *hours*. The parameters are estimated by the Maximum Likelihood Method.

The normalized bi-parametric Weibull distribution law, symbolized by Wbp , is defined by dimensionless form parameter β_1 and by the real scale parameter η_1 , measured in *hours*. Parameters are estimated by the Least Squares Method.

The tri-parametric Weibull distribution, symbolized by Wtm , is built by β_2 dimensionless form parameter, η_2 scale parameter in *hours*, and γ , initialization parameter in *hours*. The parameters are estimated by the Method of Moments.

The normalized bi-parametric Weibull distribution, symbolized by Wbv , is defined by the dimensionless form parameter β_3 and η_3 scale parameter, in *hours*, calculated by the Maximum Likelihood Method.

Table 2 synthetically shows the distribution law parameter values taken into consideration for the characterization of the travel mechanism's functionality of the bucket wheel excavator.

Table 2. The estimated values of the theoretical distribution law parameters characterizing the excavator's travel mechanism reliability

No	Distribution	$\lambda, 1/h$	m_n, h	σ_n, h	β_1	η_1, h	β_2	η_2, h	γ, h	β_3	η_3, h
1	Exponential negative, ep	$39.93 \cdot 10^{-4}$									
2	Normal (Gauss-Laplace), nv		218.566	257.641							
3	Weibull biparametric normalized, Wbp				0.899	194.527					
4	Weibull triparametric, Wtm						0.852	201.169	$1.616 \cdot 10^{-6}$		
5	Weibull biparametric normalized, Wbv									0.842	198.405

Table 3 shows:

- $R(t)$, analytical expressions of reliability functions for theoretical distributions considered in the study, whose parameters have been estimated by the previously presented analytical methods;

- D_{max} , values of maximum deviations between theoretical and empirical distribution, more specifically between theoretical and empirical (experimental) probability distributions;

- $D_{\alpha,n}$, critical values of Kolmogorov-Smirnov test, (K-S), with α risk margin,

respectively P truthfulness probability, ($\alpha + P = 1$);
 - theoretical distribution validation result.

Table 3. Comparative analysis of theoretical distributions characterizing the excavator travel system functionality

Distribution	Reliability function, R(t)	Maximum deviations, D_{max}	Risk, α (%)	Critical value, $D_{\alpha,76}$	Validation
Exponential negative, ep	$e^{-0.003993 \cdot t}$ (2)	0.172134	0.01	0.184075	Yes
Normal (Gauss-Laplace), nv	$\frac{1}{2} - \Phi\left(\frac{t - 218.566}{257.641}\right)$ (3) or $1 - \frac{1}{257.641} \frac{1}{\sqrt{2\pi}} \int_0^t e^{-\frac{1}{2}\left(\frac{x-218.566}{257.641}\right)^2} dx$ (4)	0.238371	0.005	0.195783	Not
Weibull biparametric normalized, Wbp	$e^{-\left(\frac{t}{194.527}\right)^{0.899}}$ (5)	0.084510	0.20	0.120880	Yes
Weibull triparametric, Wtm	$e^{-\left(\frac{t-1.616 \cdot 10^{-6}}{201.169}\right)^{0.852}}$ (6)	0.084075	0.20	0.120880	Yes
Weibull biparametric normalized, Wbv	$e^{-\left(\frac{t}{198.405}\right)^{0.842}}$ (7)	0.151329	0.05	0.152435	Yes

Table 3 shows that exponential and bi- and tri-parameter Weibull distributions are validated, normal distribution not being validated.

For normal distribution, maximum distance between empirical (experimental) and theoretical function is higher than the critical value of the test. The test is considered for 76 values characterizing the moment of failure occurrence, for the bucket wheel excavator travel system.

Normalized bi-parametric Weibull distribution is validated, where the parameters are calculated by the Least Squares Method, that is by the Maximum Likelihood Method. Similarly, tri-parametric Weibull distribution is validated, where the parameters are obtained by the Method of Moments.

These distribution laws approximate the experimental function the best, since the distances between the theoretical and experimental functions are the smallest. Function validation is achieved even for a large value of risk of 20%.

The exponential model is also validated, but the maximum distance between the theoretical distribution and the experimental one is close to the critical value of the Kolmogorov-Smirnov test. This suggests that the value of reliability indicators

determined with this distribution will differ from the values calculated for the other distributions. The validation of the exponential model has been anticipated, since the β form coefficients of Weibull distributions have values sufficiently close to 1. The values are $\beta_1 = 0.899$, $\beta_2 = 0.852$ and $\beta_3 = 0.842$. It is known that for the coefficient $\beta = 1$, the two distributions, exponential and Weibull, are expressed by the same relations.

In Figures 1, 2, 3 and 4 the variations of the principal reliability indicators are presented, depending on the time of operation until the failure.

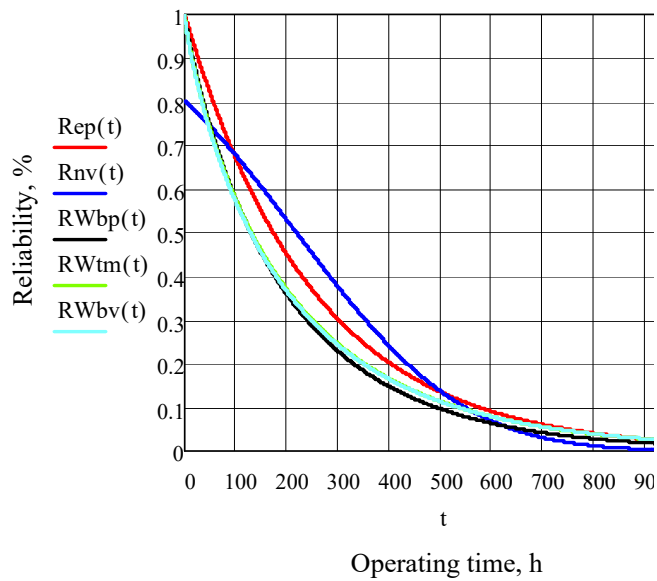


Fig. 1. Variation of travel system reliability function

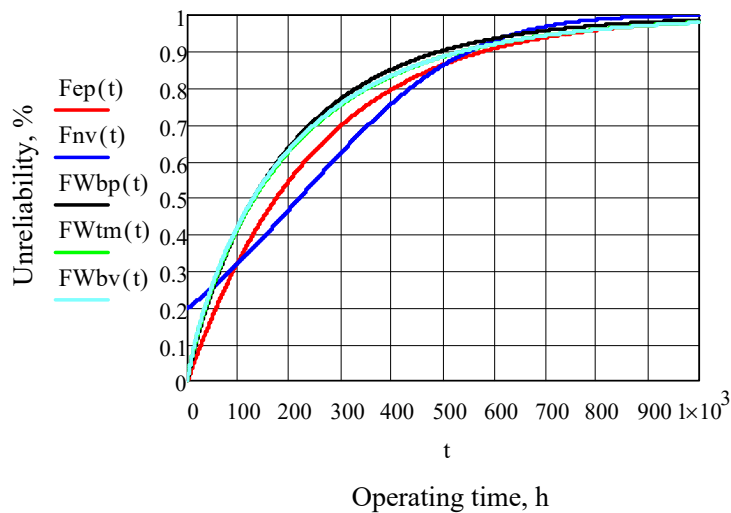


Fig. 2. Unreliability function of the travel system

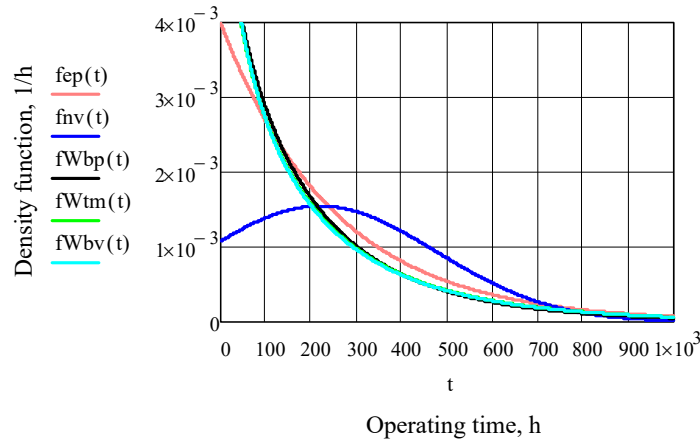


Fig. 3. Density function of time until failure

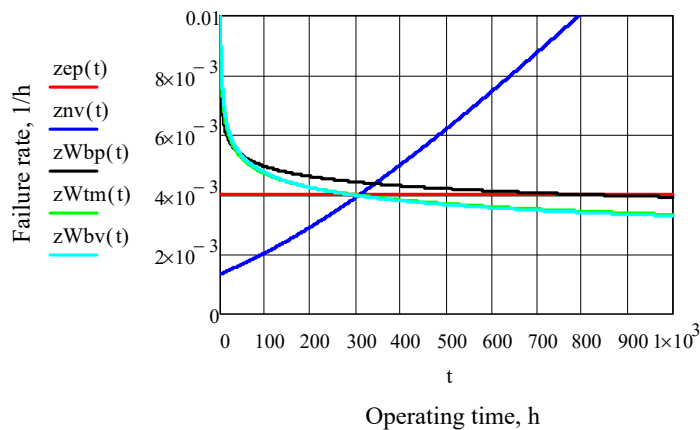


Fig. 4. Function of the failure rate

3. INTERPRETATION OF RESULTS

Table 4 presents the values for a series of indicators characterizing the travel mechanism reliability.

1. The reliability of the excavator's travel system is low, the probability of it not failing after 200 hours of operating being only 40%. The 40% trust level indicates that the travel system of the excavator is expected to fail after 13 days. The 60% risk margin is considered very high. It is necessary to point out that the excavator practically works for 15 hours a day.

2. If an 80% reliability is required, which is a reasonable value, an operating time without failure of $t_{80} = 40$ hours results. This means that after approximately 2.5 days of effective operating it is necessary to intervene to repair the excavator's travel system.

Table 4. Reliability indicators regarding operating time until failure for the travel system of the excavator

No	Parameter			Parameter value for distribution:				
	Name	Symbol	UM	Exponential negative, ep	Normal, nv	Weibull bi-parametric normalized, Wbp	Weibull tri-parametric, Wtm	Weibull bi-parametric normalized, Wbv
1	Mean	m	h	250	218	204	218	217
2	Median	t_{med}	h	173	218	129	130	128
3	Variance	D	h^2	62724	66379	52046	66379	67222
4	Standard deviation	σ	h	250	258	228	257	259
5	Coefficient of variation	CV	-	1	1.179	1.114	1.179	1.194

3. The great slope of the curve of reliability function shows its rapid degradation in time, this meaning that the failure speed of the travel system is high. This results from the graph of the density probability function of the failure time, which also rapidly decreases in time.

4. The analysis of the variation in time of the failure rate shows its stabilization tendency around the value of $4 \cdot 10^{-3}$ failures/hours. This value is high, compared to those of the order of 10^{-6} that are indicated in literature for mechanical elements. The form of relative constancy of the failing intensity shows the existence in the component of the travel system of several elements prone to degradation. Degradation manifests by wear, fatigue, corrosion or abrasion, or even moral wear, considering the travel system represents an obsolete technical solution. The great number of elements prone to continuous degradation leads to the failure of others, and even if some of those are replaced, they lead to occurrence of defects. It results that the solution adopted to keep in function the excavator's travel system is one of compromise.

5. The intensely asymmetric form of the probability density curves shows that the median time until defects occur, better characterizes the functionality of the excavator's travel mechanism. The median value of 129 hours of good operating, for validated Weibull distributions, is more realist than the value of over 200 hours indicated by the average. This is also confirmed by the reliability of only 40% of the system for only 200 hours of effective operating.

6. Standardized bi-parameter Weibull distribution with parameters calculated by the Least Squares Method, allows the calculation of the most adequate reliability indicators. The explanation is based on the demonstrated fact that, if one should opt between two validated distributions, the one for which variance has the lowest value should be chosen. This indicator is a measure of centring values towards the mean value (median), which is considered to be the closest value to the real one.

7. To increase the safety in operation of the travel mechanism, its overall design should be reconsidered, in the sense of redesigning the overall solution. Deficient composing elements should be redesigned, execution technology of the composing

elements should be improved, its maintenance and repair technology should be reconsidered.

4. CONCLUSIONS

The reliability analysis performed regarding the EsRc-1400 bucket wheel excavator system leads to the following main conclusions:

1. The scientific approach of determination of reliability indicators is correct. This is confirmed by the validated Weibull distributions, which are characterized by variable failure rates in time, specific to mechanical elements. Similarly, the specifications found in the literature are confirmed, specifications indicating that these distributions describe the best the mechanical degradation phenomena (wear, corrosion, fatigue, abrasion). Moral wear may also be included in the same category. All these phenomena are characteristic to the bucket wheel excavator's travel mechanism in general.

2. The excavator's travel mechanism reliability is very low, only 40% for the 200 hours of effective operation.

3. To increase the operational safety of the travel mechanism, the overall construction thereof should be reconsidered. Imperfect composing elements should be redesigned, execution technology of the composing elements should be improved, and maintenance and repair technology should be reconsidered.

REFERENCES

- [1]. **Dhillon, B.S.**, *Design reliability. Fundamentals and applications*, CRC Press LLC, 1999.
- [2]. **Gilma, I.**, *Studiu privind îmbunătățirea siguranței în funcționare a unor utilaje din industria minieră*, Raport de cercetare științifică nr. 1, Universitatea din Petroșani, Petroșani.
- [3]. **Jula, D., Praporgescu, G., Mihăilescu, S., Tomuș, O.B., Deaconu, I.**, *Aspecte privind determinarea fiabilității utilajelor din carierele de lignit*, Lucrările științifice ale simpozionului internațional multidisciplinar "Universitaria SIMPRO", Volumul: Mașini și echipamente tehnologice, Editura UNIVERSITAS, Petroșani, 2006.
- [4]. **Jula, D., Dumitrescu, I.**, *Fiabilitatea sistemelor de transport*, Editura Focus, Petroșani, 2009.
- [5]. **Jula, D., Dinescu, S., Tomuș, O.B.**, *Reliability Analysis of EsRc 1400 Bucket Wheel Excavators Operating in Oltenia Lignite Open Pit Mines*, MicroCAD2015, International Scientific Conference, University of Miskolc, Hungary, 2015.
- [6]. **Roșu (Gîrjob), E.**, *Studiul corelației dintre calitate, fiabilitate și mentenabilitate la echipamentele miniere*, Teză de doctorat, Universitatea din Petroșani, Petroșani, 2012.
- [7]. **Smith, J. D.**, *Reliability, Maintainability and Risk. Practical methods for engineers*, Sixth Edition, Butterworth-Heinemann Ltd, New York, 2001.
- [8]. * * *, *Excavatorul cu roată portcupe ERC 1400-30/7 modernizat. Instrucțiuni de exploatare, întreținere și reparare*, Rominex SA Timișoara, 2009.
- [9]. * * *, *Fișe de urmărire a funcționării mașinilor și instalațiilor la EMC Jilț*.

ASPECTS REGARDING MAINTAINABILITY ANALYSIS OF EsRc-1400 BUCKET WHEEL EXCAVATOR

ION GÎLMA¹, CRISTIAN ILIONI²

ABSTRACT: The paper presents the results obtained in the analysis of maintainability of the EsRC-1400 bucket wheel excavator travel system. The main maintainability indicators are determined that quantify maintenance actions and define the adopted maintenance strategy. The defining elements result from the interpretation of maintainability indicators on which the excavator quality level determination is based.

Keywords: bucket wheel excavator, travel system, maintainability, maintenance, probability, mathematical statistics, repair rate, law of distribution, repair time.

1. GENERAL CONSIDERATIONS

The studies performed on the EsRc-1400 excavator showed that the travel system is a principal source of failure. These defects require corrective intervention to reinstate the state of functioning of the excavator, decisively influencing its operating capacity. Generally, a maintainability study carried out on a product involves seven stages.

Stage 1. Establishing a data base regarding the repair periods or restarting time for the product

Stage 2. Determination of the empirical probability distribution

Stage 3. Estimation of parameters of theoretical probability distribution characterizing the repair process of the product

Stage 4. Calculation of punctual values of theoretical distribution functions

Stage 5. Testing concordance of empirical and theoretical distributions

Stage 6. Calculation and graphic representation of maintainability indicators for validated distributions

Stage 7. Interpretation of results and decision making

¹ *Eng. Ph. D. Student, at University of Petroșani*

² *Assistant, Ph. D. Eng., at University of Petroșani*

2. DETERMINATION OF MAINTAINABILITY INDICATORS

To establish corrective repair times for the travel system, two data bases have been used:

- files regarding situation of defects, showing the day and hour of failure occurrence, as well as the time required to remedy the defect and the travel system restarts its functioning;

- files showing the effective operating period, per days, of each excavator, considering only the time in which the excavator was effectively functioning in coal or rock, and taking into consideration the nature of all causes leading to the non-functioning of the excavators.

From the data regarding the operation of the excavators, t_{ri} values result, representing the effective duration of repair of the travel mechanism, represented by the statistic series made up of $n=71$ values, in *hours*, until the effect is remedied: 0.25; 0.33; 0.5; 0.5; 0.5; 0.5; 0.53; 0.66; 0.66; 0.66; 0.66; 0.83; 1; 1; 1; 1.08; 1.08; 1.08; 1.08; 1.16; 1.16; 1.16; 1.25; 1.25; 1.3; 1.33; 1.33; 1.33; 1.42; 1.42; 1.5; 1.5; 1.5; 1.5; 1.5; 1.5; 1.53; 1.53; 1.53; 1.6; 1.7; 1.92; 2; 2; 2.16; 2.33; 2.42; 2.42; 2.66; 2.83; 3.16; 3.5; 3.75; 4; 4.16; 4.16; 4.16; 4.5; 5; 5.83; 5.83; 6; 6.92; 7.16; 8.25; 8.75; 9.16; 13; 17.5; 21.5.

The statistic series presented is (S2) type, since there are sufficient repetitive values.

The empirical or theoretical probability distribution of repair times represents the function of maintainability, respectively, the probability that the travel mechanism would be repaired in a certain period of time and conditions given.

Table 1 presents the values of the empirical (experimental) probability distribution for repair times, t_{ri} , respectively, empirical (experimental) maintainability function, $\hat{M}(t_{ri})$, whit the cumulative relative frequency it is.

Table 1. Values of empirical (experimental) maintainability function

i	Repair time t_{ri} , <i>hour</i>	Absolute frequency, n_i	Relative frequency, f_i	Empirical probability distribution, $\hat{M}(t_r)$
1	0.25	1	0.014085	0.014085
2	0.33	1	0.014085	0.028169
3	0.50	4	0.056338	0.084507
4	0.53	1	0.014085	0.098592
5	0.66	4	0.056338	0.154930
6	0.83	1	0.014085	0.169014
7	1.00	3	0.042254	0.211268
8	1.08	4	0.056338	0.267606
9	1.16	3	0.042254	0.309859
10	1.25	2	0.028169	0.338028
11	1.30	1	0.014085	0.352113
12	1.33	3	0.042254	0.394366

i	Repair time t_{ri} , hour	Absolute frequency, n_i	Relative frequency, f_i	Empirical probability distribution, $\hat{M}(t_r)$
13	1.42	2	0.028169	0.422535
14	1.50	6	0.084507	0.507042
15	1.53	4	0.056338	0.563380
16	1.60	1	0.014085	0.577465
17	1.70	1	0.014085	0.591549
18	1.92	1	0.014085	0.605634
19	2.00	2	0.028169	0.633803
20	2.16	1	0.014085	0.647887
21	2.33	1	0.014085	0.661972
22	2.42	2	0.028169	0.690141
23	2.66	1	0.014085	0.704225
24	2.83	1	0.014085	0.718310
25	3.16	1	0.014085	0.732394
26	3.50	1	0.014085	0.746479
27	3.75	1	0.014085	0.760563
28	4.00	1	0.014085	0.774648
29	4.16	3	0.042254	0.816901
30	4.50	1	0.014085	0.830986
31	5.00	1	0.014085	0.845070
32	5.83	2	0.028169	0.873239
33	6.00	1	0.014085	0.887324
34	6.92	1	0.014085	0.901408
37	7.16	1	0.014085	0.915493
36	8.25	1	0.014085	0.929577
37	8.75	1	0.014085	0.943662
38	9.16	1	0.014085	0.957746
39	13.00	1	0.014085	0.971831
40	17.50	1	0.014085	0.985915
41	21.50	1	0.014085	1.000000
		$\sum n_i = n = 71$	$\sum f_i = 1$	

In the system's maintainability study exponential negative, normal, lognormal and bi and triparametric Weibull distribution laws are considered.

Negative exponential distribution law, having ep as symbol, is characterized by parameter μ , representing the rate of repair or restarting functioning in *repairs/hour*. Parameter μ is estimated by the Least Squares Method.

Normal distribution law (Gauss-Laplace), symbol nv, is defined by parameters m_m , mean repair time, in *hours*, and σ_m , the mean square deviation or standard deviation, in *hours*. Parameters are estimated by the Maximum Likelihood Method.

Lognormal distribution law, symbol lgv, is defined by the parameter m_{rlg} , mean repair time, in *hours*, and mean square deviation, σ_{rlg} .

Normalized biparametric Weibull distribution law, symbol Wbp, is defined by the dimensionless form parameter β_{1r} and real scale parameter η_{1r} , measured in *hours*. Parameters are estimated by the Least Squares Method.

Triparametric Weibull distribution, symbol Wtm, is built by β_{2r} dimensionless form parameter, η_{2r} scale parameter, in *hours*, and γ initialization parameter, in *hours*. Parameters are estimated by the Method of Moments.

Normalized biparametric Weibull distribution, symbol Wbv, is defined by dimensionless form parameter β_{3r} and scale parameter η_{3r} , in *hours*, calculated by the Maximum Likelihood Method.

Table 2 shows the synthesis of distribution parameters values of laws taken into consideration to characterize the maintainability of the travel mechanism of the bucket wheel excavator.

Table 2. Estimated values of theoretical distribution laws parameters characterizing maintainability of excavator travel system

No	Distribution	μ, h^{-1}	m_{rn}, h	σ_{rn}, h	m_{rlg}, h	t_{rmed}, h	σ_{rlg}, h	β_{1r}	η_{1r}, h	β_{2r}	η_{2r}, h	γ_r, h	β_{3r}	η_{3r}, h
1	Exponential negative, ep	0.720												
2	Normal (Gauss-Laplace), nv		5.251	4.571										
3	Lognormal, lgv				0.895	2.448	1.039							
4	Weibull biparametric normalized, Wbp							1.276	2.795					
5	Weibull triparametric, Wtm									0.879	3.204	$-1.5 \cdot 10^{-9}$		
6	Weibull biparametric normalized, Wbv												1.015	3.029

Table 3 shows:

- $M(t_r)$, analytical expressions of maintainability functions for theoretical distributions considered in the study, whose parameters are estimated by the analytical methods presented previously;
- D_{max} , maximum deviation values between theoretical and empirical distribution, more specifically between theoretical and empirical maintainability functions;

- $D_{\alpha,n}$, critical values of Kolmogorov-Smirnov test, (K-S), with α risk margin, respectively, P truthfulness probability, ($\alpha + P = 1$);
- result of theoretical distribution validation.

Table 3. Comparative analysis of theoretical distributions characterizing excavator travel system maintainability

Distribution	Maintainability function, $M(t_r)$	Maximum deviations, D_{max}	Risk, α (%)	Critical value, $D_{\alpha,76}$	Validation
Exponential negative, ep	$1 - e^{-0.720 \cdot t_r}$ (1)	0.344219	0.5	0.264824	NOT
Normal (Gauss-Laplace), nv	$\frac{1}{2} + \Phi\left(\frac{5.251 - t_r}{4.570}\right)$ (2) or $\frac{1}{4.571} \frac{1}{\sqrt{2\pi}} \int_0^{t_r} e^{-\frac{1}{2}\left(\frac{x-5.251}{4.571}\right)^2} dx$ (3)	0.422341	0.5	0.264824	NOT
Lognormal, lgv	$\frac{1}{2} + \Phi\left(\frac{1}{1.039} \cdot \ln \frac{t_r}{2.448}\right)$ (4) or $\frac{1}{1.039} \frac{1}{\sqrt{2\pi}} \int_0^{t_r} \frac{1}{x} e^{-\frac{1}{2}\left(\frac{\ln x - 0.895}{1.039}\right)^2} dx$ (5)	0.237858	1	0.249036	YES
Weibull biparametric normalized, Wbp	$1 - e^{-\left(\frac{t_r}{2.795}\right)^{1.276}}$ (6)	0.192382	5	0.207599	YES
Weibull triparametric, Wtm	$1 - e^{-\left(\frac{t_r + 1.5 \cdot 10^{-9}}{3.204}\right)^{0.879}}$ (7)	0.158384	20	0.163492	YES
Weibull biparametric normalized, Wbv	$1 - e^{-\left(\frac{t_r}{2.795}\right)^{1.76}}$ (8)	0.170061	10	0.186865	YES

From table 3 it is seen that exponential and normal distributions are not validated, even for a very low risk level. On the other hand, the three Weibull distributions, as well as lognormal distribution are validated.

Among Weibull distributions, triparametric Weibull distribution, where parameters are calculated by the method of moments, approximate the best the theoretical function. This is demonstrated by the maximum distance between the two functions, experimental and theoretical, whichever is the smallest.

It is noticed the closeness to the non-validation limit of biparametric Weibull distribution with the calculated parameters by the Least Squares Method. For this case, the validation risk is of only 5%.

Lognormal distribution is also validated, frequently indicated by the literature, in order to characterize the process of reparation of products of mechanical nature. Distribution is recommended when reparation times are known.

Figures 1, 2, and 3 show the variations of the principal indicators of maintainability, function of the corrective repair time.

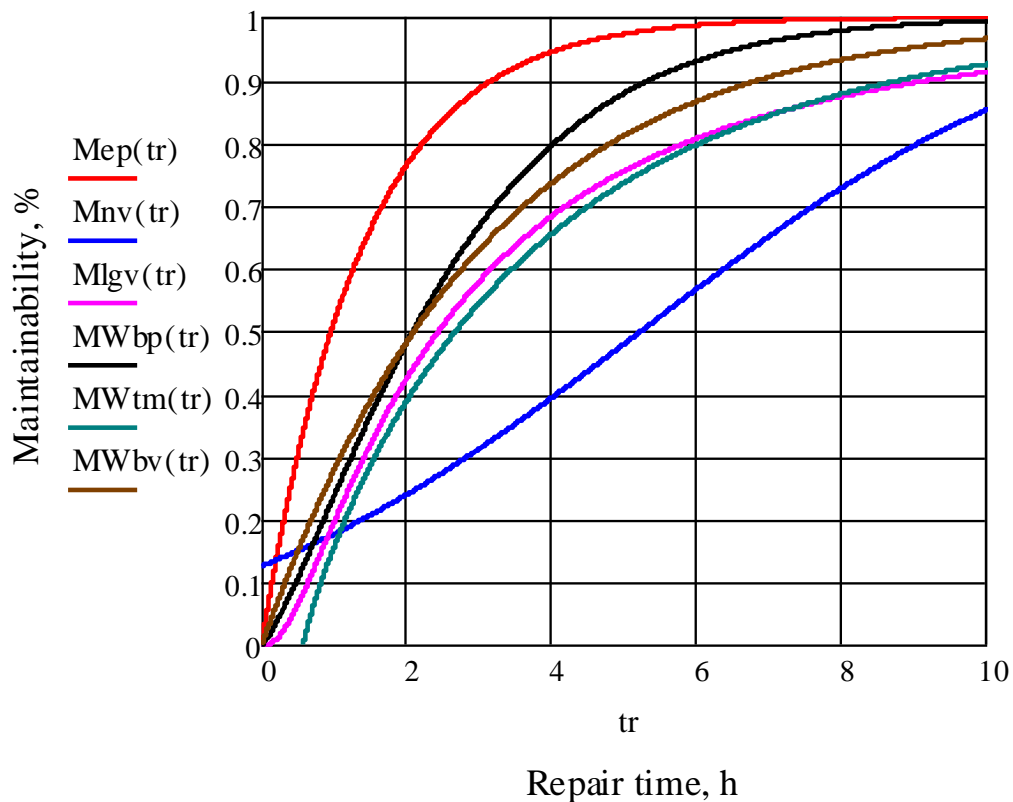


Fig. 1. Variation of the maintainability functions depending on the repair time

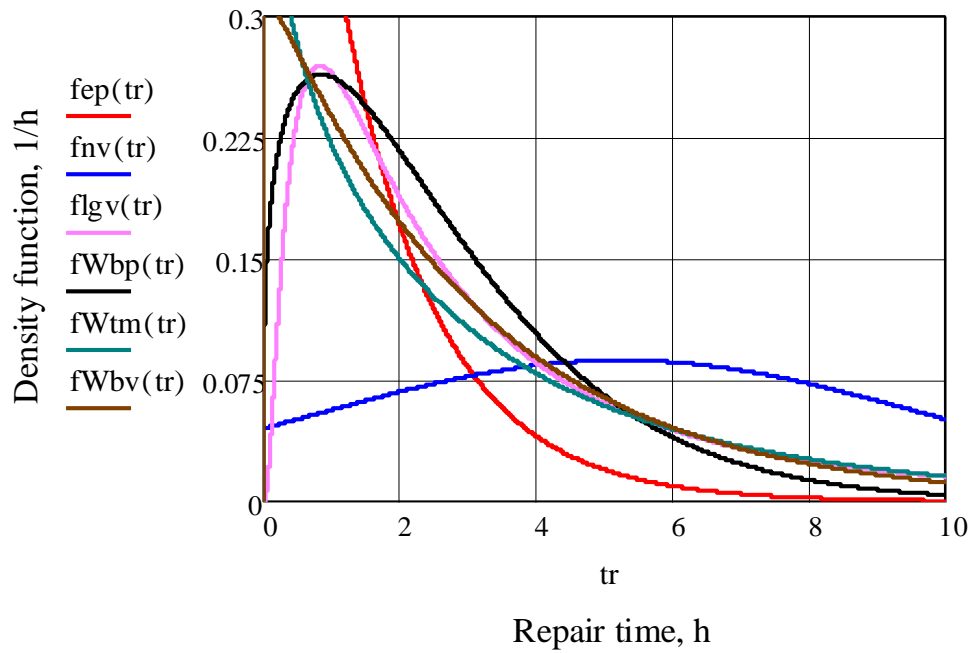


Fig. 2. Density function of repair time

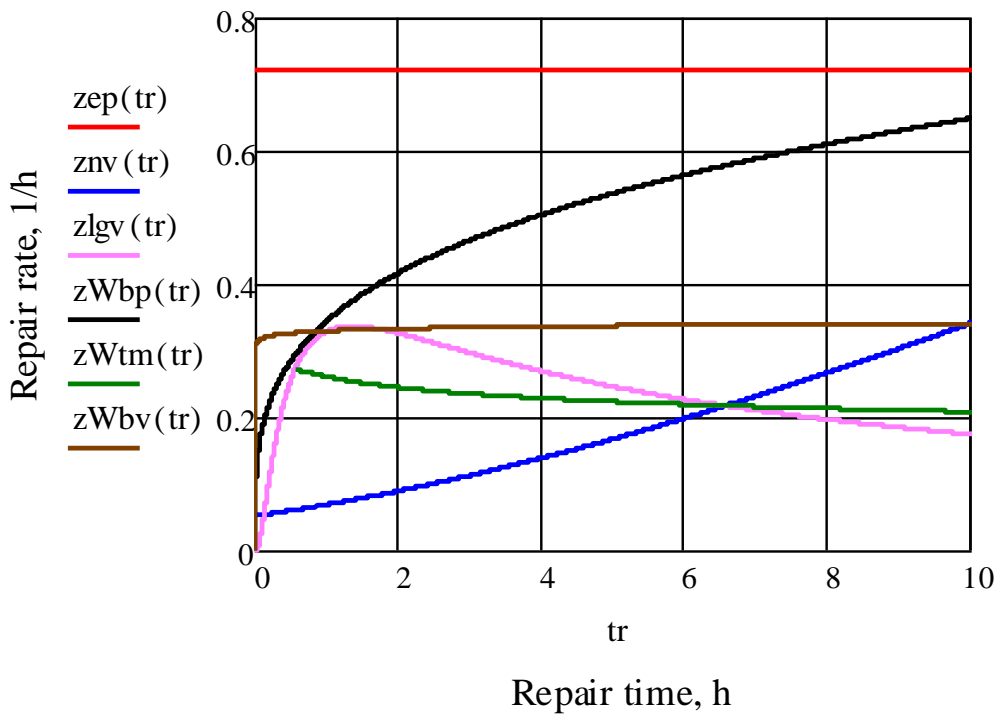


Fig. 3. Variation of the repair rate functions

Table 4 shows the values for a series of indicators characterizing the maintainability of the travel system.

Table 4. Indicators of maintainability regarding the repair time of the travel system

Parameter		Parameter value for distribution:						
Name, Symbol	UM	Exponential negative, ep	Normal, nv	Lognormal, lgv	Weibull biparametric normalized, Wbp	Weibull triparametric, Wtm	Weibull biparametric normalized, Wbv	
Mean, MTR	h	1,389	5,536	4,203	2,591	3,416	3,011	
Median, $TMMC$	h	0,963	5,251	2,448	2,097	2,981	2,111	
Maximum time	$T_{max}90\%$	h	3,198	11,386	9,361	5,374	8,274	6,891
	$T_{max}95\%$	h	4,161	13,077	13,469	6,606	11,161	8,932
Variance, D_r	h^2	1,929	12,858	34,392	4,188	15,182	8,806	
Standard deviation, σ_r	h	1,389	3,586	5,864	2,046	3,896	2,968	

3. INTERPRETATION OF RESULTS

1. The probability for the travel system to be repaired in two *hours* is 40%. This value is considered to be small, towards acceptable, the justification being that only unpairing the tracks require a longer remedy time, the times to remedy the other defects being smaller by far. This is also shown by the average value of the reparation time, which is around three *hours*.

2. When a 80% maintainability is required, frequently applicable, we expect a time for reparation of five *hours*. This value is also rather high.

3. Variation in time of the reparation rate shows an increasing tendency, followed by a stabilization in the range of (0,2...0,33) *repairs/hour*. The very low values of the reparation rate shows once again the deficient character of the maintenance applied. The relatively constant value of the reparation rate proves the homogeneous character of the corrective maintenance activity as a whole. Homogeneous character refers to availability of spare parts and various materials, promptitude of intervention by human operators, qualification of operators. Correctness of defect diagnosis is added to this, as well as the quality level of the spare parts and tools.

4. The asymmetrical shape of the probability density curves show that the median time of corrective repair characterizes the best the maintenance activity applied to the travel mechanism. The median values, between 2 and 3 *hours*, are lower than the mean, which is between 2,5 and 4 *hours*, for all validated distributions. For these values of median time the maintainability level for the system is in the range of 40 ...60%, corresponding to the real situation in exploitation.

5. There is a correspondence between the lowest values of dispersion for tri-parametrical Weibull distribution. Where the parameters are calculated by the Method of Moments this distribution is considered to be the first in the reparation process characterization, having the smallest distance as to the empirical distribution.

6. The maximum time of corrective intervention of approximately 13 *hours* is acceptable, if we consider the high level of confidence for which it was calculated.

4. CONCLUSIONS

The maintainability analysis carried out on the ExRc-1400 wheel bucket excavator travel system leads to the following five main conclusions:

1. The scientific demarche of determination of the maintainability indicators is correct, being confirmed by the lognormal Weibull distribution that is validated. These distributions are characterized by the repair rates variable in time, specific to elements and components of mechanical nature. Confirmation is also emphasized by the points made in literature indicating these distributions as describing best the reparation phenomena of the mechanical components.

2. To increase safety in operation of the travel system, and implicitly of the wheel bucket excavator, maintenance activity should be reconsidered. It is necessary for another maintenance strategy to be adopted, in detriment of the corrective one, applied at the apparition of the defect.

3. Application of the preventive-planned maintenance strategy involves planned maintenance activities outside the productive activity. The essential conditions for the application of such a strategy are insuring high quality spare parts and elimination of improvisations. This is impossible to be achieved in EsRc-1400 excavators, since the travel system is morally worn out, the constructive-functional solution being obsolete. Even if the spare parts are of good quality, they are used in improper conditions, premature defects occurring.

4. Maintenance activities applied show that the applied maintenance strategy is not the corrective one applied at the occurrence of failure, but a palliative one. According to this palliative strategy, the intervention is on the defect occurred at the travel system, to ensure the momentary functionality of the excavator in general. The moral wear of the travel system, to which the generalized, significant physical wear is added, leads to the premature apparition of the same defect. This is proved by the large number of defects of the same nature occurred at the same components.

5. The existing situation in the maintenance activity is confirmed by the modernizations done as a whole on the EsRc-1400 excavator. The rotating, lifting-lowering, cutting systems of the arm with the bucket wheel and with energy supply have been modernized. The travel system and the haulage with roller belts from the excavator remained as 35 years ago. These systems are the principal failure sources at the moment of the excavator. Once again it is proved that the modernization of the travel system for the ExRc-1400 bucket wheel excavator is necessary from the point of view of maintainability.

REFERENCES

- [1]. **Andraș, A., Andraș, I., Radu, S.M.**, *Study regarding the bucket-wheel excavators used in hard rock excavations*, Annals of the University of Petroșani, Mechanical Engineering, Vol. 18 (XLV), 2016, pag. 11-22, ISSN 1454-9166;
- [2]. **Dhillon, B.S.**, *Design reliability. Fundamentals and applications*. CRC Press LLC. 1999.
- [3]. **Gilma, I.**, *Studiul privind îmbunătățirea siguranței în funcționare a unor utilaje din industria minieră*. Teză de doctorat. Universitatea din Petroșani. Petroșani. 2017.
- [4]. **Jula, D., Dumitrescu, I.**, *Fiabilitatea sistemelor de transport*. Editura Focus. Petroșani. 2009.
- [5]. **Roșu, (Gîrjob), E.**, *Studiul corelației dintre calitate, fiabilitate și mentenabilitate la echipamentele miniere*. Teză de doctorat. Universitatea din Petroșani. Petroșani. 2012.
- [6]. **Smith, J. D.**, *Reliability. Maintainability and Risk. Practical methods for engineers*. Sixth Edition. Butterworth-Heinemann Ltd. New York. 2001.
- [7]. * * *, *Excavatorul cu roată portcupe ERC 1400-30/7 modernizat. Instrucțiuni de exploatare, întreținere și reparare*. Rominex SA Timișoara. 2009.
- [8]. * * *, *Fișe de urmărire a funcționării mașinilor și instalațiilor la EMC Jilț*.

RESULTS OBTAINED ON THE OPTIMIZATION OF LABOR USE IN WORK EXERCISES FOR SALVATORS FOR THE SURFACE INDUSTRY

**ANDREI-LUCIAN GIREADĂ¹, MARIN SILVIU NAN²,
MARCEL RAD³, CRISTIAN NICOLESCU⁴,
IZABELLA KOVACS⁵, DĂNUȚ GREACEA⁶**

Abstract: To highlight changes in blood oxygen saturation and heart rate, tests were conducted for two teams of three rescuers are protected by protective breathing apparatus open circuit based air and positive pressure.

The measurements were performed in blood oxygen saturation and pulse rate from each Save at the ambient temperature of 200C. Measurements were repeated in each stage of temperature increase of 50C to 450C maximum.

In the work, it has been observed that as the temperature and humidity in the chamber increase the workout, the rescuer and the pulse increase blood oxygen saturation decreases.

Following tests carried out by rescuers on the shooting training there was a direct correlation, according to the submission of a significant amount of effort between the growth temperature and humidity environment and changing the parameters of physiological of rescuers (pulse and oxygen saturation in the blood), which will allow for the identification of higher temperature limits in the intervention area so that saviors can operate safely.

Keywords: Saving, intervention and rescue, work consumption, workout.

1. INTRODUCTION

During effort, the adaptation of the body is assured on the one hand by nervous

¹ Eng. PhD student, University of Petroșani

² Prof., Ph.D. Eng., University of Petroșani, nan.marins@gmail.com

³ Eng. PhD student, University of Petroșani

⁴ Eng. PhD student, Eng., University of Petroșani

⁵ Psychologist, INCD Insemex Petroșani

⁶ Eng. PhD student, University of Petroșani

regulation and on the other by neuro-hormonal regulation. During the effort, a number of changes in the apparatuses and systems in the body are produced as an expression of the functional adaptation trend, the changes that most outwardly manifest in the cardiovascular system activity. The most attractiveness of this device is the acceleration of heart rate, increased heart rate, which reflects the rhythm of the heart. Heart rate can be reached at a level of 60-70 beats per minute, 120-150 or 200 beats per minute in exceptional cases at very high effort.

Rescue teams have conducted several exercises with varying degrees of difficulty for each of the calculated consumption of work, according to relations :

$$A_1 = 0,5 \cdot P \cdot S \text{ [Kgm]} \quad (1)$$

$$A_2 = 0,25 \cdot P \cdot S \text{ [Kgm]} \quad (2)$$

$$A_3 = 0,1 \cdot P \cdot S \text{ [Kgm]} \quad (3)$$

$$A_4 = 0,055 \cdot P \cdot S \text{ [Kgm]} \quad (4)$$

$$A_5 = p \cdot h \cdot n \text{ [Kgm]} \quad (5)$$

$$A_6 = 0,35 \cdot P \cdot S \text{ [Kgm]} \quad (6)$$

$$A_7 = 0,25 \cdot P \cdot S \text{ [Kgm]} \quad (7)$$

$$A_8 = 0,055 \cdot P \cdot S \text{ [Kgm]} \quad (8)$$

$$A = \sum A_i \div A_n \text{ [Kgm]} \quad (9)$$

Testing was conducted for 6 activities:

- crossing the trail of narrow spaces;
- traction ergometers;
- walking on the treadmill ergometer;
- up and down the ladder metal;
- climbing and lowering the shaft ladder;
- covering the circuit module.

The measurements were performed in blood oxygen saturation and pulse rescuer in each part, which is repeated after each of the six tested activities..

2. THE TRAIL SURFACE - FOR RESCUERS IN TRAINING

In the polygon training, a team of three rescuers, surface profile, are the first training conducted several exercises with varying degrees of difficulty:

- two circuits of the route crevice;
- three series of 80 traction ergometers;
- five minutes walk on the treadmill ergometer;
- ascending and descending on the metallic scale 50 times;
- climbing and lowering the shaft ladder;
- two laps of the circuit module.

For each type of exercise part of the work consumption was calculated as follows:

I. The amount of work submitted for the passage of a narrow section of the gallery with the length of 12 meters and the section of 0,54 m² in the sloping position, with the activity repeating twice:

$$A_1 = 0,5 \cdot 100 \cdot 12 \cdot 2 = 1200 \text{ [Kgm]} \quad (10)$$

II. The amount of work done for the passage of a reduced section of the gallery with a length of 12 meters and a section of 0,9 m² in the walking position with palm and knee support, with a repetition of the activity twice:

$$A_2 = 0,25 \cdot 100 \cdot 12 \cdot 2 = 600 \text{ [Kgm]} \quad (11)$$

III. The amount of work done for a section of a reduced profile gallery of 12 meters in length and the 1.5 m² section in the bending position with the repetition of the activity twice:

$$A_3 = 0,125 \cdot 100 \cdot 12 \cdot 2 = 300 \text{ [Kgm]} \quad (12)$$

IV. The amount of work done for driving a labyrinth works with normal profile, having a length of 50 meters, with 2-fold repetition of activity:

$$A_4 = 0,055 \cdot 100 \cdot 50 \cdot 2 = 550 \text{ [Kgm]} \quad (13)$$

V. The amount of work carried out in order to cover a portion of the creepage, having a length of 3 meters and 0.9 m² section in the support position away by hands and knees, repeating activity 2 times:

$$A_5 = 0,25 \cdot 100 \cdot 3 \cdot 2 = 150 \text{ [Kgm]} \quad (14)$$

VI. The amount of work carried out in order to cover a portion of the creepage, having a length of 3 meters and area of 0.54 m², the crawling position, by repeating activity 2 times:

$$A_6 = 0,5 \cdot 100 \cdot 3 \cdot 2 = 300 \text{ [Kgm]} \quad (15)$$

VII. The amount of work performed for the ascent and descent of stairs at an angle of 90° with a height of 3 meters, with 2-fold repetition of activity:

$$A_7 = 0,35 \cdot 100 \cdot 6 \cdot 2 = 232 \text{ [Kgm]} \quad (16)$$

VIII. The amount of work done for lifting a load of 20 kg in the ergometer, the height of 1.2 m, and a repetition of 50 times the activity of 2 series:

$$A_8 = 20 \cdot 1,2 \cdot 50 \cdot 2 = 2400 \text{ [Kgm]} \quad (17)$$

IX. The amount of work done for getting on and off a ladder at an angle of 900, with a height of 9 meters, with repeated activity 2 times:

$$A_9 = 0,35 \cdot 100 \cdot 18 \cdot 2 = 1260 \text{ [Kgm]} \quad (18)$$

X. The amount of work performed for completion of a work with the normal profile (horizontal), the ergometric treadmill, the speed of 5 km / h for 5 minutes:

$$A_{10} = 0,055 \cdot 100 \cdot 400 = 2200 \text{ [Kgm]} \quad (19)$$

XI. The amount of work performed for completion of a job, the ascent and descent on the scale of 5 stages, at an angle of 450 with 50 times repetition of activity:

$$A_{11} = 0,25 \cdot 100 \cdot 100 = 2500 \text{ [Kgm]} \quad (20)$$

XII. The amount of work carried out in order to cover a portion of the creepage, having a length of 6 meters and 0.6 m² area, the crawling position, by repeating activity 2 times:

$$A_{12} = 0,5 \cdot 100 \cdot 6 \cdot 2 = 600 \text{ [Kgm]} \quad (21)$$

XIII. The amount of work performed in order to cover a portion of creepage, having a length of 41 meters and area of 0.9 m², the position went to support hands and knees, with repeated activity 2 times:

$$A_{13} = 0,25 \cdot 100 \cdot 41 \cdot 2 = 2050 \text{ [Kgm]} \quad (22)$$

XIV. The amount of work done for driving a labyrinth works with normal profile, having a length of 36 meters, by repetition of two times the activity of:

$$A_{14} = 0,055 \cdot 100 \cdot 36 \cdot 2 = 400 \text{ [Kgm]} \quad (23)$$

XV. The amount of work done for climbing and lowering two stairs at an angle of 900, 3 meters high, with repeating the activity twice:

$$A_{15} = 0,35 \cdot 100 \cdot 6 \cdot 2 = 460 \text{ [Kgm]} \quad (24)$$

The total amount of work performed is:

$$A = \sum A_i \div A_{13} = 1200 + 600 + 300 + 550 + 150 + 300 + 232 + 2400 + 1260 + 2200 + 2500 + 600 + 2050 + 400 + 460 = 15.200 \text{ [Kgm]} \quad (25)$$

3. RESULTS

The total amount of work performed by a rescuer from the surface, the trainee to practice crossing the first path was 15.200 kgm.

Also, measurements were made of the blood oxygen saturation and pulse each rescuer in part, measurements are repeated after each (Figure 1).



Fig. 1. Output measurements

For this route, the blood oxygen saturation and pulse rate are represented in Table 1, and graphically in Figures 2 and 3.

Table 1 Surface track table - rescuers in training

Nr. crt	GROUPS - TRAINING	Subject 1		Subject 2		Subject 3	
		Pulse	SpO ₂	Pulse	SpO ₂	Pulse	SpO ₂
1	Narrow spaces	133	98	137	98	126	98
2	ergometers	162	98	138	97	115	96
3	Conveyor belt	120	96	103	97	120	96
4	Metal ladder	144	98	107	97	116	98
5	Well	101	96	116	96	113	97
6	Modular circuit	127	97	121	99	135	98

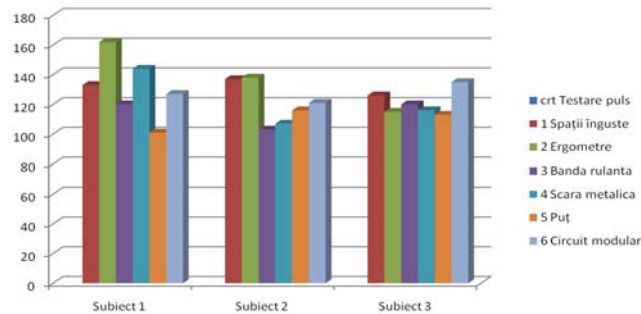


Fig. 2. Variation of the pulse at the surface route - rescuers

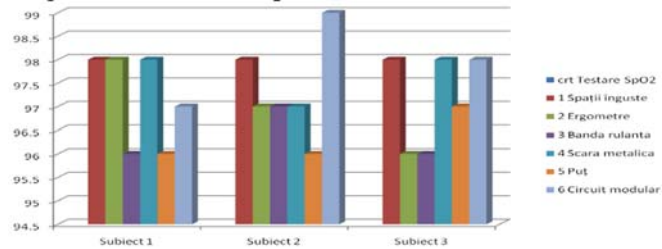


Fig. 3. Variation route SpO2 surface - rescuers.

REFERENCES

- [1]. Găman, G. A., et al., *Organization of salvage of personnel and goods in areas affected by underground and surface damages*, International Seminar on Security in Coal Mines, Călimănești, 1996
- [2]. Găman, G. A., et al., *Rescue in toxic environments*, Sigma Plus Publishing House, Petrosani, 1997
- [3]. Găman, G. A., et al., *Considerations regarding the activity of mining-rescuers in conditions of high temperature and humidity*, Jubilee Session of Petrosani University, 1998
- [4]. Găman, G. A., et al., *Assessment of the methodology of training miners in order to intervene under specific conditions*, 28th International Conference of Mining Security Research Institutes, Sinaia, 1999
- [5]. Găman, G. A., et al., *Analysis of factors that can lead to improvement of the mining rescue activity*, 28th International Conference of Mining Security Research Institutes, Sinaia, 1999
- [6]. Găman, G. A., et al., *Optimizing rescue work in mining by reducing the risk factors to which rescuers are subjected in the act of liquidating the damage and / or evacuating the remaining persons in the areas affected by these events*, INCD INSEMEX, 2000
- [7]. Găman, G. A., et al., *Experimental determination for rescue selection and training methods of mine rescuers operating at high temperatures and humidity*, International conference on mine rescue works, Bytom, Poland, 2000
- [8]. Găman, G. A., et al., *Changes in Physiological Parameters at Rescuers in Action*, Communication Session Petrosani National Company, 2002
- [9]. Găman, G. A., et al., *Particularities of the mining rescue activity*, SANOSCU Mining Security Salon, 2002
- [10]. Găman, G. A., et al., *Neuropsychological system responses of rescuers in operation*, SANOSCU Mining Security Salon, 2002

THE EQUATIONS OF MOTION OF THE EXTRACTION DRIVE WHEEL CABLE SYSTEM AND THE RELATION BETWEEN THE TENSIONS BETWEEN THE EXTREME POINTS OF THE WRAPPING OF THE CABLE ON THE DRIVE WHEEL

RĂZVAN BOGDAN ITU¹, IOSIF DUMITRESCU², VILHELM ITU³

Abstract: This work presents the establishment of the equations for the motion without slipping of the extraction cable on the rotating drive wheel. The equations of motion established for the cable – drive wheel elements allow for the determination of tension in the area of the wrapping of the cable on the drive wheel, in the extreme points of the wrapping. The determination of the tensions is based on the equations of motion in the most general functioning dynamic conditions of the cable – drive wheel system.

Key words: equations of motion; relation between the tensions

1. INTRODUCTION

It's a known fact that, in the case of the classification of extraction installations, based on the criterion of the type of the organ for wrapping the extraction cable, these are either installations with a constant radius of wrapping or with a variable radius of wrapping. The ones with a constant radius of wrapping can have a cylindrical drum, a sectioned cylindrical drum, two cylindrical drums, a friction (drive) wheel. Those with a friction wheel can be monocable drive wheels (KÖPE) (fig. 1) and multicable drive wheels with two (fig.2) or four cables (fig.3). The drive wheel can be placed on the ground (fig. 1 and fig. 2) or in the extraction tower (fig.3). In what regards the extraction installations that use drive wheels (with friction), the cable is no longer wrapped but passed over them. The motion of the cable and of the extraction vessels that are fastened at its ends is done due to the friction forces between the cable and the drive wheel.

¹ Assistant, Eng. Ph.D., University of Petroșani, raz.van4u@yahoo.com

² Assoc.Prof, Eng. Ph.D., University of Petroșani, iosif_dumi@yahoo.com

³ Lecturer, Eng. Ph.D., University of Petroșani, drituv@yahoo.com



Fig. 1. Monocable drive wheel (Köpe)



Fig. 2. Two cable drive wheel



Fig. 3. Four cable drive wheel

In the case of the motion without slipping of a flexible cable wrapped on a drive wheel (rotating circular disc), the wheel and the cable form a mechanical system with interconditionate motions. This situation appears in the case in which the cable involves the wheel, or in the case in which the wheel involves the cable. The present paper approaches the study of the dynamic behaviour of the cable – drive wheel mechanical system, based on the hypotheses mentioned below.

The equations of motion for the cable and the wheel will be established for the general case, when the kinematic parameters of the cable – wheel mechanical system are time functions, a situation that corresponds to the transitory regimes of functioning, characterised by the constant values of the sizes of kinematic parameters.

The normal and tangential specific reactions that correspond to the continuous distributions of reaction forces that act on the cable in the cable – wheel contact area are polar angle functions and possibly time functions, through the medium of kinematic parameters, but their rapport is constant, independent of time and polar angle.

2. MOTION EQUATIONS FOR THE CABLE – WHEEL SYSTEM

Distribution of the forces that act on a cable element with the centre in current point P is shown in fig. 4, and the one acting on the wheel is shown in fig 5.

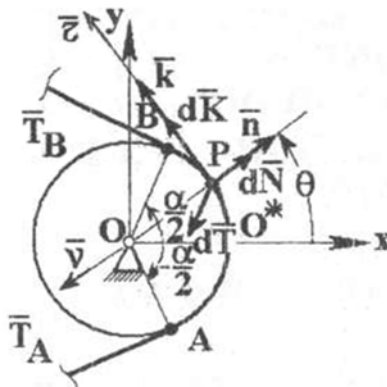


Fig. 4. Distribution of the forces that action a cable element

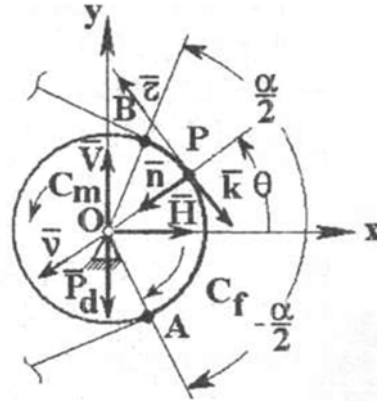


Fig. 5. Distribution of the forces that action the drive wheel (disc)

Considering, first of all, the state of dynamic equilibrium of the cable (fig. 4), the vectorial equation of its absolute motion will be:

$$dm\bar{a} = d\bar{T} + d\bar{N} + d\bar{K} \quad (1)$$

where:

$$dm = \rho_1 ds = \frac{rd\theta}{Nm}, \quad (2)$$

(dm , the mass of the cable element; Nm , the metric number of the cable)

$$\bar{a} = \dot{v}\bar{\tau} + \frac{v^2}{r}\bar{\nu}, \quad (3)$$

(\bar{a} , acceleration of the current point P)

$$d\bar{T} = d(T\bar{\tau}) = dT\bar{\tau} + Td\bar{\nu} \quad (4)$$

($d\bar{T}$, the variation of the tension of the cable element)

$$d\bar{N} = \bar{n}ds = -md\bar{\nu}; \quad d\bar{K} = \bar{k}ds = +rkd\bar{\nu} \quad (5)$$

($d\bar{N}$ and \bar{n} , normal elementary and specific $d\bar{K}$ and \bar{k} reactions, elementary and specific tangential reactions);

Taking into consideration the relations (2) – (5), to the vectorial equation (1) the following scalar equations will correspond:

$$\frac{rvd\theta}{Nm} = dT + rkd\theta; \quad \frac{v^2}{Nm} = T - rm \quad (6)$$

Moving on to the determination of the equations of motion of the drive wheel, we will first calculate the components of the torsors in pole O of the two continuous distributions of specific forces of reactions of the cable – wheel connections, $\bar{n} = n(\theta)\bar{v}$ and $\bar{k} = k(\theta)\bar{r}$.

The elementary force $d\bar{N}$, that acts on the spring of contact with the cable, with the centre in point P , determined by the polar angle θ (fig. 1b), will be expressed by:

$$d\bar{N} = \bar{n}ds = n(\theta)r d\theta\bar{v} = rn(\theta)[- \cos \theta \cdot \bar{i} - \sin \theta \cdot \bar{j}], \quad (7)$$

The components of the resulting torsor in pole O of this distribution of elementary forces on the contact quadrant AB will be expressed by:

$$\bar{N} = -rN_x(\alpha) \cdot \bar{i} - rN_y(\alpha) \cdot \bar{j}; \quad \bar{M} \cdot \bar{n} = \bar{0}, \quad (8)$$

the functions N_x and N_y , from relation (8) will be expressed by:

$$N_x = \int_{\frac{\alpha}{2}}^{\frac{\alpha}{2}} n(\theta) \cos \theta d\theta = N_x(\alpha); \quad N_{xy} = \int_{\frac{\alpha}{2}}^{\frac{\alpha}{2}} n(\theta) \sin \theta d\theta = N_{xy}(\alpha), \quad (9)$$

The elementary force $d\bar{K}$, which acts on the circle element in point P , will be expressed by:

$$d\bar{K} = -r\mu^* [- \sin \theta \cdot \bar{i} + \cos \theta \cdot \bar{j}]n(\theta)d\theta, \quad (10)$$

and the moment in pole O :

$$dM = -r|dK| - r(kds) = -\mu^* r^2 n(\theta)d\theta, \quad (11)$$

Consequently, the components of the torsor in pole O of this continuous forces distribution will be given by the relations:

$$\bar{K} = -r\mu^* (-N_x \bar{i} + N_y \bar{j}); \quad M_k = -r^2 \mu^* \sqrt{N_x^2 + N_y^2}, \quad (12)$$

with functions N_x and N_y expressed by relations (9).

The equations of motion will have the forms:

$$\bar{O} = \bar{P}_d + \bar{H} + \bar{V} + \bar{N} + \bar{K}, \quad J\ddot{\phi} = C_m - M_K - C_f, \quad (13)$$

where P_d , is the weight of the disc, H and V are the components according to the axes

of the fixed benchmark Oxy of the reaction of articulation, φ is the angle of rotation of the disc, C_m , is the moment of the engine torque that must be applied to the disc, $C_f = \mu_0 r_0 \sqrt{H^2 + V^2}$ is the torque moment of friction in bearing, μ_0 , is the coefficient of friction in bearing, r_0 , is the radius of the bolt (the articulation).

From (13) and by considering relations (7) – (12) the following system of equations will be obtained:

$$\begin{cases} 0 = H - rN_x - r\mu^* N_y \\ 0 = -P_d + V - rN_y + r\mu^* N_x \\ J\ddot{\varphi} = C_m - \mu_0 r_0 \sqrt{H^2 + V^2} - r^2 \mu^* \sqrt{N_x^2 + N_y^2} \end{cases}, \quad (14)$$

3. THE CABLE TENSION IN THE AREA OF WRAPPING ON THE WHEEL

Euler's formula for wires wrapped on circular discs is also extended to dynamic cases, when the wheel rotates, either independently, or it forms a mechanical system with the cable.

In this last situation, the speed of a peripheral point on the wheel in contact with the cable has the same size and orientation like the speed of the cable's travel, and the relative speed of the cable's points in contact with the wheel is null.

Onward, we establish the relation between the tensions from the extreme points of a cable wrapped on the rotating wheel, in the conditions in which the cable travels without slipping on the wheel.

In this purpose, we use the motion equations determined in &2, (The establishment of the equations of motion for the mechanical system cable – wheel) both for the cable and the wheel, in the conditions in which the mechanical system cable – wheel functions in a transitory regime.

These relations are particularised for the permanent regime of functioning of the considered mechanical system, characterised by constant values of the size of kinematic parameters of order I.

By considering the state of dynamic equilibrium of the cable (fig. 4), in &2 the following scalar equations have resulted:

$$\frac{r\dot{v}d\theta}{Nm} = dT + rkd\theta; \quad \frac{v^2}{Nm} = T - rm \quad (15)$$

The same &2 also gives us the equations of motion that correspond to the wheel:

$$\begin{cases} 0 = H - rN_x - r\mu^* N_y \\ 0 = -P_d + V - rN_y + r\mu^* N_x \\ J\ddot{\varphi} = C_m - \mu_0 r_0 \sqrt{H^2 + V^2} - r^2 \mu^* \sqrt{N_x^2 + N_y^2} \end{cases}, \quad (16)$$

The significations of the values contained in relations (15) and (16) are specified in &2 (the first part). By using the relations:

$$v = r\dot{\varphi} \quad \dot{v} = r\ddot{\varphi} \quad (17)$$

equations (15), (16) and the notation:

$$\phi(\alpha) = \frac{r^2}{P_d^2} (N_x^2 + N_y^2) + \frac{2r}{P_d} (N_y + \mu^* N_x), \quad (18)$$

the following equations of motion will be obtained:

$$\begin{cases} \left(\frac{r\ddot{\varphi}}{Nm} - rk \right) d\theta = dT \\ rn = T - \frac{r^2 \dot{\varphi}^2}{Nm_x} \\ J\ddot{\varphi} = C_m - \mu_0 r_0 P_d \sqrt{1 + \phi(\alpha)} - r^2 \mu^* \sqrt{N_x^2 + N_y^2} \end{cases}, \quad (19)$$

To these equations, we add the relation:

$$k(\theta) = \mu^* n(\theta), \quad (20)$$

where μ^* represents an unknown constant that must verify the condition $(k(\theta, t) = \mu^* n(\theta, t); \mu^* \leq \mu)$

$$\mu^* \leq \mu, \quad (21)$$

The system of equations (19) contains the unknown functions $\varphi = \varphi(t)$, $T = T(\theta)$, $n = n(\theta)$, $k = k(\theta)$ and $C_m = C_m(\theta)$. This dynamics problem is very complicated. System (19) is simplified if we impose the law of motion of system $\varphi = \varphi(t)$ and what we have to do is determine the functions $T = T(\theta)$, $n = n(\theta)$, $k = k(\theta)$, as well as the way in which the engine torque C_m must vary in time.

These equations will be especially simplified in the case of the functioning of the cable – wheel system in a permanent regime, meaning in the conditions:

$$\dot{\phi} = \omega_0 = \text{const.} > 0; \quad \ddot{\phi} = 0, \quad (22)$$

In this situation, system (19) has the particular form:

$$\begin{cases} dT = -rkd\theta \\ rn = T - \frac{r^2 \omega_0^2}{Nm_x} \\ J\ddot{\phi} = C_m - \mu_0 r_0 P_d \sqrt{I + \phi(\alpha)} - r^2 \mu^* \sqrt{N_x^2 + N_y^2} \end{cases}, \quad (23)$$

with

$$\frac{k}{n} = \mu, \quad (24)$$

In this situation, from the first two equations of system (23) we obtain the differential equation:

$$\frac{dT}{T - \frac{r^2 \omega_0^2}{Nm}} = -\mu^* d\theta, \quad (25)$$

which integrated between $-\alpha/2$ and θ leads to the following relation between the tensions from point A and P of the wrapping of the cable on the wheel:

$$T(\theta) = T_A e^{-\mu^* \left(\frac{\alpha}{2} + \theta\right)} + \frac{r^2 \omega_0^2}{Nm} \left[1 - e^{-\mu^* \left(\frac{\alpha}{2} + \theta\right)} \right], \quad (26)$$

For $\theta = \alpha/2$, relation (26) becomes:

$$T_B = T_A e^{-\mu^* \alpha} + \frac{r^2 \omega_0^2}{Nm} \left[1 - e^{-\mu^* \alpha} \right], \quad (27)$$

Equation (27) will give the law according to which the moment of the engine torque varies, according to the wrapping angle.

4. CONCLUSIONS

Departing from the hypothesis according to which - in the case of the travelling without slipping of a cable wrapped on a rotating drive wheel – the wheel and the cable form a mechanical system with interconditionate movements, this work ended by establishing the equations of motion for the two elements of the considered mechanical system. The system formed by equations (6) and (14) leads to the determination of the tension of the cable in the area of its wrapping on the wheel and of the law of variation of the moment of the engine torque applied to the wheel.

The system formed by the equations of movement corresponding to the cable and the wheel have led to:

- obtaining the relation between the tensions from the extreme points of the wrapping of the cable on the wheel, which, besides the friction coefficient and the wrapping angle, also depends on the wheel's speed and radius and on the metric number of the cable;

- obtaining the law of variation of the moment of the engine torque applied to the wheel, according to the wrapping angle;

For determining the total tension of the cable in the area of its wrapping on the drive wheel we must also add the weight per linear metre of the cable and of the extraction vessels attached to its ends.

REFERENCES

- [1]. **Buzescu F.L.**, *A mathematical model of the travelling without slipping of a wire wrapped on a rotating circular disc*, Scientific materials of the National XXXI Conference for the mechanics of solid bodies –Chişinău, 2007.
- [2] **Dumitrescu I., Cozma B. Urdea Gh. B.**, *Study of Coal Transportation Flow from the face to the Ground in Lonea Mine*, 15 th GeoConference on Science and Technologies in Geology, Exploration and Mining SGEM 2015, Conference Proceedings, vol. III, pp. 603 – 610, ISBN 978-619-7105-09-4, ISSN 1314-2704
- [3] **Dumitrescu I., Jula D., Kovacs I., Cozma B.**, *Numerical analzsis of cable connecting devices for one side wedged winding engine vessels*, KOD 2008 Proceedings, The Fifth International Symposium about forming and design in mechanical engineering, , pag. 195-198,. ISBN 978-86-7892-104-9
- [4]. **Mangeron D., Irimiciuc N.**, *The mechanics of rigids applied to engineering*, Technique Publishing House, Bucureşti. Vol I - 1978, Vol II- 1980.
- [5]. **Radu, S.M, Rosianu, C., Stoicoiu, I.**, *Upgrading Electrical Drives Control At The Bucket Wheel Excavators*, Proceedings of the 14th Conference On Environment And Mineral Processing, Pages: 97-100, 2010. WOS:000396179300017

ASPECTS REGARDING DETERMINATION OF RELIABILITY CHARACTERISTICS FOR BUCKET WHEEL EXCAVATOR TEETH

DUMITRU JULA¹, ION GÎLMA²

ABSTRACT: The paper presents the results obtained in determining the reliability characteristics of bucket wheel excavator teeth used in Oltenia Basin. The main reliability indicators are determined, which quantify the life time of teeth. A special attention is given to reliability indicator interpretation.

Keywords: wheel bucket excavator, bucket, tooth, reliability failure rate, probability, distribution law, mathematical statistics, life time.

1. GENERAL CONSIDERATIONS

Excavators are high capacity equipment, at which displacement and haulage of materials from the face are done with the help of buckets equipped with teeth mounted on bucket wheels. The bucket wheel is the leading sub-assembly of the equipment, which decisively influence the excavator's cutting performances.

The teeth of the bucket wheel excavator have the role of displacing the material in the face, guiding it towards the inside of the bucket. The teeth are mounted to the buckets by screws or by wedging them in cases. During operation, the teeth support combined strains, bending in two perpendicular directions, and compression according to the direction of the longitudinal axis. Crushing strains also occur in the mounting areas to the buckets and at shocks, due to the lack of homogeneity of the excavated rocks. What is important is the highly aggressive mechanical abrasion, in the area of the active part, this being decisive in the establishing of the reliability level of the teeth.

For such tools, it is important to carry out a reliability study, from two points of view. First, based on reliability indicators, the life time of a tooth type can be determined, that is its operating time, until an admitted wear limit is established. This is important when a decision is

¹ *Assoc. Professor Eng. Ph.D., University of Petrosani, juladumitru@yahoo.com*

² *Eng. Ph.D. Student, University of Petrosani*

made in purchasing a certain type of tooth, required to function an mean operating time. Second, reliability characteristics are the basis for the determination of a necessary spare parts of teeth.

2. DETERMINATION OF RELIABILITY INDICATORS

The reliability study has been performed on a sample made up of seventy 1400-MII type teeth, with which EsRc-1400 excavator buckets were equipped.

The effective functioning times, until failure, that is until changing caused by reaching the admitted wear limit, measured in *hours*, make up a (S1) type statistics series, with $n = 70$ number of elements, with the values: 95; 97; 97; 98; 99; 100; 100; 100; 165; 170; 172; 180; 180; 185; 185; 189; 198; 200; 200; 200; 200; 200; 245; 259; 261; 265; 273; 279; 283; 286; 291; 295; 300; 300; 300; 300; 352; 359; 362; 378; 382; 387; 392; 395; 398; 400; 400; 400; 463; 465; 489; 493; 495; 500; 500; 500; 552; 580; 580; 590; 591; 592; 594; 595; 597; 600; 600; 600; 688; 693.

Table 1 presents the values of empirical (experimental) probability distribution of effective functioning times of the teeth until changing.

Table 1. Empirical (experimental) probability distribution values $\hat{F}(t_i)$

i	$\hat{F}(t_i)$	i	$\hat{F}(t_i)$	i	$\hat{F}(t_i)$	i	$\hat{F}(t_i)$	i	$\hat{F}(t_i)$	i	$\hat{F}(t_i)$
1	0,009943	13	0,180398	25	0,350852	37	0,521307	49	0,691761	61	0,862216
2	0,024148	14	0,194602	26	0,365057	38	0,535511	50	0,705966	62	0,876420
3	0,038352	16	0,208807	27	0,379261	39	0,549716	51	0,720170	63	0,890625
4	0,052557	16	0,223011	28	0,393466	40	0,563920	52	0,734375	64	0,904830
5	0,066761	17	0,237216	29	0,407670	41	0,578125	53	0,748580	65	0,919034
6	0,080966	18	0,251420	30	0,421875	42	0,592330	54	0,762784	66	0,933239
7	0,095170	19	0,265625	31	0,436080	43	0,606534	55	0,776989	67	0,947443
8	0,109375	20	0,279830	32	0,450284	44	0,620739	56	0,791193	68	0,961648
9	0,123580	21	0,294034	33	0,464489	45	0,634943	57	0,805398	69	0,975852
10	0,137784	22	0,308239	34	0,478693	46	0,649148	58	0,819602	70	0,990057
11	0,151989	23	0,322443	35	0,492898	47	0,663352	59	0,833807		
12	0,166193	24	0,336648	36	0,507102	48	0,677557	60	0,848011		

In the study of 1400-MII type tooth reliability the exponential negative, normal and bi and triparametrical Weibull distribution laws are taken into consideration.

The negative exponential distribution law, ep, is characterized by λ parameter, representing the failure intensity or rate, in *failure/hour*. Parameter λ is estimated by the Least Squares Method.

The normal distribution law (Gauss-Laplace), symbol nv, is defined by parameters m_n , mean operating time, in *hours*, and σ_n , the mean square deviation or standard deviation, in *hours*. The parameters are estimated by the Maximum Likelihood Method.

The normalized biparametric Weibull distribution law, symbolized by Wbp, is defined by dimensionless form parameter β_1 and by the real scale parameter η_1 , measured in *hours*. Parameters are estimated by the Least Squares Method.

The triparametric Weibull distribution, symbolized by Wtm, is built by β_2 dimensionless form parameter, η_2 scale parameter in *hours*, and γ , initialization parameter in *hours*. The parameters are estimated by the Method of Moments.

The normalized biparametric Weibull distribution, symbolized by Wbv, is defined by the dimensionless form parameter β_3 and η_3 scale parameter, in *hours*, calculated by the Maximum Likelihood Method.

Table 2 presents a synthesis of the parameter values of the distribution laws taken into consideration for the characterisation of the 1400-MII type teeth functionality.

Table 2. Estimated values of theoretical distribution parameters characterizing the 1400-MII teeth reliability

Distribution	λ, h^{-1}	m_n, h	σ_n, h	β_1	η_1, h	β_2	η_2, h	γ, h	β_3	η_3, h
Exponential negative, ep	$32,66 \cdot 10^{-4}$									
Normal (Gauss-Laplace), nv		347,271	171,997							
Weibull biparametric normalized, Wbp				2,085	393,987					
Weibull triparametric, Wtm						2,124	392,114	$3,429 \cdot 10^{-8}$		
Weibull biparametric normalized, Wbv									2,009	395,848

Table 3 presents the quantitative comparison between the laws of theoretical distribution considered to characterize the functionality of the 1400-MII type tooth.

Table 3 presents:

- column (1), theoretical distribution laws considered to characterize the tooth functionality;

- column (2), analytical expressions of the reliability functions for the theoretical distributions considered, whose parameters are estimated by the analytical methods previously presented;

- column (3), values of maximum deviations between theoretical and empirical distribution, D_{max} , more exactly between the functions of theoretical and empirical (experimental) probability distributions;

- column (4), assumed risk margin, α , respectively the truth probability P , between which there is the relation $\alpha + P = 1$;

- column (5), critical values of Kolmogorov-Smirnov test (K-S), $D_{\alpha,n}$, for α risk margin and $n = 70$ number of sample elements;

- column (6), theoretical distribution validation results.

Table 3. Comparative analysis of theoretical distributions characterizing 1400-MII type tooth functionality

Distribution	Reliability function, R(t)	Maximum deviations, D_{max}	Risk, α (%)	Critical value, $D_{0.570}$	Validation
(1)	(2)	(3)	(4)	(5)	(6)
Exponential negative, ep	$e^{-0.003266 \cdot t}$ (1)	0.307194	0.5	0.203855	NOT
Normal (Gauss-Laplace), nv	$\frac{1}{2} - \Phi\left(\frac{t - 347.271}{171.997}\right)$ <p style="text-align: center;">or</p> $1 - \frac{1}{171.997} \frac{1}{\sqrt{2\pi}} \int_0^t e^{-\frac{1}{2}\left(\frac{x-347.271}{171.997}\right)^2} dx$ (2) (3)	0.115382	20	0.125858	YES
Weibull biparametric normalized, Wbp	$e^{-\left(\frac{t}{393.987}\right)^{2.085}}$ (4)	0.088134	20	0.125858	YES
Weibull triparametric, Wtm	$e^{-\left(\frac{t-3.429 \cdot 10^{-8}}{392.114}\right)^{2.124}}$ (5)	0.095357	20	0.125858	YES
Weibull biparametric normalized, Wbv	$e^{-\left(\frac{t}{395.848}\right)^{2.009}}$ (6)	0.084148	20	0.125858	YES

Table 3 indicates that exponential distribution is not validated, maximum distance between empirical and theoretical distribution being higher than the critical value of the test. Normal (Gauss-Laplace) and Weibull bi and triparametrical laws, with parameters calculated by various analytical methods are validated.

Normalized biparametrical Weibull distribution, where parameters are calculated by the Least Squares Method, and by Maximum Likelihood Method, respectively, approximate the best theoretical distribution.

However, one can definitely state that any of the validated distributions can characterize the functionality of the teeth of the wheel bucket excavator.

Validation of normal distribution can also be noticed. This is indicated by the literature of speciality for the characterization of mechanical, electrical and thermal ageing, phenomena that can also be found in the analyzed case.

For the form parameter $\beta = 2$, ($\beta_1 = 2,085$; $\beta_2 = 2,124$; $\beta_3 = 2,009$) resulted from calculations, Rayleigh distribution law is found. This distribution law represents a

particular case of Weibull distribution law, and it is characterized by linear variation of failure intensity.

Figures 1, 2, 3 and 4 show variations of the main reliability indicators, function of the operating time until failure.

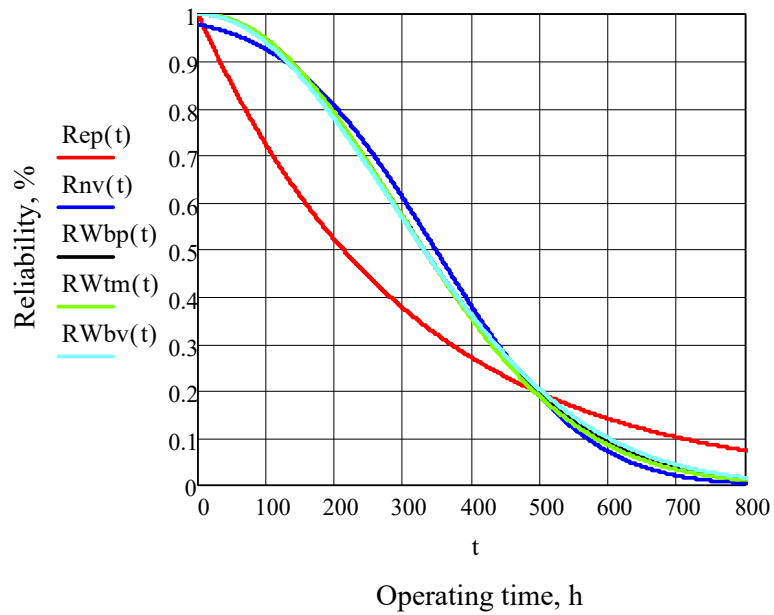


Fig. 1. Variation of 1400-MII type tooth reliability function

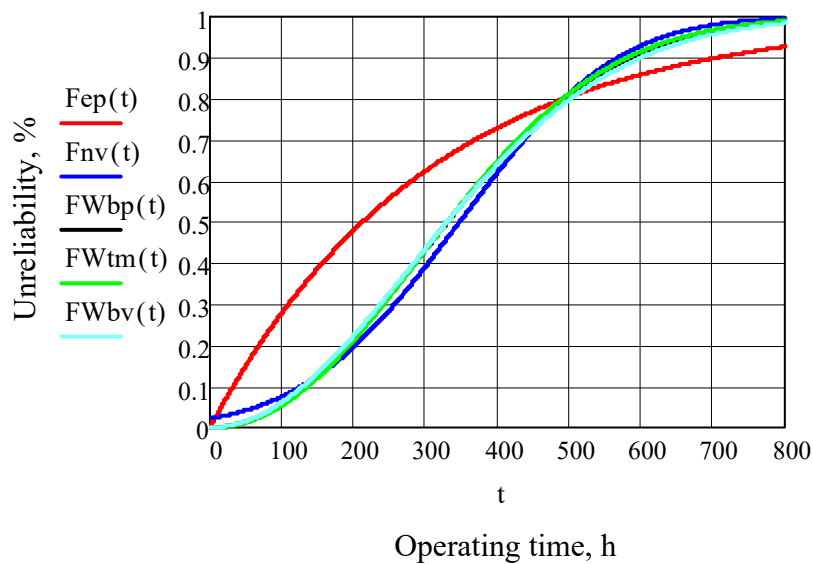


Fig. 2. Variation of unreliability function

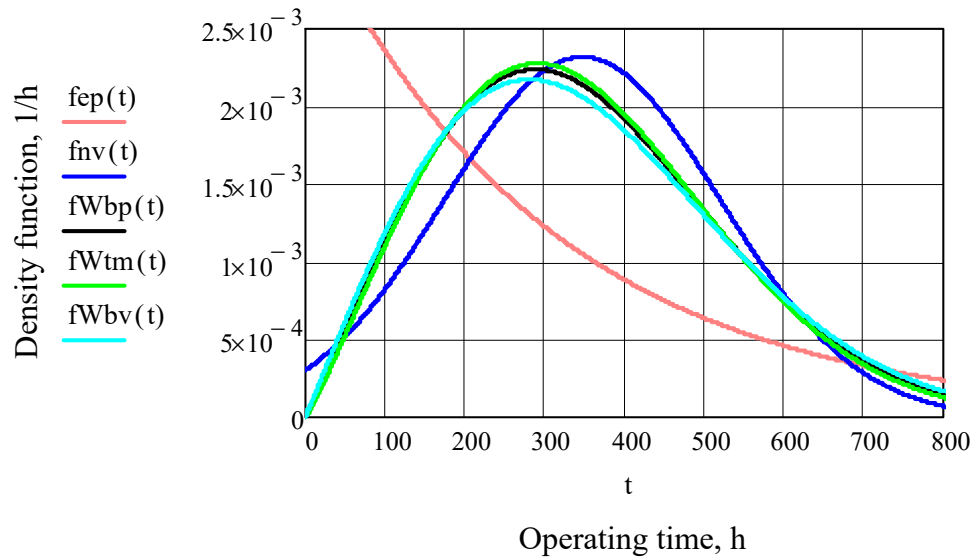


Fig. 3. Density function of operating time until failure

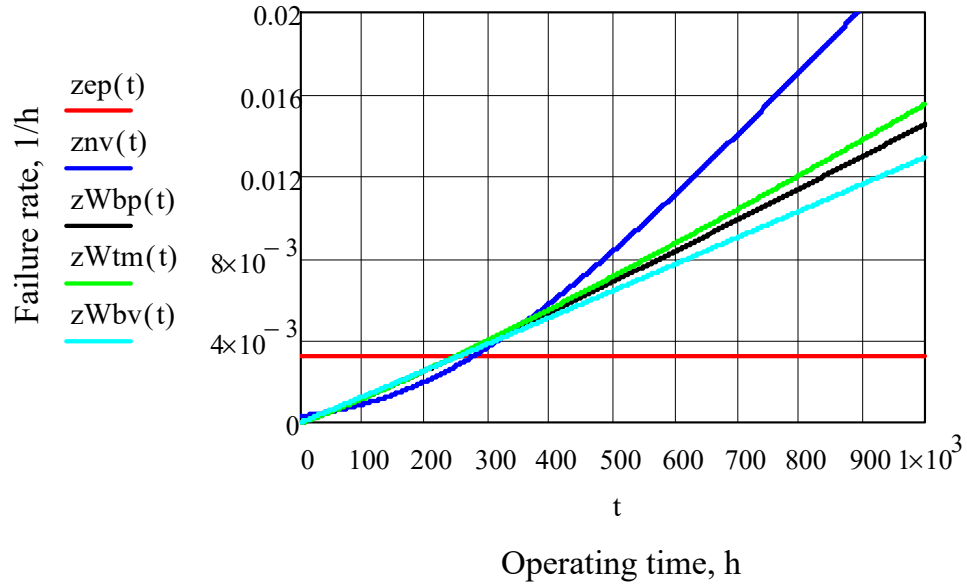


Fig. 4. Variation of failure rate functions of 1400-MII type tooth

Table 4 shows values for a series of indicators characterizing tooth reliability.

Table 4. Reliability indicators regarding operating time until 1400-MII type tooth failure

No. crt.	Parameter			Parameter value for distribution:				
	Name	Symbol	UM	Exponential negative, ep	Normal, nv	Weibull bi-parametric normalized, Wbp	Weibull tri-parametric, Wtm	Weibull bi-parametric normalized, Wbv
1	Mean	m	h	306	347	349	347	350
2	Median	t_{med}	h	212	347	330	330	330
3	Variance	D	h^2	93771	29583	30865	29583	33353
4	Standard deviation,	σ	h	306	172	176	172	183
5	Coefficient of variation	CV	-	1	0.495	0.503	0.495	0.521

3. INTERPRETATION OF RESULTS AND PRINCIPAL CONCLUSIONS

1. A first remark resulting from the graphs presented is the tendency of grouping and even total overlap of validated distribution law curves. The large gap between the exponential distribution law and the other validated laws is obvious. The comparatively smaller values of dispersion recommend the use of normal and bi- and tri-parametrical Weibull distributions in a more attentive characterization of the tooth reliability.

2. Since the variation curve of the density function of likelihood is approximately symmetrical, it results that the 348 *hours* mean time characterizes the best the tooth functionality. The value is calculated from table 4, as an average of average values for the four validated distributions.

3. Analyzing the variations of the reliability and non-reliability functions it results that for an effective functioning time of the excavator of 200 *hours*, reliability is 80%. This means that after approximately 13 working days we should anticipate that it would not be necessary to replace the teeth. The time in days is calculated in the hypothesis that the excavator effectively works an average of 15 *hours* a day. The reliability value of 1400-MII type tooth for 200 *hours* of functioning is very good.

4. For up to 100 *hours* of functioning, a decrease of the reliability value down to approximately 93% occurs. This decrease is normal mainly due to a small value of the reliability curve slope, which suggests a small value of the wear speed. After 100 *hours* the curve slope increases, which denotes an increase of the wear speed of the tooth. This behaviour also results from the failure intensity variation curves, for which, the same interval is characterized by smaller failure intensities.

5. A 50% reliability corresponds to the average of 348 *hours* of use of the teeth. If a 500 *hours* average time of good functioning is required, the tooth reliability is only 20%. This means that out of 100 new teeth mounted in the same time, after 500 hours of functioning, only 20 will stay in function. The other 80 teeth are replaced due to reaching

the admitted limit of wear. The rapid decrease of reliability from 80 to 20%, in increasing time from 200 to 500 *hours* shows the increase of the wear speed. This increase is shown by the increase of the slope of the reliability curve and the increase of the wear intensity.

6. The approximately linear variation of the failure rate or intensity is noticed, function of the functioning time of the tooth for bi- and tri-parametrical Weibull distributions. The slope of the line shows the quality level of the tooth.

7. The overall behaviour of the tooth functioning is explained by the existence of a much harder material at the level of the cutting edges of the teeth. The hardness decreases toward the middle, along with the increase of the worn size. This totally depends on the solutions adopted by the manufacturer in the design and manufacturing of this type of teeth.

REFERENCES

- [1]. **Dhillon, B.S.**, *Design reliability. Fundamentals and applications*. CRC Press LLC. 1999.
- [2]. **Gîlma, I.**, *Studiul privind îmbunătățirea siguranței în funcționare a unor utilaje din industria minieră*. Teză de doctorat. Universitatea din Petroșani. Petroșani. 2017.
- [3]. **Jula, D., Praporgescu, G., Mihăilescu, S., Tomuș, O.B., Deaconu, I.**, *Aspecte privind determinarea fiabilității utilajelor din carierele de lignit*. Lucrările științifice ale simpozionului internațional multidisciplinar “Universitaria SIMPRO”. Volumul: Mașini și echipamente tehnologice. Editura UNIVERSITAS. Petroșani. 2006.
- [4]. **Jula, D., Dumitrescu, I.**, *Fiabilitatea sistemelor de transport*. Editura Focus. Petroșani. 2009.
- [5]. **Jula, D., Dinescu, S., Tomuș, O.B.**, *Reliability Analysis of EsRc 1400 Bucket Wheel Excavators Operating in Oltenia Lignite Open Pit Mines*. MicroCAD2015. International Scientific Conference. University of Miskolc. Hungary. 2015.
- [6]. **Mitran, I., Popescu, F.D., Nan, M.S., Soba, S.S.**, *Computer Assisted Statistical Methods for Process Reliability Analysis*, Proceedings Of The 15th American Conference On Applied Mathematics And Proceedings Of The International Conference On Computational And Information Sciences 2009, Vols I And II, Page: 166+, 2009, WOS:000266634600026.
- [6]. **Roșu (Gîrjob), E.**, *Studiul corelației dintre calitate, fiabilitate și mentenabilitate la echipamentele miniere*. Teză de doctorat. Universitatea din Petroșani. Petroșani. 2012.
- [7]. **Smith, J. D.**, *Reliability. Maintainability and Risk. Practical methods for engineers*. Sixth Edition. Butterworth-Heinemann Ltd. New York. 2001.
- [8]. **Tomuș, O.B., Andraș, A.**, *Analysis Of Rock Cutting With Bucket Wheel Excavators Using The Chip Breakout Pattern Method*, North University Baia Mare Scientific Bulletin Series C, Volume XXII (2008) Fascicle Mechanics, Tribology, Machine Manufacturing Technology, pag. 463-466, ISSN 1224-3264;
- [9]. * * *, *Excavatorul cu roată portcupe ERC 1400-30/7 modernizat. Instrucțiuni de exploatare, întreținere și reparare*. Rominex SA Timișoara. 2009.
- [10]. * * *, *Fișe de urmărire a funcționării mașinilor și instalațiilor la EMC Jił.*

IMPROVING THE FUNCTIONAL PERFORMANCES OF THE BUCKET WHEEL EXCAVATORS (BWEs) CUTTING-TEETH

**ILDIKO KERTÉSZ (BRÎNAȘ)¹, ANDREI ANDRAȘ²,
FLORIN DUMITRU POPESCU³**

Abstract: The value of the resultant forces acting on the BWEs cutting-teeth can be determined by calculation or by experimental methods so that the parameters of the working organs and their position during the exploitation process are appropriate to the magnitude of these forces. The deformations and stresses of the cutting-tooth during the excavation process is influenced by its position relative to the working organ (excavator bucket), which is determined by the cutting-tooth fitting mode. In this paper we will analyze the deformations and the stresses in the situation of the currently used cutting-tooth holder and propose another type of holder for which we will do the same determinations. The stress and deformation analysis was performed using SolidWorks® software.

Key-words: BWE, rotor, cutting-tooth, tooth holder, FEM, FEA, stress, deformation.

1. THE INFLUENCE OF THE LOCATION OF CUTING-TEETH ON THE BUCKET, ON THE GEOMETRIC AND STRENGTH PARAMETERS

The positioning and orientation of the cutting-teeth on the cutting edge of the bucket influences their geometry and strength. Overall, the magnitude and direction of the velocity vector are determined by the variation of swiveling velocity v_p (the range of variation being determined by the type of swiveling mechanism). The swiveling velocity v_p is composed with the cutting speed v_t which is considered constant.

¹ *Ph.D. Student, University of Petroșani*

² *Lecturer, Ph.D., Eng., University of Petroșani*

³ *Prof. Habil., Ph.D., Eng, University of Petroșani, fpopescu@gmail.com*

To study the influence of cutting-teeth placement on buckets, on the geometric and strength parameters, the following planes are defined by which the position of each cutting-tooth can be expressed:

1. the setting plane, defined by the cutting edge of the tooth and its positioning face (figure 1);

2. the rake plane, defined by the cutting edge of the tooth and its rake face (Figure 1);

3. the symmetry plane is perpendicular to the cutting edge of the tooth and passes through the middle of the cutting edge of the tooth (Figure 1);

4. the cutting plane, defined by the tooth cutting edge and the resultant vector of velocity (Figure 2);

5. the velocity plane is perpendicular to the cutting plane and contains the resultant vector of velocity (Figure 2).

If the resultant vector of velocity is perpendicular to the cutting edge of the tooth, then the velocity plane and the symmetry plane overlap.

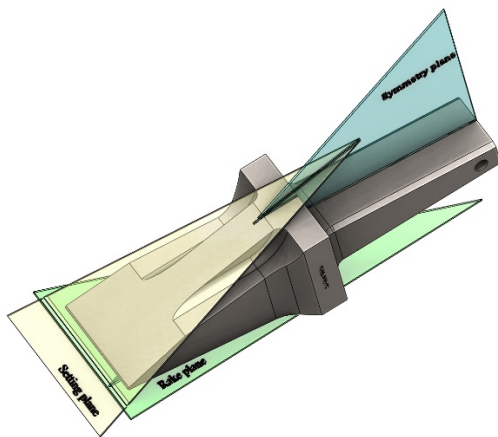


Fig. 1. Planes of setting, rake and symmetry

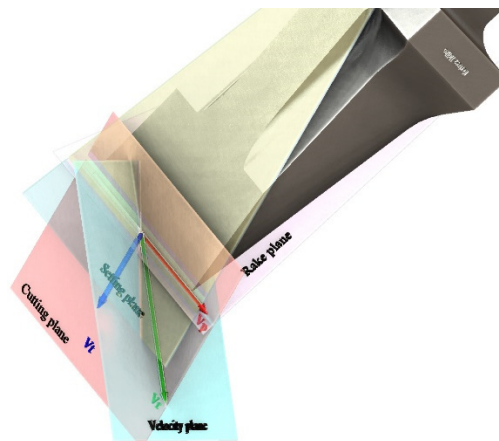


Fig. 2. Swiveling, cutting and resultant velocities; Cutting and velocity planes.

In Figure 2, the setting angle is measured between the setting plane and the cutting plane, and the angle of sharpening is measured between the cutting plane and the rake plane. Here we noted with v_p the swiveling velocity, with v_t the cutting speed and with v_r the resultant speed.

The angle between the line resulting from the intersection of the cutting plane with the symmetry plane and the resultant velocity vector designates the angle of the tooth positioning on the cutting edge of the bucket. Placing the tooth on the cutting edge is done through its holder.

In operation the characteristic angles (figure 3) are:

- the set angle of operation β_f , which is the angle between the resultant velocity direction and the intersection line between the set plane and the velocity plane;
- the cutting angle in operation, which is the angle between the resultant velocity, direction and the intersection line between the rake plane and the velocity plane;
- the sharpening angle in operation, which is the angle between the intersection line of the set planes and the velocity plane, respectively the intersection line between the clearance plane and the velocity plane;
- the raking angle in operation α_f is complementary to the set angle β_f .

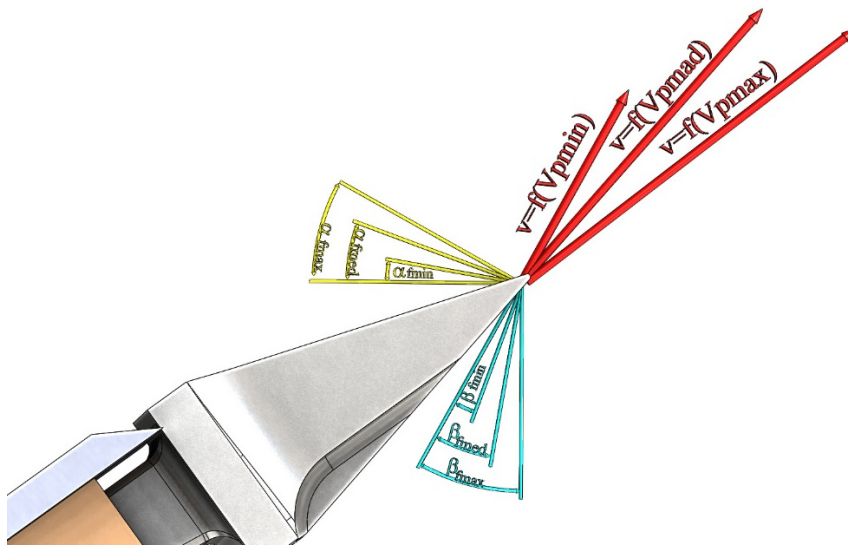


Fig. 3. Characteristic angles in operation.

2. DETERMINATION OF STRESSES AND DEFORMATIONS FOR CHISEL TYPE CUTTING-TEETH USING OLD TOOTH HOLDER

In the past research the University of Petroșani conducted for the Oltenia Power Complex, three types of cutting-teeth for BWEs were proposed. Figure 4 shows the construction of such a tooth, Figure 5 shows the typo-dimensional differences between the three types of teeth. The dimensions correspond to the three distinct categories of excavated material, each having its specific cutting resistance:

1. Overburden rocks that are easily dislocated, having a low specific cutting resistance $A = 200...450$ N/cm;
2. Overburden rocks and lignite with a medium specific cutting resistance $A = 450...800$ N/cm;
3. Lignite having a higher specific cutting resistance $A = 800...1200$ N/cm.



Fig. 4. The cutting-tooth chosen for analysis

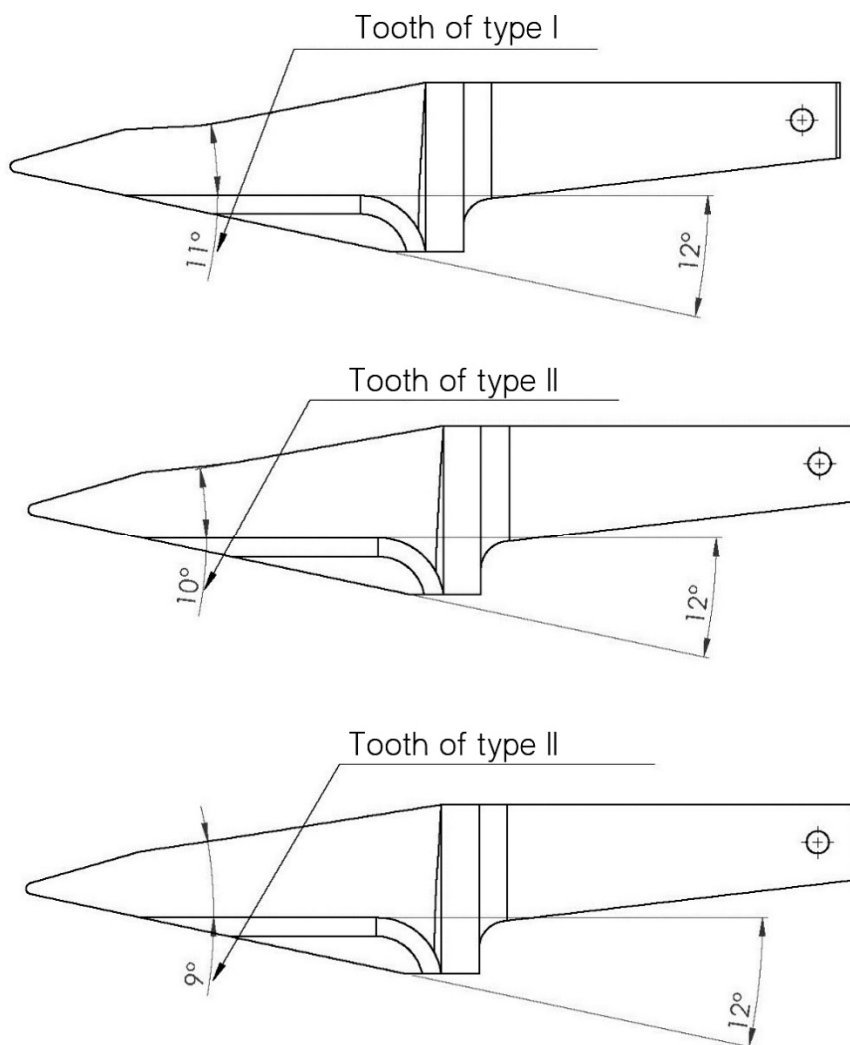


Fig. 5. Typo-dimensions of the proposed cutting-tooth

The stresses on the cutting-tooth are: $F_x = 60 \text{ kN}$; $F_y = 18 \text{ kN}$; $F_z = 10 \text{ kN}$.
 In relation to tooth surfaces we will have the following component forces:

$$F_{y1} = F_x \cos \alpha - F_y \cos \gamma = (60 \times \cos 52^\circ - 18 \times \sin 38^\circ) \times 10^3 = 29 \times 10^3 \text{ N} \quad (1)$$

$$F_{x1} = F_x \sin \alpha - F_y \sin \gamma = (60 \times \sin 52^\circ - 18 \times \sin 38^\circ) \times 10^3 = 41,2 \times 10^3 \text{ N} \quad (2)$$

$$F_{z1} = 10 \times 10^3 \text{ N} \quad (3)$$

Figure 6 shows deformation and in Figure 7 the von Mises stress resulting from the FEA on type I when the tooth is mounted with the old tooth holder.

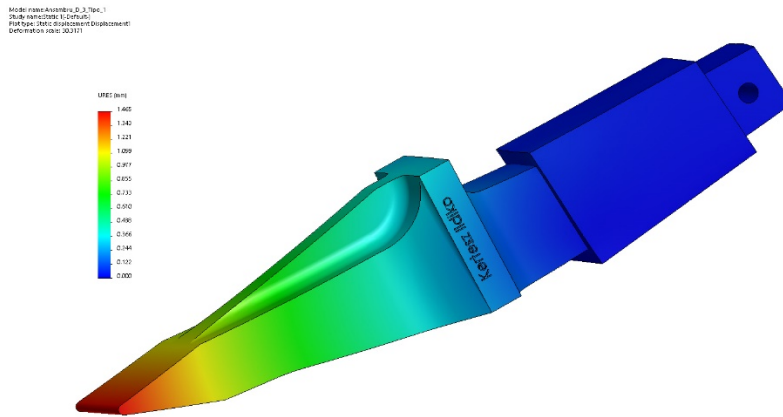


Fig. 6 Type I cutting-tooth deformation, when mounted with the old tooth holder

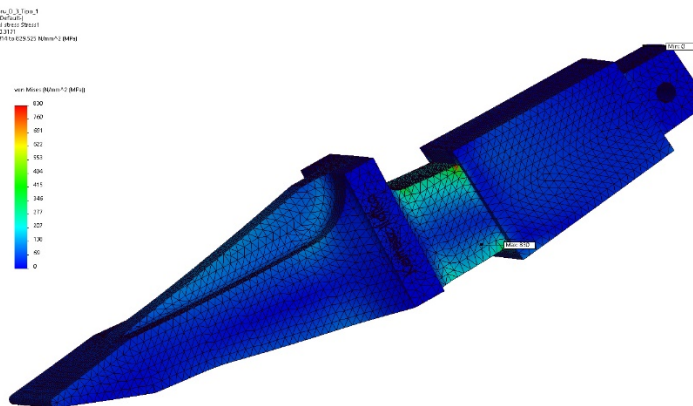


Fig. 7 Type I cutting-tooth von Mises stress, when mounted with the old tooth holder

One can observe that the maximum deformation occurs in the area of the tip of the tooth, and the most stressed points of the tooth structure are those corresponding to its tail, between the tooth-support and the shoulder of the tooth.

3. PROPOSED SOLUTION TO REDUCE STRESSES ACTING ON THE CUTTING-TOOTH

As shown in the previous paragraph, the maximum stress points are located where the section of the tooth - holder assembly presents vaulting. In the present case, it is the area of switching from the tooth holder section to the actual tooth section. Next, we propose and analyze a type of tooth holder that will better encompass the tooth's tail. Figures 8 and 9 show the details of this new version of the tooth holder.



Fig. 8 Proposed holder for fitting the cutting-tooth to the bucket

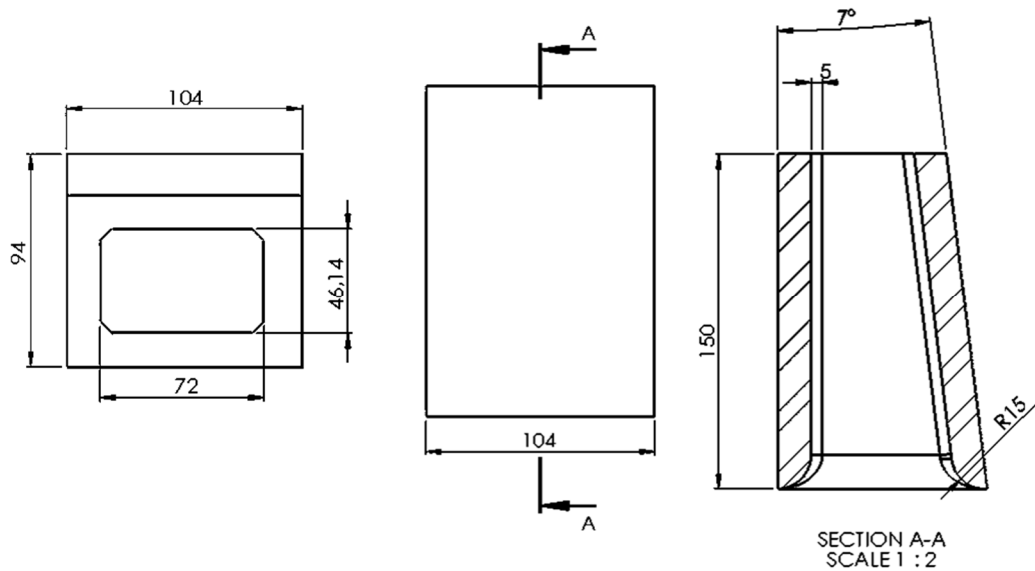


Fig. 9. Dimensions and geometry of the proposed new tooth-support

4. DETERMINATION OF STRESSES AND DEFORMATION FOR THE CHISEL TYPE CUTTING TOOTH USING THE NEW TOOTH HOLDER

By imposing the stresses from paragraph 2, we determined the deformations and stresses of the three typo-dimensions of the tooth proposed for analysis when it is mounted on the buckets with the new tooth holder proposed in paragraph 3.

Figures 10, 12 and 14 show deformations, and figures 11, 13 and 15 shot the von Mises stresses corresponding to the three types. The results obtained using the FEA for these tooth-type dimensions are summarized in Table 1.

The results obtained after FEA of the three types of teeth are summarized in Table 1.

Table 1 Summarized results obtained for the three types of teeth after FEA

No.	Type of tooth	Holder type	Angle	Deformation	Stress
			°	mm	N/mm ²
1	I	Old	11	1,465	829
2		New		0,581	224
3	II	New	10	0,548	215
4	III	New	9	0,523	211

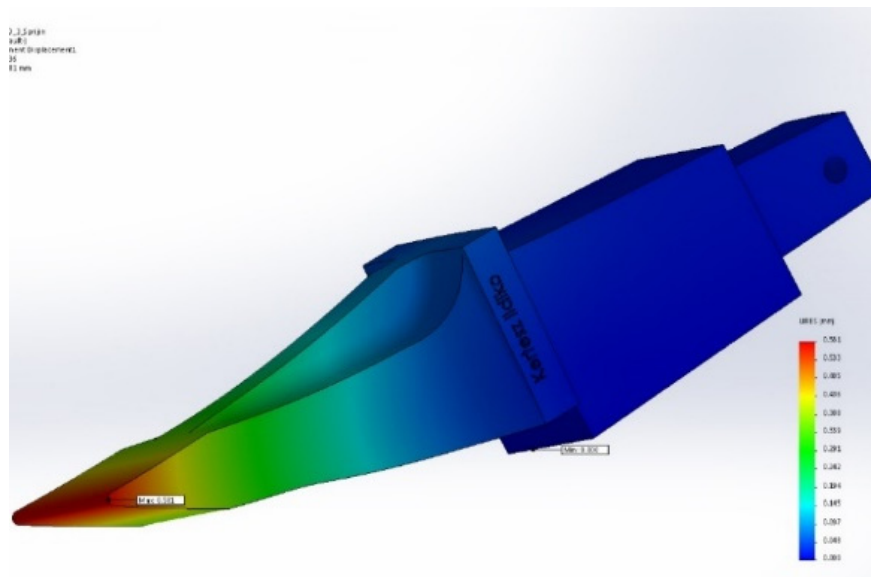


Fig. 10. Type I tooth deformation, when mounted with the new proposed tooth holder

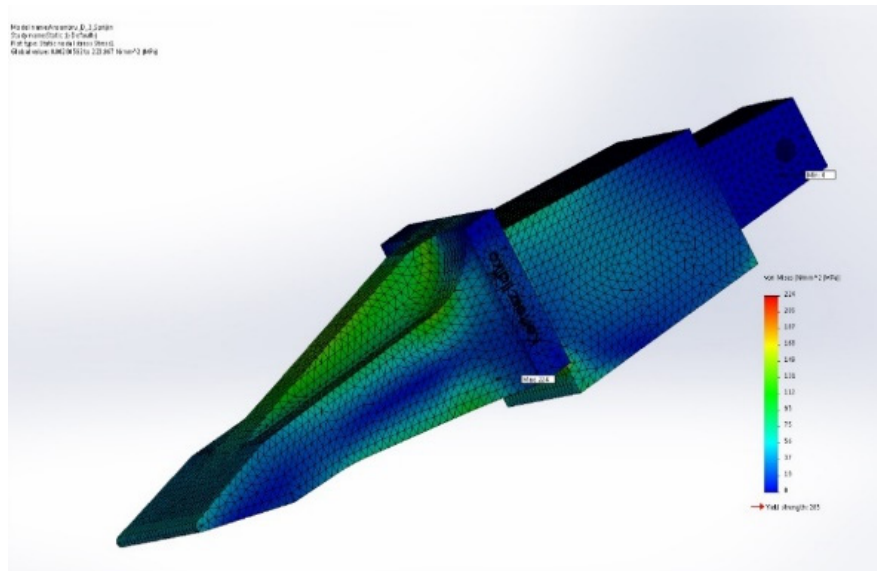


Fig. 11. Type I tooth von Misses stress, when mounted with the new proposed tooth holder

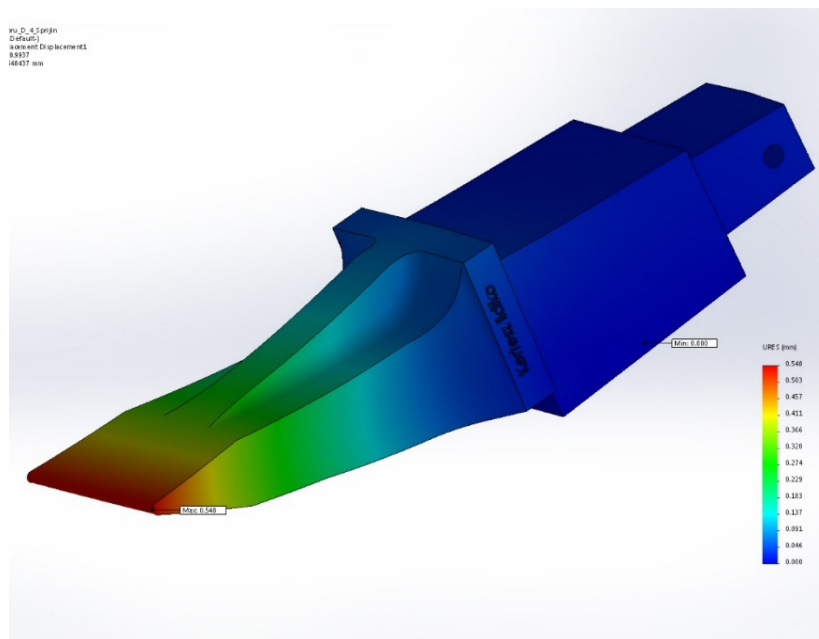


Fig. 12. Type II tooth deformation, when mounted with the new proposed tooth holder

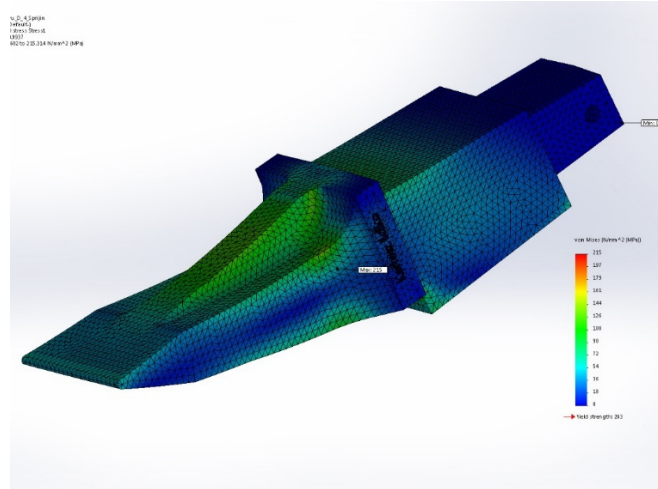


Fig. 13. Type II tooth von Mises stress, when mounted with the new proposed tooth holder

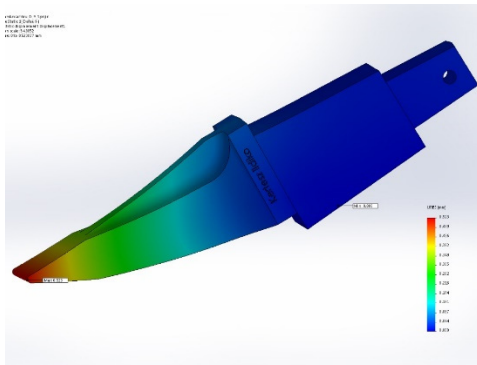


Fig. 14. Type III tooth deformation, when mounted with the new proposed tooth holder

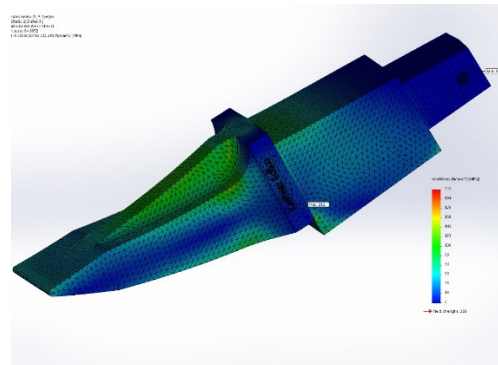


Fig. 15. Type III tooth von Mises stress, when mounted with the new proposed tooth holder

5. CONCLUSIONS

FEA is a numerical analysis method used to solve problems in various fields of engineering. From mathematical point of view, it resolves a set of partial differential equations by methods specific to numerical analysis. In mechanical engineering it is widely used to solve structural, vibration and thermal problems, and because of its numerical versatility and efficiency, this method imposed itself on the engineering analysis software market, while other methods have become niche applications.

The simulation of the cutting-teeth behavior when mounted on the BWEs using FEA, was based on the results obtained over the years by the Department of Mechanical, Industrial and Transports Engineering during research contracts aimed at improving the performance of BWEs operating in the Oltenia Coal Basin.

The analysis was done on three type-dimensions of teeth using FEA. An assembly of tooth and tooth-support was used in all cases. For every scenario we created CAD geometry, FEA geometry, stresses, restrictions and material.

For type I tooth we conducted the analysis in two cases: with the existing, old cutting-tooth holder and the proposed new teeth- holder which better encompass the tooth's tail when mounted. For all three types of teeth it was concluded that:

- in the case of tooth mounting by a holder of the old type, the von Mises tension is maximal in the area of the tooth's tail being located between the holders and the shoulder;

- Mounting the cutting-tooth into the old tooth holder causes the von Mises stress to be maximal in the tail area of the tooth, at the intersection of support and the joint;

- Mounting the cutting-tooth into the proposed new tooth holder makes the von Mises stress to be maximal at the clearance area corresponding to the setting plane of the tooth;

- Regardless of the tooth holder type used, the maximum deformation appears at the tip of the cutting-tooth. It was observed that in the case of the old tooth holder , the deformations are larger than in the case of the proposed new tooth holder;

- It is shown that increasing the sharpening angle results in the decreasing of both the deformations and the von Mises stresses of the cutting-tooth.

The results of this analysis is similar to past results, obtained using analytical methods, of research conducted by the Mechanical, Industrial and Transports Engineering Department.

REFERENCES:

- [1]. Dimirache, G., Zamfir, V., *Ingineria sistemelor mecanice*, Editura Focus, Petroşani 2002;
- [2]. Iliaş, N., *Maşini miniere, exemple de calcul*, Editura Tehnică Bucureşti, 1993;
- [3]. J. Ed Akin, *Finite Element Analysis Concepts via SolidWorks*, World Scientific, 2009;
- [4]. Kovacs, I., Iliaş, N., Nan, M.S., *Regimul de lucru al combinelor miniere*, Editura Universitas, Petroşani, 2000;
- [5]. Kurowski, P., M., *Engineering Analysis with SOLIDWORKS Simulation* 2015;
- [6]. Ladányi, G., Virág, Z., *Examining The Bucket Wheel Excavator's Bucket After Renewal*, Annals Of The University Of Petroşani, Mechanical Engineering, 18 (2016), Pag. 93-98
- [7]. Lazăr, M., Andraş, I., Faur, F., Andraş, A. *Influence Of Physical, Mechanical And Technological Characteristics Of Coal And Overburden Rocks On The Excavation Process*, SGEM2017 Conference Proceedings, ISBN 978-619-7105-00-1 / ISSN 1314-2704, 29 June - 5 July, 2017, Vol. 17, Issue 13, 445-452 pp, DOI: 10.5593/sgem2017/13/S03.057
- [8]. Marian, I. *Utilaje de încărcare și transport minier*, Editura Tehnică, Bucureşti, 1991;
- [9]. Ovidiu-Bogdan, T; Iosif, A; Dumitru, P.F., *Comparative study regarding the break-out angle and specific energy consumption at overburden rock and lignite cutting from Oltenia coalfield*, Quality-Access To Success, Vol. 18, S1, Bucharest, Jan 2017, 386-389 pp. ISSN: 1582-2559. WOS:000417405000072
- [10]. Nan, M., S., *Parametrii procesului de excavare la excavatoarele cu rotor*, Editura Universitas, Petroşani, 2007;

THE ANALYSIS OF THE DEFORMATIONS AND STRESSES OF THE CUTTING-TEETH OF BUCKET-WHEEL EXCAVATORS (BWEs) DURING OPERATION, USING FINITE ELEMENTS METHOD (FEM)

**ILDIKO KERTÉSZ (BRÎNAȘ)¹, FLORIN DUMITRU POPESCU²,
SORIN MIHAI RADU³, CRISTIAN ILIONI⁴**

Abstract: For BWEs, the digging process is influenced by the forces opposing the working elements and cutting tools. These forces determine both the choice of the operating method and the choice of machines and their parameters. The value of the resistance forces can be calculated or determined by experimental methods so that the parameters and positioning of the cutting tools during the excavation process are appropriate to the magnitude of these forces. Studies conducted on failure causes of the mechanical parts show that the cutting and loading systems are causing the highest rate of failure, about 32% of all recorded mechanical failures. In the paper we will use FEM to analyze the deformations and stresses acting on the cutting tooth mounted on the rotor of BWEs. For this, SolidWorks® software was used, both as CAD tool to design the tooth as well as for modeling and simulation of the phenomena.

Key-words: BWE, rotor, cutting-teeth, cutting-teeth support, FEM, force, strain, deformation.

1. STEPS FOR A FEM/FEA APPROACH

The starting point for any project using FEA and simulation is a model that can be a part or a set of parts. First, the characteristics of the material(s) of the parts, the tasks to which they are subject and the restrictions are defined. Subsequently, as with any FEA-based analysis tool, the geometry of the model is divided into relatively small entities called finite elements. Creating finite elements is commonly called meshing.

¹ *Ph.D. Student, University of Petroșani*

² *Prof. Habil., Ph.D., Eng., University of Petroșani, fpopescu@gmail.com*

³ *Prof., Ph.D., Eng., University of Petroșani*

⁴ *Assistant, Ph.D., Eng., University of Petroșani*

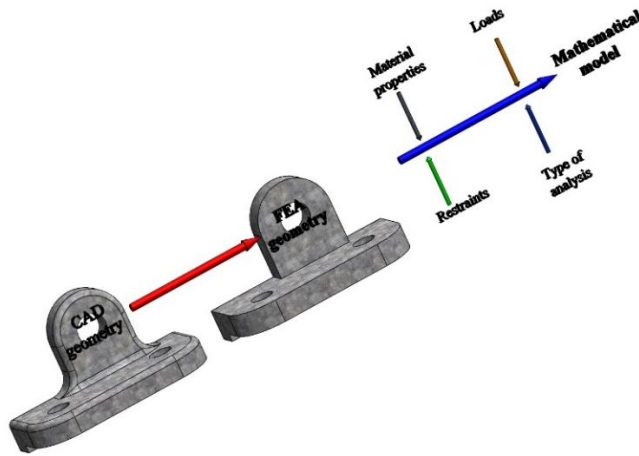


Fig. 1. Creation of the mathematical model.

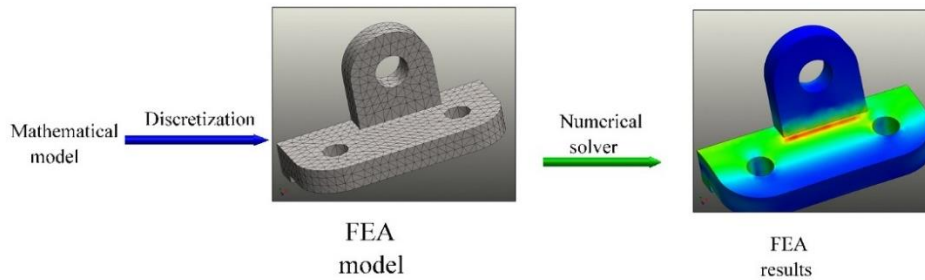


Fig. 2. Building of the FEA model.

Creating the mesh network often requires changes in CAD geometry, which means *canceling* geometric elements, *idealization*, and / or *cleaning*:

- *Canceling* - is the process of removing parts of the geometry that are insignificant to the analysis, such as fillets or bevels;
- *Idealization* - is a more aggressive process of change of the geometry, for example thin walls are replaced with surfaces or beams replaced by lines;
- *Cleaning* - It is necessary for the geometry to satisfy the requirements imposed by the meshing process.

Creating a mathematical model consists of: modifying the CAD geometry (ie – Figure 1 – we removed fillets), defining the loads and strains, imposing the restrictions, defining the properties of the material and the type of analysis (static, dynamic, etc.) to be carried out. The properties of the material, the tasks and the restrictions imposed on the model are the input information for a certain type of analysis.

The mathematical model based on the FEA geometry, the information and properties of the material, the requirements to which the model is subjected, and the imposed restrictions can be divided into finite elements using the meshing process (Figure 2). The discrete loads and restrictions are applied to the nodes of the finite element mesh.

Often, the most difficult step of a FEA study is the analysis of the results. The correct interpretation of the results implies understanding all the simplifications and errors that they induce in the first three stages: defining the mathematical model, meshing, and solving it.

2. VON MISES YIELD CRITERION

The Von Mises stress test criterion, also known as the Huber criterion, is a stress test that represents all six components of a general 3-D state (Figure 3). The general stress is represented by three normal stresses σ_x , σ_y , σ_z and six tangential or shear stresses. Due to the symmetry of shear stresses, the 3D general tension state is characterized by six components: σ_x , σ_y , σ_z and $\tau_{xy} = \tau_{yx}$, $\tau_{yz} = \tau_{zy}$, $\tau_{zx} = \tau_{xz}$. Von Mises stress can be expressed by the equation:

$$\sigma_{vm} = \sqrt{0,5 \times \left[(\sigma_x - \sigma_y)^2 + (\sigma_y - \sigma_z)^2 + (\sigma_z - \sigma_x)^2 \right] + 3 \times (\tau_{xy}^2 + \tau_{yz}^2 + \tau_{zx}^2)} \quad (1)$$

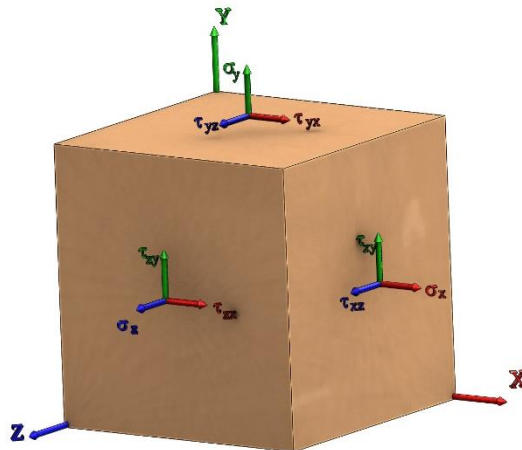


Fig. 3. The general state of stresses

Von Mises stress is frequently used for the structural safety analysis of materials with elasto-plastic properties (such as steel or aluminum alloys). In theory, a ductile material yields when the von Mises stress equals the permissible stress limit. In most cases, the flow limit is used as stress limit. According to the von Mises criterion in case of failures, the factor of safety (*FOS*) is expressed as:

$$FOS = \frac{\sigma_{limit}}{\sigma_{vm}} \quad (2)$$

where σ_{limit} is the flow limit.

3. THE GEOMETRIC PARAMETERS OF THE TEETH OF BWEs

The geometry of the cutting- teeth of the BWEs is influenced by:

- the functional parameters of the excavator;
- the constructive parameters of the cups (Figures 4) and the rotor (Figure 5);
- the shape and the type of the cutting-teeth used;
- the type of excavated material;
- cost.



Fig. 4. The bucket with cutting teeth of a BWE

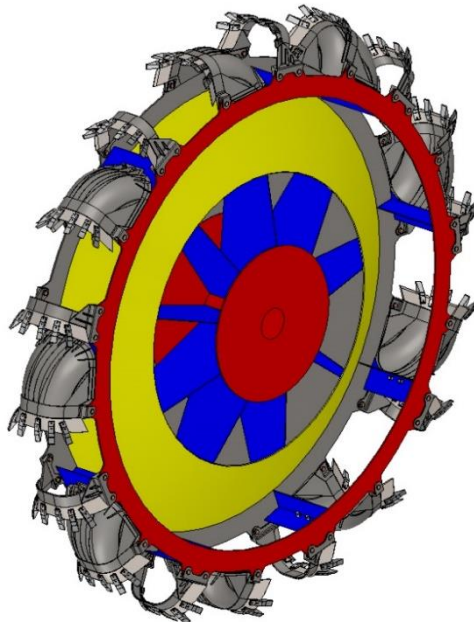


Fig. 5. The rotor assembly of a BWE

There are two types of cutting-teeth: 1 - chisel shaped cutting-teeth used on BWEs. 2 - Conically shaped cutting-teeth, used on both single bucket excavators and shearer-loader machines.

In figures 6 and 7 we present a chisel shaped cutting-tooth that is mounted on E_sR_C – 1400 type BWEs used in Oltenia Basin open-pit lignite mines. From the point of view of the geometric parameters, two types of cutting-teeth are needed. One for overburden excavation and the other one for lignite excavation. In Table 1 the geometric parameters of the analyzed cutting-teeth are shown.

Table 1 Geometric parameters of the analyzed cutting-teeth

No.	Geometric parameters	Symbol	Dimensions of the cutting-tooth		Obs.
1.	Angle of clearance	α	55°	52°	$\alpha+\beta+\delta=90^0$
2.	Set angle	β	7	7°	
3.	Angle of sharpening	δ	28°	31°	
4.	Cutting angle	γ	35°	38°	$\gamma+\alpha=90^0$
5.	Longitudinal lateral angle	ξ	5°	5°	-
6.	Transverse lateral angle	θ	3°	3°	-
7.	Rake angle	φ	13°	13°	-
8.	Cutting edge width	b	120	120	-

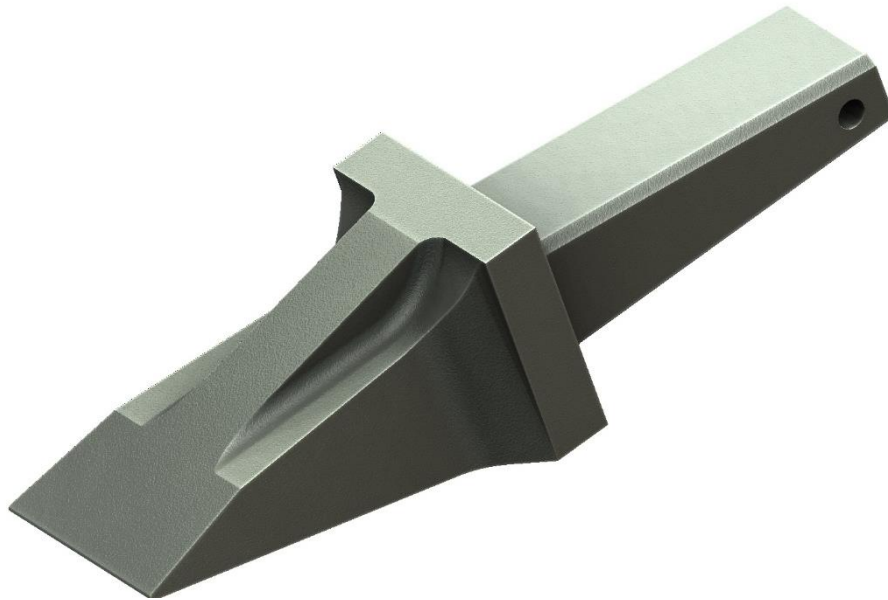


Fig. 6. Chisel shaped cutting-tooth with support bracket used in open-pit coal mines in Oltenia Basin

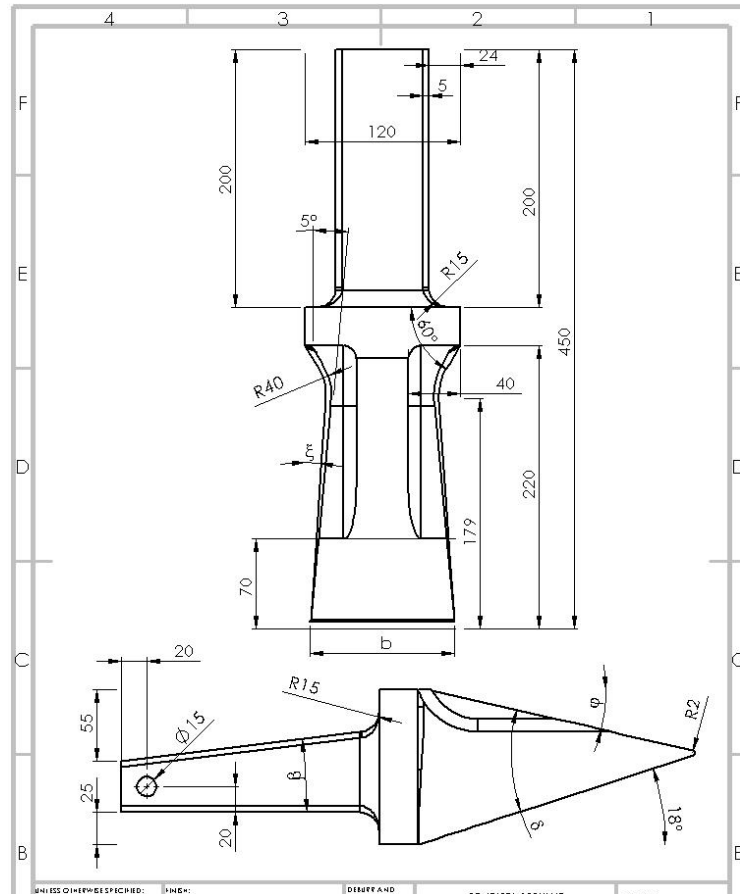


Fig. 7. Geometric dimensions of the chisel shaped cutting-tooth with support bracket used in open-pit coal mines in Oltenia Basin

4. DETERMINATION OF STRAINS AND STRESSES OF THE CUTTING-TOOTH USING SOLIDWORKS®

For a realistic approach, the FEA was conducted on an assembly of a cutting-tooth and its cup holder support bracket. When creating this assembly, we set up the geometrical links between the two components. Figure 8 shows the restrictions (fixation condition) imposed on the analyzed assembly.

The maximum tangential and normal cutting forces at the tooth's trajectory were considered, as well as the lateral force generated by the pivoting movement. These forces have the following values:

$F_x = 60 \text{ kN}$; $F_y = 18 \text{ kN}$; $F_z = 10 \text{ kN}$. With respect to the tooth surfaces we will have the following component forces:

$$F_{y1} = F_x \cos \alpha - F_y \cos \gamma = (60 \times \cos 52^\circ - 18 \times \sin 38^\circ) \times 10^3 = 29 \times 10^3 \text{ N} \quad (3)$$

$$F_{x1} = F_x \sin \alpha - F_y \sin \gamma = (60 \times \sin 52^\circ - 18 \times \sin 38^\circ) \times 10^3 = 41,2 \times 10^3 \text{ N} \quad (4)$$

$$F_{z1} = 10 \times 10^3 \text{ N} \quad (5)$$

For these forces, the state of stresses for a cutting-tooth with a sharpening angle of 28° - which has a more lean construction - were determined. These forces are the resultant forces of specific loads having a random distribution on the active faces of the cutting-tooth, which, for calculations, were considered as applied to the tip of the cutting-tooth (Figure 9).

The material used for simulation is *41MoCr11*, or equivalent to $\sigma_{02} = 750 \text{ N/mm}^2$, $\sigma_r = 950 \text{ N/mm}^2$ (medium hardened alloy steel, recommended for thermal treated parts).



Fig. 8. Fixation conditions of the cutting-tooth

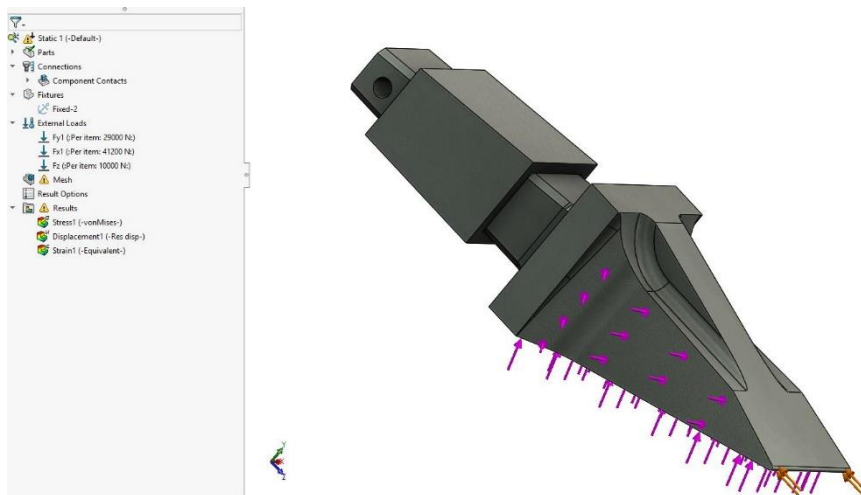


Fig. 9. The forces that act on the tooth

Figure 10 shows the cutting-tooth mesh nodal network, and Figure 11 shows the deformations of the cutting-tooth resulting from the FEM analysis. It can be noticed that the maximum deformation is 0,665 mm and occurs at the tip of the cutting-tooth.

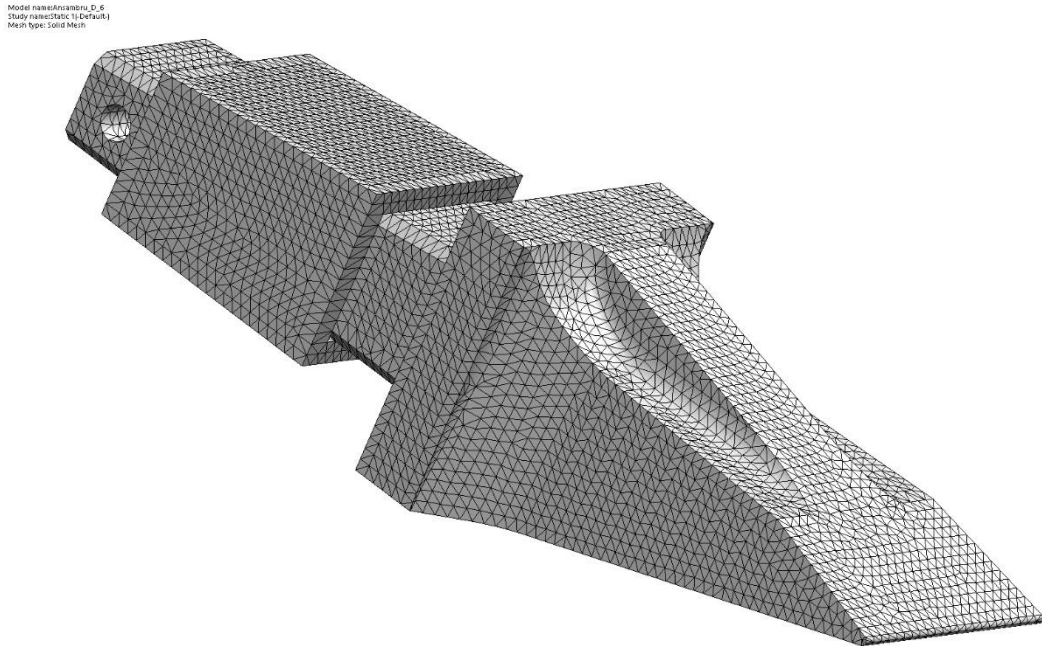


Fig. 10. The mesh nodal network

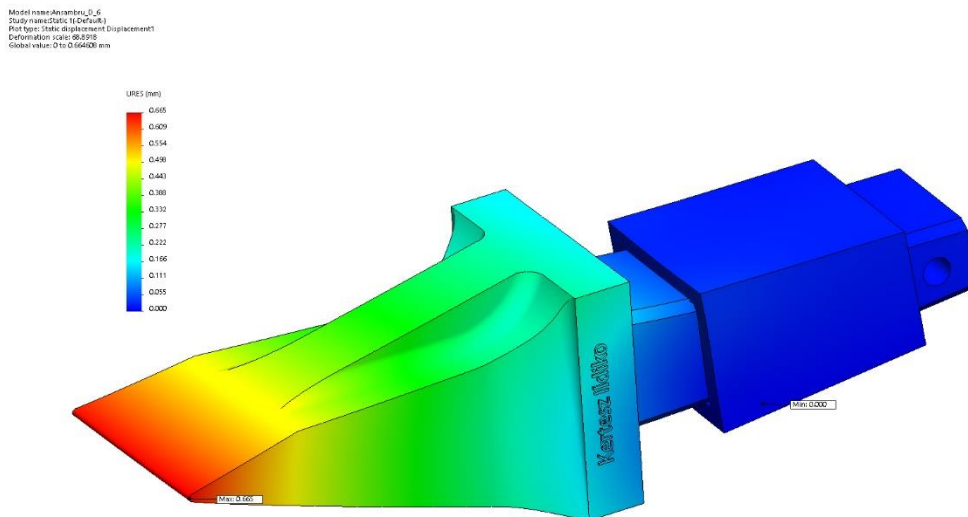


Fig. 11. Deformation of the cutting-tooth and its cup holder support bracket assembly

Based on Figure 12 it can be observed that the most stress occurs on the tail part of the cutting-tooth, between its holder and joint. The maximum von Mises stress is 332 N/mm².

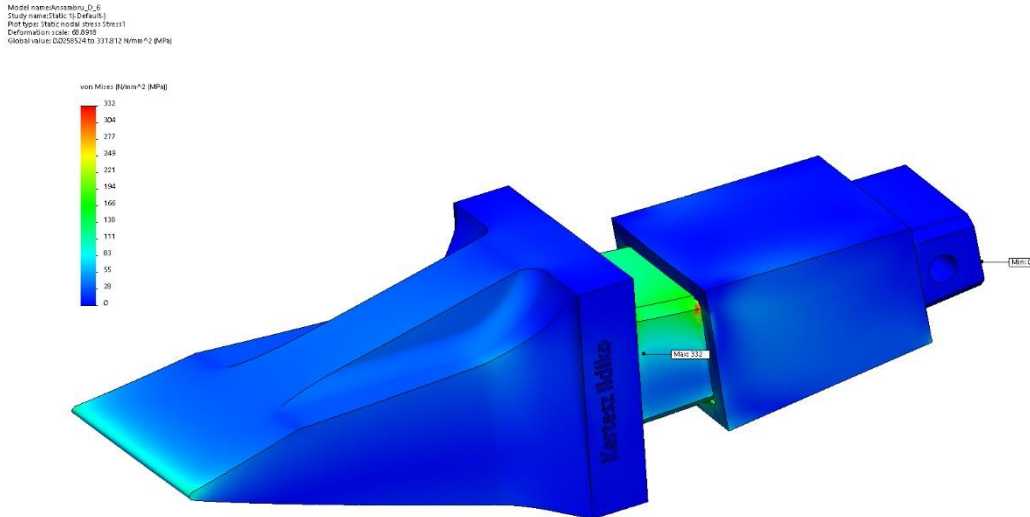


Fig. 12. Stress of the cutting-tooth and its cup holder support bracket assembly

CONCLUSIONS

FEM is a numerical analysis method used to solve problems in various engineering fields. In mechanical engineering it is widely used to solve structural, vibration and thermal problems, and because of its numerical versatility and efficiency, this method imposed itself on the engineering analysis software market, while other methods have become niche applications.

FEM/FEA is mainly used during the product development phase to analyze a project. The ultimate goal of using FEA as a design tool is to change the standard repetitive cycle of design → prototype → test into a simplified process in which prototypes are not used as design tools, but rather as validation of the final design.

Using FEA makes design iterations shift from the physical space of prototypes and testing into the virtual space of computer simulation.

The simulation of the behavior of cutting-teeth mounted on the BWEs using FEA was based on the results - obtained over the years by the Department of Mechanical, Industrial and Transport Engineering – of the research contracts aimed at improving the performance of BWEs used in open-pit mining in the Oltenia Basin

The results obtained using this method are consistent with those determined by analytical methods in the research studies conducted within the MITE Department:

- Mounting the cutting-tooth into a cup holder causes the von Mises stress to be maximal in the tail area of the tooth, holder and the joint;
- The maximum deformation occurs at the tip of the cutting-tooth.
- It is necessary to design a new holder that will encase the cutting-tooth better, and to carry out a study, using simulation and modeling, of the deformations and the stresses in this new configuration;

REFERENCES:

- [1]. **Andraş, A., Andraş, I., Tomuş, O.B.**, *Optimization of geometric and strength parameters of teeth for bucket wheel excavator in view to increasing the cutting efficiency*, 17th International Multidisciplinary Scientific GeoConference, SGEM 2017, Conference Proceedings, ISBN 978-619-7105-00-1 / ISSN 1314-2704, 29 June - 5 July, 2017, Vol. 17, Issue 13, 607-612 pp, DOI: 10.5593/sgem2017/13/S03.077
- [2]. **Dimirache, G., Zamfir, V.**, *Ingineria sistemelor mecanice*, Editura Focus, Petroşani 2002;
- [3]. **Iliş, N.**, *Maşini miniere, exemple de calcul*, Editura Tehnică Bucureşti, 1993;
- [4]. **J. Ed Akin**, *Finite Element Analysis Concepts via SolidWorks*, World Scientific, 2009;
- [5]. **Kovacs, I., Iliş, N., Nan, M.S.**, *Regimul de lucru al combinelor miniere*, Editura Universitas, Petroşani, 2000;
- [6]. **Kurowski, P., M.**, *Engineering Analysis with SOLIDWORKS Simulation 2015*;
- [7]. **Ladányi, G., Virág, Z.**, *Examining The Bucket Wheel Excavator's Bucket After Renewal*, Annals Of The University Of Petroşani, Mechanical Engineering, 18 (2016), Pag. 93-98
- [8]. **Marian, I.**, *Utilaje de încărcare şi transport minier*, Editura Tehnică, Bucureşti, 1991;
- [9]. **Nan, M., S.**, *Parametrii procesului de excavare la excavatoarele cu rotor*, Editura Universitas, Petroşani, 2007;
- [10]. **Nan, M.S., Kovacs, J., Popescu, F.D.**, *Balance control by weighting and tensiometric measurements of bucket wheel excavators*, WSEAS Transactions On Systems And Control, Issue 11, Volume 3, November 2008, ISSN: 1991-8763, pp. 927...936;
- [11]. **Pop, I.A., Itu, R.B., Radu, S.M.**, *Applications of forces reduction in the calculation of technological mechanical loads transmitted to the tower of a winding engine trough extraction pulley bearings*, 16th GeoConference on Science and Technologies in Geology, Exploration and Mining SGEM 2016, Conference Proceedings, Albena, Bulgaria, 30.06-6.07.2016, Book 1, vol. II, pp. 49 – 56, ISBN 978-619-7105-56-8, ISSN 1314-2704, DOI: 10.5593/SGEM2016/B12/S03.017
- [12]. **Popescu, F.D.**, *Aplicaţii industriale ale tehnicii de calcul*, Editura AGIR, Bucureşti, 2009, ISBN 978-973-720-234-5;
- [13]. **Radu, S.M., Chmielarz, W., Andras, A.**, *Mining Technological System's Performance Analysis*, Annals of the University of Craiova for Journalism, Communication and Management, nr. 2/2016, pp. 56-64, ISSN 2501-3513.
- [14]. **Zamfir, V., Dimirache, G.**, *Teoria mecanismelor pentru sisteme automate şi roboţi industriali: Notiţe de curs*, Editat la Universitatea din Petroşani, 1996.

STRENGTH ASSESSMENT OF A TRUSS BRIDGE FOR BELT CONVEYORS

GÁBOR LADÁNYI¹

ABSTRACT: The paper presents the results obtained after a stress assessment of a reusable truss bridge used for belt conveyors. This analysis was conducted at the request of Mátrai Erőmű ZRt (Matra Powerplant SA). The results were in favor of reusing this truss bridge, as it has a sufficient reserve up to the limit stress producing remaining deformation.

Keywords: truss bridge, strength assessment, conveyor belt, safety factor, slenderness ratio

1. INTRODUCTION

The Visonta open-pit mine belonging to Mátrai Erőmű ZRt (Matra Powerplant SA) has reached a state where the changes which have to be applied require the radical modification of the conveying system. According to the new structure, the overburden rock conveying route will cross the track of lignite one. One possible solution to this problem is to lift one conveying line over the other one. The mine 's specialists decided to do this. That implies the re-use of an already built in, but long time not used belt conveyor gangway truss bridge, which can be seen in the photo below (Figure 1).

However, in the new function, the belt conveyor to be incorporated in the bridge is wider than the previous built-in unit, and then the total mass of the conveyor elements is also greater than the previous operation load of the bridge.

Another substantial difference is that before, the unit was installed in the lignite conveying track, and, according to the new function it will convey overburden rock. As the bulk density of the two material is different, the overburden's one being significantly higher than the lignite's one. This fact is also producing extra load relative to the previous operating situation.

¹ *Assoc. Professor Eng. Ph.D., University of Miskolc, gtblaga@uni-miskolc.hu*



Fig. 1. Conveyor gangway truss bridge to be assessed

Taking into account the previously presented facts, the strength assessment of the bridge in order to verify the possibility to be used in the new conditions became compulsory. The task has been accomplished buy the author with the support of a team from the Institute of Technical Mechanics from the University of Miskolc.

2. STRENGTH ASSESMENT OF RELIABILITY INDICATORS

Before the strength assessment, a visual inspection of the bridge at its actual setting location has been performed. This inspection revealed o high level of corrosion on all the elements, which suggested the possibility of a possible cross section reduction of the constitutive parts.

In the strength assessment we used the actual state of the elements, obtained by a precise measurement of each member actual cross section, dimension and the nodes (joints) exact coordinates. This survey revealed that the structure is asymmetric, from two points of view:

- The entire truss of 23m length is composed by ten equal length (2,3m) cells. In these cells, the diagonal brackets are reciprocally perpendicular to the symmetrical one, but their arrangement among the ten cells is not symmetrical, as usual, from ten they are six in one direction and only four oriented on the perpendicular direction with the first ones. (see fig. 2)

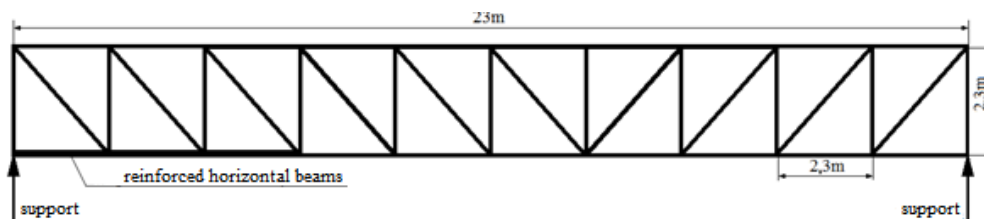


Fig. 2. Schematic drawing of the truss

- The lower beams, on the first three cells on one end are significantly reinforced (on left and right side)

During the calculations, this reinforcement of the longitudinal beams was not taken into account. It was calculated as if the original support structure and cross section worked at the full length of 23m.

However, the asymmetrical lattice structure was considered, and in the model, we used the cell structure shown in Figure 2.

2.1. The loads taken into account during the inspection

The self-weight of the structure is calculated using the actual geometric data by the FE program and it is taken into account as a constant load. In our case, the weight is 60 kN (considering $\rho_{Fe} = 7.8 \text{ t/m}^3$). In addition, the weights from the following masses were taken into account:

1. The weight of the steel structure elements of the belt conveyor skeleton = 60 kN

2. The weight of the belt = 30 kN

3. Weight of the transported material = 180 kN

The total weight calculated under points 1, 2 and 3 together: $G = 60 + 30 + 180 = 270 \text{ kN}$

During the calculations, this force was operated as uniformly distributed to eighteen parts. Then, the resulting partial forces were assigned as concentrated force to the 9 - 9 nodes between the ten cells of the truss. (See Figure 3)

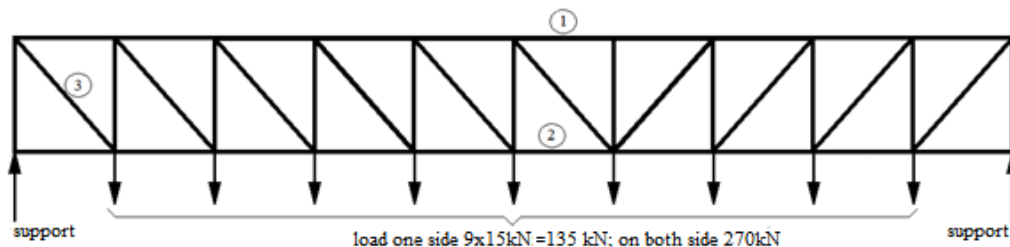


Fig. 3. Distribution of supplementary load on the nodes

2.2. The results of the assessment and the deductible conclusions

So, the load on the lattice structure was given, out of the self-weight by the 270 kN force. This last was allocated for calculation as 18 equal loads to 9+9 nodes located in the lower plane of the structure (left and right side). (See explanatory figure 3.) Thus, in the load-bearing structure, the 15 kN force applied at the nodes, out of the self-weight has been applied. This is the load status A.

As in the case of structures similar to the tested bridge, the bars with the highest load are at 3 typical locations of the grid, indicated in Fig. 3, in Table 1 the forces and stresses in these bars are shown.

Table 1 The A load status results on 3 typical bars

No of bar	Load [kN]	Stress value [MPa]	Stress direction
1	205	60	Compressed
2	197	90	Tensioned
3	129	70	Tensioned

Since the yield strength of structural steels (σ_f or R_m) in general applications reaches 310 MPa, it can be concluded that the stress on the highest load bearing rods is significantly below the residual deformation limit of 310 MPa.

The overall width of the metallic skeleton of the belt conveyor to be implemented on the bridge (~2800mm) exclude the installation of any walking pad inside the structure, because the available space between the two-lateral gridlers is about 3000mm. By our opinion, it is possible, in order to solve accessibility, to mount on one of the lateral gridlers a cantilever support for the walking pad.

This construction is similar to what the on the mining machinery - excavators, spreaders etc. - we can observe. Due to the weight of the cantilever mounted walking pad on the truss structure, there is some extra weight compared to the A state. This was modeled in another calculation by increasing the force applied at the nine load points on one side by 1,5 kN.

So, in this case, $9 \times (15 + 1.5) = 148.5$ kN was operated on one side. Thus, the asymmetric load produces torsional stress on the structure as well as the slight increase in overall load. ($\Sigma = 283,5$ kN) This is the load status B. The forces and stresses in the selected rods are given in Table 2 when using the B load.

Table 2 The B load status results on 3 typical bars

No of bar	Load [kN]	Stress value [MPa]	Stress direction
1	225	66	Compressed
2	216	98	Tensioned
3	142	81	Tensioned

Comparing the results in the two tables, it can be stated that the increase from A to B is about 10%.

In the third load state C, the dual U-holder in the lower plane of the structure was loaded with a distributed force resulted from the previous test, with two 15 and 16.5kN partial forces at the end of the support, totaling $15 + 16.5 = 31.5$ kN. The value of the forces acting on the selected rods and the stresses awaiting them in the state C are given in Table 3.

Table 3 The C load status results on 3 typical bars

No of bar	Load [kN]	Stress value [MPa]	Stress direction
1	206	70	Compressed
2	195	91	Tensioned
3	128	85	Tensioned

Looking at the reduced stresses of the three load states, we see that the highest value, 98 MPa, occurs in the case of type B load. Compared to this, an average steel yield flow stress is $\sigma_f = 310 \text{ MPa}$. The ratio of the two values can be interpreted as a static safety factor (n):

$$n = \frac{310}{98} = 3,16 \quad (1)$$

This can characterize the reserve available in the structure up to the failure. From this point of view, 3,16 is a really comforting value.

Since the rods of the upper chord of the grid structure are compressed, the buckling safety of these rods must be examined separately. According to the tables, the highest compressive load is given by the 225 kN force, so we count further with this value.

Basic data of the analyze:	Bar length:	$l = 2,3 \text{ m}$
	Cross section:	$A = 3800 \text{ mm}^2$
	Load:	$F = 225 \text{ kN}$
Calculated values:	Effective length:	$l_0 = l/2 = 1,15 \text{ m}$ (fixed ends)
	Radius of Gyration:	$i = 30,8 \text{ mm}$
	Slenderness ratio:	$\lambda = l_0 / i = 1,15/0,0308 = 38$

The slenderness ratio $\lambda = 38$ is smaller than the critical value $\lambda_{cr} = 105$ for steel rods. This means that the studied rod is so called short rod in which the failure stress can be calculated from the yield limit of the material by the Tetmajer's relationship.

$$\rho_k = \rho_f - 1,14 \cdot \lambda = 310 - 1,14 \cdot 38 = 267 \text{ MPa} \quad (2)$$

The stress in the rod as the result of the load:

$$\rho = \frac{F}{A} = \frac{(225 \cdot 10^3) \text{ N}}{3800 \text{ mm}^2} = 59 \text{ MPa} \quad (3)$$

From the previous two results we obtain the safety factor to buckling

$$k = \frac{267}{59} = 4,52 \quad (4)$$

The 4,52 safety factor is a guarantee that the compressed bars do not fail by buckling.

3. CONCLUSIONS

In summary, it can be concluded that the forces and stresses awakening under the loads taken in consideration do not cause the bridge failure because it has a sufficient reserve up to the limit stress producing remaining deformation.

4. ACKNOWLEDGEMENTS

The described work/article was carried out as part of the „Sustainable Raw Material Management Thematic Network – RING 2017”, EFOP-3.6.2-16-2017-00010 project in the framework of the Széchenyi2020 Program. The realization of this project is supported by the European Union, co-financed by the European Social Fund.

REFERENCES

- [1] **Korányi, I.**, *Tartók sztatikája II/1-2.* (TK)
- [2] **Dr. Szabó, J., Dr. Roller, B.** *Rúdszerkezetek elmélete és számítása*
- [3] **Hopkins D.A., Halford, G.R., Patnaik, S.N.**, *Integrated Force Method Solution to Indeterminate Structural Mechanics Problems*
- [4] **Nan, M.S., Kovacs, I., Popescu, F.D.**, *Research regarding the improvement of the methodology and means used for the balancing by weighting of bucket wheel excavators*, SMO 08: Proceedings Of The 8th Wseas International Conference On Simulation, Modelling And Optimization, Page: 94-+, 2008. WOS:000262950300013

VIBRATION AND CURRENT SIGNATURE MONITORING EXPERIENCES AT THE MÁRKUSHEGY MINE PLANT

GÁBOR LADÁNYI¹

ABSTRACT: The paper presents the results obtained during the years of vibration and current signature monitoring at Márkushegy mining plant, before its final closure. The large amount of recorded data has been used for a statistical analysis, being useful for deriving conclusions regarding the incidence of different kind of faults occurred at main underground and surface equipment of an underground coal mine. The importance of inter-inspection time period on the capability of monitoring to increase up-times is revealed. The gained experience, which is disseminated in the paper could be a valuable guideline to design the condition-based maintenance of operating mines.

Keywords: condition-based maintenance, vibration monitoring, current signature inspection, fault prediction

1. FOREWORD

The mining plant in Márkushegy, Hungary's last underground coal mine, which has been continuously producing since 1981, was closed in 2016. At the end of the mining activity, complementary activities also ended, the execution of which supported, (sometimes being indispensable) the core activity, coal production.

Such activity was the running of vibration diagnostic measurements for information on status-dependent maintenance of the units operating in the mine, in production and transportation.

At the end of the 1990s, the tools of vibration diagnostics were used in the mine to assess the status of individual units. The actual paper aim is the dissemination of knowledge gained and experience accumulated between 2005 and 2016, as result of this activity.

Initially, only the drive units of the belt conveyors in the surface transport flow were supervised. Over the years, the surveillance was expanded to other equipment that

¹ *Assoc. Professor Eng. Ph.D., University of Miskolc, gtblaga@uni-miskolc.hu*

played the same important role in the good operation of the mine. In the last few years, the following groups of machines were submitted to vibration monitoring and diagnostics:

- belt conveyor drives, both surface and underground operating units;
- sieves
- breakers (crushers)
- longwall drum shearer-loaders
- mine hoists
- ventilators.

2. MATERIAL AND METHOD

The extent limitations of the paper do not allow to present the schemes of measuring set-up for each group of above listed equipment.

The most important measurement requirements were imposed by the belt conveyor driving unit (electric drives, clutches, gear unit), therefore we show in fig. 1. the measuring set-up layout of this one.

As it can see, for the diagnosis of one driving unit we used several measuring points and directions. In the case presented in fig. 1, their number is 18, which is motivated by the extent of the unit and the number of bearings from inside.

In the table 1 we summarized the equipment groups listed above, with their number of units and the corresponding number of measuring points (directions), their total amount being 550.

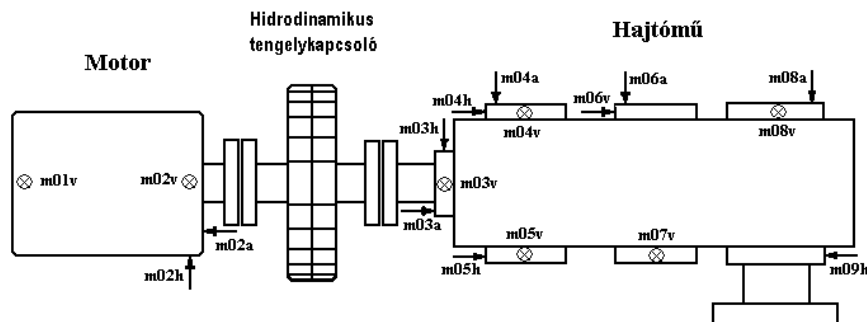


Fig.1. Measuring set-up layout of a belt conveyor driving unit

For each point, at least two spectra were recorded, which means 1100 spectra. As the inspection of a unit is performed twice per year, and for certain units, three times per year, that means 2200 spectra.

Given the huge amount of measurements, the recorded spectra in ten years of monitoring activity represents a strong data warehouse, from which, valuable information can be gained by using simple statistical tools.

Table 1. Machines which were examined by vibration diagnosis

	Equipment	Components	Number of examined equipment	Number of measuring points
1.	Belt conveyor driving units	Electric motors Gear drives Clutches	21	450
2.	Sieves	Electric motors Shaft bearings Belt drives	2	24
3.	Breakers	Electric motors Shaft bearings Belt drives	2	18
4.	Mine hoists	Electric motors Gear drives Clutches	1	18
5.	Drum shearer-loaders Ranging arms	Electric motors Drum drive gear-chain	3	30
6.	Ventilators	Electric motors Bearings	3	12

Starting with October 2008, additionally to vibration diagnosis measurements, electric current signature diagnosis measurements were performed. The mine's numerous machines and equipment are actuated with three phases, squirrel-cage rotor electric motors.

At this kind of motors, after long operating time, damage of the rotor's conductor bars (cage) occurs, mainly when they are frequently started under load. As a result, the internal electric resistance of the rotor increases, the characteristic of the motor became weak, and consequently even at reduced load its speed decreases rapidly.

This kind of harm is easy to be detected by analyzing the motor's current signature. For detailed description of this issue see [5]. This diagnosis monitoring method has been introduced for the critical electric motors, as presented in the table 2.

Table 2. Electric motors monitored by the current signature analysis method

Equipment	Rated voltage	Rated power	Number
3 – phase electric motor	1kV; 6kV	160-500kW	>80

The motor's rated power range was 160-500 kW and their rated voltage was mainly 6 kV, for which the measurements were performed using current measuring transformers. Smaller amount of motors was mainly those from the face equipment driving units, at 1 kV voltage and power at the bottom of the range. As they are operating in harsh environment, their monitoring was very motivated.

3. RESULTS

In the tables 3 to 8 the location, description and occurrence number of detected damages are presented.

Table 3. Bearing faults

	Equipment	No.	Symptom description
1.	Mine hoist	1	Motor is noisy, vibrate
2.	Inclined shaft driving unit	1	High vibration level at the fast stage shaft
3.	Belt conveyor drum bearing	1	Dry (not lubricated) run
4.	Belt conveyor drum bearing is tightened	1	Diagnosed based on temperature increase
5.	Inclined shaft driving unit fast stage shaft bearing	1	High vibration level
6.	Belt conveyor in the 67 roadways	1	Shaft is loose in the bearing
7.	Inclined shaft NU324 electric motor bearing	2	Detected by vibration signal
8.	Lubrication improvement proposals	5	Improper lubrication consequences
9.	Sieve's motor bearing	1	Noisy bearing
10.	Breaker bearing housing destroyed	1	NOT foreseen by diagnosis because of long inter-inspection time
11.	Breaker bearing housing loose	1	Wear of a crushing beam (disc) from breaker (crusher) rotor
	Total	16	

Table 4. Clutches faults

Equipment	No.	Symptom description
Misalignment of coupled shafts	5	High vibration level both side of the coupling clutch
Unbalanced, loose connection	11	Usually sealing rings fault
Crackling noise	1	
Total	17	

Table 5. Gear faults

Equipment	No.	Symptom description
Toothed wheel fault	6	Usually bevel gear toothed wheel pair
Mine hoist main gear	1	Unusual frequency
Total	7	

Table 6. Broken cage bars

Equipment	No	Symptom description
Rotor cage damaged	12- From current signature measurement	Broken bars in the cage
High vibration; Vibration, rubbing	3- From vibration measurement	Many cage bars broken and/or bearing fault
Total	15	

Table 7. Loosening

Equipment	No	Symptom description
Sieves	1	Loose bearing support
Electric motor	1	Resonance of support
Gear casing loose	1	Fasteners fault
Motor casing rubbing	1	Rotor-stator contact
Shaft eccentricity	1	Loose
Total	5	

Table 8. Other faults

Equipment	No	Symptom description
Ventilation problem at L3 motor	1	Obturation by dirt
Overheating of K1/1 motor	1	The brake is not released in operation
Torque compensator tighten	1	
Two driving units temperature difference	1	Thermal imaging
Shearer -loader case rubbing	1	Cap pressed the bearing
Total	5	

4. CONCLUDING REMARKS

The conclusions to be drawn from the figures presented in tables are easier to be formulated, if one calculates the relative frequencies of each group of faults. These frequencies are summarized in Fig. 2

The first notice is that the greatest frequency (~ 26%) belongs to faults that appears in the bearings. It is no coincidence, therefore, that manufacturers of the vibration monitoring devices afford much weight to develop and manufacture support tools (hardware, software) for early diagnosis of the bearings.

The second most common fault detected in the studied set (24.6%) belongs to the misalignment of clutches. Such a fault, of course, has an impact on the development of the previous group of faults. In fact, the inaccurately set clutches causes overloads on the bearings supporting the coupled shafts.

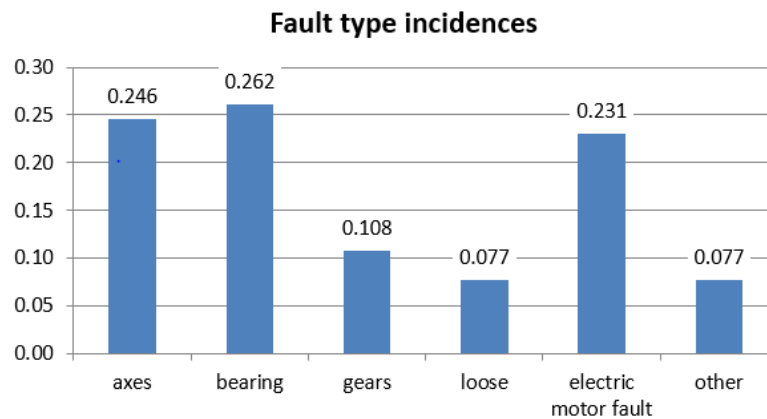


Fig. 2. Relative incidence of the faults

Related to the electric motor's diagnosis, it is well known that the damage of the rotor cage is a common issue. The mechanical vibrations in this case have often as a source the pulsating electromagnetic force, so, the use of electrical measurements brings additional information related to a machine status.

The correct choice of the control period is extremely important for enhancing the efficiency of the diagnosis. A good example is the fault presented in the row 10 from Table 3, which has not been detected, because the 4-month inter-testing period was too long. At this equipment, the reduction of the time between checks would be desirable.

We can conclude that the vibration and current signature diagnosis activity performed in the past ten years before closure, at the Márkushegy mine plant contributed to increase the availability of the involved equipment, and to reduce the downtimes produced by unexpected faults.

The described work/article was carried out as part of the „Sustainable Raw Material Management Thematic Network – RING 2017”, EFOP-3.6.2-16-2017-00010 project in the framework of the Széchenyi2020 Program. The realization of this project is supported by the European Union, co-financed by the European Social Fund.

REFERENCES

- [1] **Dömötör Ferenc (szerk.):** *Rezgésdiagnosztika I-II. kötet*; Főiskolai kiadó
- [2] **Brüel & Kjaer application notes,** *Vibration measurement in predictive maintenance* (BO 0094-11)
- [3] **Brüel & Kjaer application notes,** *Machines-Condition Monitoring using Vibration Analysis*, (The use of Spectrum Comparison for Bearing fault Detection) A Case Study from Alma Paper Mill, Quebec, Canada (BO 0253-11)
- [4] **Gilmore, R. J., Thomson, W. T.,** *Motor current signature analysis to detect Faults in induction motor drives – fundamentals, data interpretation, and industrial case histories.* Proceeding of the thirty-second turbomachinery symposium; 2003.
- [5] **Ladányi Gábor, Ladányi Gergő:** *Kalickás indukciós motor hibadiagnosztizálása rezgés és motoráram analízis együttes alkalmazásával.* GÉP 2013:(3) pp. 16-20.

CATIA V5 – SOFTWARE IN MODELING AND SOLVING ENGINEERING APPLICATIONS WITH FINITE ELEMENT METHOD AS A WORK TOOL

RADU MAREȘ¹, ANA-PETRINA PĂUN², MIHAI POPESCU-STELEA³

Abstract: Knowledge the application of finite element method - FEM, represents an approximate solving method to the problems of field (elastic field movements, tension field, temperature field, etc.), that is to determine in a given field to one or more unknown functions, characteristics of the physical nature of researched field, when we can't solve differential equations of the phenomenon. This paper contains the application of FEM on two auto inferior arms which differ only in the material from which they are made. It is also described the FEM, by means of which was performed the manner in which the two auto inferior arms behaves, subject to the same forces.

Key words: finite element method, software, differential equations

1. INTRODUCTION

Finite element method – FEM, It was initiated by formulating matrix method of bar displacements structures. Subsequently it demonstrated that FEM is closely related to classical methods of solving formulated problems. Historically the method is relatively new. In the general view, the first scheme with finite element is made of COURANT in 1943 to solve a torsion problem. The next stage was once the matrix formulation of J.H.ARGYRIS in 1954 computational structures in bars.

The concept of continued discretization through finite element was introduced by M. J. Turner, H.C.Martin, R.W.Clough, L.C.Topp in 1956, which solves the problem of plane elasticity theory using finite element triangular and rectangular. The notion of finite elements was introduced by R.W. Clough in 1960 [1].

¹ *Ph.D. student, University of Petroșani,*

² *Ph.D. student, assistant, University of Petroșani,*

³ *Lecturer, Eng. Ph.D., University of Petroșani, popescustealeamihai@yahoo.ro*

2. THEORETICAL FUNDAMENTALS OF FEM

The finite element method is a general method for solving approximate differential equations or integral describing phenomena or physical systems with an infinite number of degrees of freedom with their conditions to limit reduced to a system of algebraic equations and to a system with finite number of degrees of freedom. In other words, it is a method that transforms study of finite fields with infinite subdomains study finished about the same fields but with a finite number of finite elements, which could be applied known numerical calculation scheme [3].

To solve applications with MEF, the following notions: structure, discretization, node, finite element.

The concept of the structure implies acceptance of the hypothesis of plane section for the bars of Bernoulli and the hypothesis of normal rectilinear of Kirchhoff for plates and coatings. Acceptance of these assumptions makes it possible to replace real external forces through internal results of efforts N, T, M which are statically equivalent.

To perform a finite element analysis of a structure, we have developed a computational model of the structure. FEM models are mathematical models that approximate the structure to be analyzed.

Discretization is to shift from continues structure (with an infinite number of points) to a discrete model with a finite number of points (nodes) and sharing structure model in any number of fragments or elements as triangles or rectangles that bind to each other by nodes [4].

In order to solve the problems of the field and those of continue mechanical environments, it is used three equivalent mathematical formulations:

- a differential formulation, which led to the finite difference method;
- a variational formulation, which led to the finite element method;
- an integral formulation, which led to the contour element method.

Catia V5 uses finite difference method as follows:

For solving a system of differential equations with unknown field u as:

$$L(u) = \{L_1(u), L_2(u), \dots\}^T = 0 \quad (1)$$

within a given field, with the satisfaction of certain conditions limit on the boundary Γ of the domain:

$$C(u) = \{C_1(u), C_2(u), \dots\}^T = 0 \quad (2)$$

Where $L_1(u), L_2(u) \dots$ are partial differential equations, L_1, L_2, \dots the differential operators; analog C_1, C_2 . [1]

Using the computer to solve a problem involves the following steps:

- Clarification of the problem and formulation data input;
- The development of the calculation model which start from a coherent ensemble of hypotheses lays down a diagram of the calculation which describes both

quantitatively and qualitatively the phenomenon;

- The selection of the most suitable methods of calculation. The selection of the numerical calculation method starts with the development of the algorithm. From the criteria which are the basis of the choice of the numerical calculation method remember: simplicity, accuracy, speed of calculation;

- The development of logical diagram for describing the algorithm of numerical method. Logical diagram actually represents a graphic of the calculation algorithm, through the record of sequence of the main stages of calculation and logical decisions necessary to obtain the solution;

- Development of the calculation program. At this stage the calculation algorithm revealed the logical diagram and is given in a programming language;

- Verifying the results are usually applying numerical method developed for simple problems of whose analytical solution: - the exact considered - is known;

- Data processing and interpretation of results for the studied problem [2].

3. CASE STUDY

Euler's formula for wires wrapped on circular discs is also extended to dynamic cases, when the wheel rotates, either independently, or it forms a mechanical system with the cable.

For the application of the method FEM, by using the Catia V5 was carried out a comparative analysis of the dynamic behavior mode of two lower arms of a car, identical from the point of view of construction on which differ only the material from which are made. One of the lower arms will be built of aluminum, other of steel.

In the simulation carried out in the case study it was accepted the hypothesis according to which the two bodies will be subject to certain forces uniformly distributed as follows:

- Seating area of the pivot axis Z will act with force of F 150 N;
- Seating area of the of alignment telescope and spring Z axis should be taken with F -20 N

Also, the two auto lower arms will be housed in the area of the bearings.

Procedure:

It starts design software Catia V 5 in the library and is selected drawings of the lower arm made of aluminum (steel), modeled in 3D.

From the Start menu submenu choose Analysis & Simulation Generative Structural Analysis, Static Analysis, where it works acting OK.

In this way we enter in the menu to analyze with FEM.

The next step is choosing the method and place of embedding with Clamp menu.

Proceed to step where choosing forces module, the size and direction (equally distributed forces, moments, load bearing, etc.).

The next stage is the mathematical calculation, which are made based on the number of finite elements which in our case is the 2109 and 710 nodes.

Once completed these commands, proceed to choosing which graphics program

Catia V 5 shows how the body behaves studied when applied forces or tensions results: photo (1,2), how they interact with each other finite elements , respectively resultant displacement: photos (4,5).

All these elements can be photographed or filmed using the menu Tools - Image Capture or Image Animate.

To see how Catia V 5 has reached the results from the images photo (1,2,3,4), from the Tools menu Generated Report - a report is generated in which are to be found all the elements of the physical and mathematical that the program Catia V5 it has taken into account in the development of the animations. In the table (1) are represented as compared, several physical characteristics of the two lower arms of which has to be taken into account when carrying out simulations.

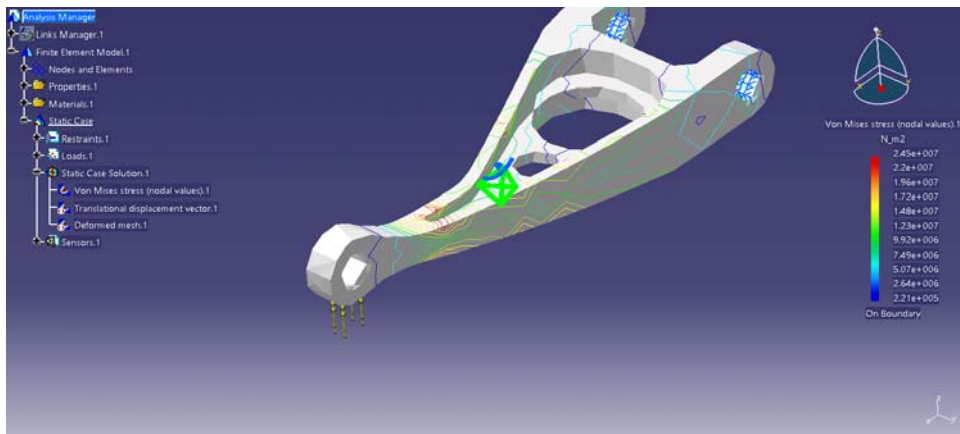


Fig. 1. Tensions aluminum arm

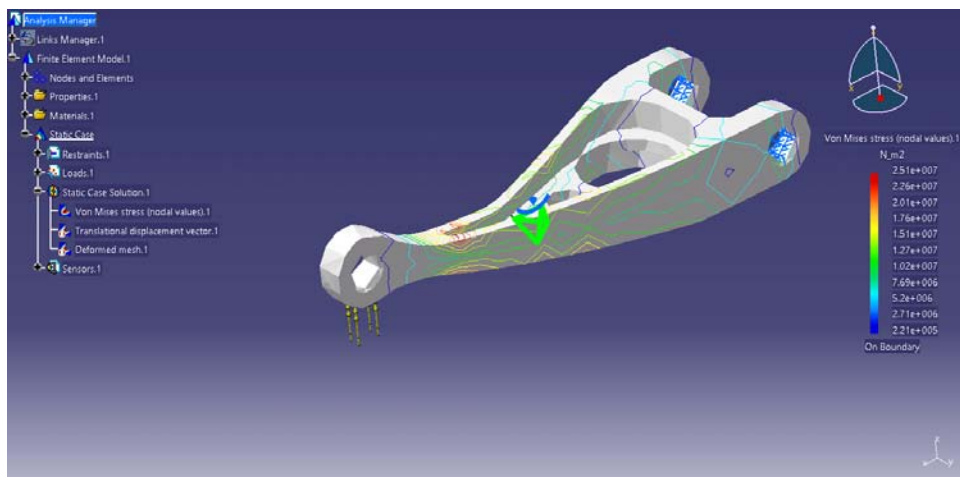


Fig. 2. Tensions steel arm

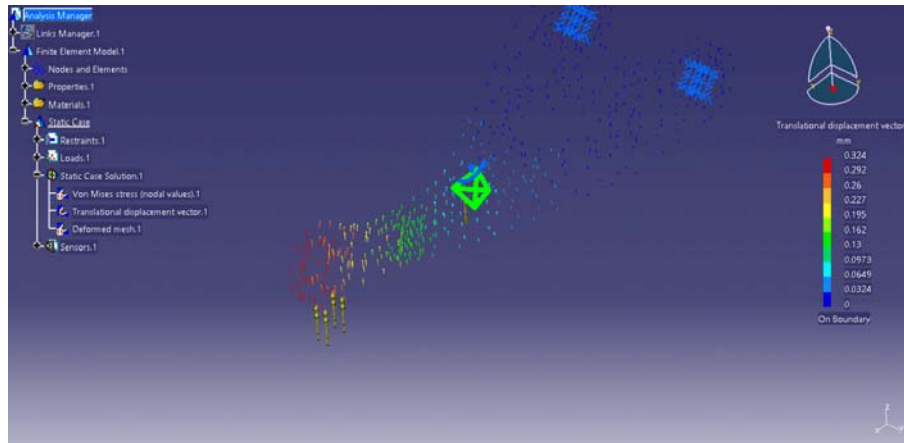


Fig. 3. The resultant displacement - aluminum arm

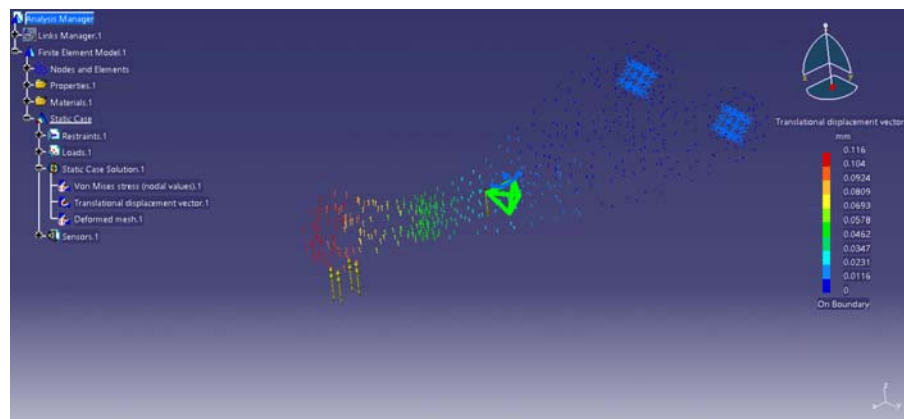


Fig. 4. The resultant displacement - steel arm

Table 1. Physical characteristics

Material	Aluminum	Steel
Young module (elasticity)	$70 \frac{N}{mm^2}$	$210 \frac{N}{mm^2}$
Poisson coefficient	0,346	0,266
Density	$2710 \frac{kg}{dm^3}$	$7860 \frac{kg}{dm^3}$
Von Misses stress- voltage maximum equivalent	$2,45 \times 10^7 N/m^2$	$2,51 \times 10^7 N/m^2$
Translational displacement- The resultant displacement	0,324 mm	0,110 mm
Sensors - Energy – the voltage used for the displacement of each node	0,02J	0,007J

4. CONCLUSIONS

Knowledge the application of finite element method - FEM by design engineers using CATIA V5 software, is an important step in choosing the correct constructive solutions as well as shortening design guys. Also this tool can be applied subassemblies and assemblies to study the behavior of their uniform under the influence of forces, moments to which they are subjected in virtual reality. By comparing the two arms from the case study, the designer can decide which are the correct solution, as well as constructive material corresponding to the aim pursued by research theme.

REFERENCES

- [1]. **Moţica, Adriana-Minerva**, *Noţiuni de teoria elasticităţii şi metode numerice de calcul*, Editura Universităţii Aurel Vlaicu, (2007).
- [2]. **Faur, Nicolae**, *Elemente finite – Fundamente*, Timisoara, (2002)
- [3]. isb.pub.ro/planuri_inv/Master/Tematica_CPTSB.pdf
- [4]. [www.resist.pub.ro/Cursuri_master/PMEF/PMEF_Curs 02](http://www.resist.pub.ro/Cursuri_master/PMEF/PMEF_Curs_02).

DEADLY MASS CASUALTY INCIDENTS - A CONSTANT CHALLENGE IN THE COOPERATION BETWEEN THE FORENSIC PATHOLOGIST AND CRIMINAL PROSECUTOR TO IDENTIFY THE VICTIMS

DAN OCTAVIAN MĂRCULESCU¹, GEORGHE LAZĂR²

ABSTRACT: A “sine qua non” prerequisite within the investigations unfolded by the legal institutions under the circumstances of mass casualty incidents is represented by the cooperation with the forensic pathologist in order to determine the identity of the deceased. This is absolutely necessary to determine the cause and the origin of the deflagrations by corroborating the injury elements with locating the victims, aspects which can only be attained through the interdisciplinarity and professionalism of the forensic pathologist/the investigator.

Keywords: mass casualty incidents, mixed team, forensic pathology, explosions, mine

1. INTRODUCTION

Mass casualty incidents are unfortunate events determined by various causes which generate the death of two or more persons and this category includes work casualty events, aircraft and naval casualty incidents or road casualty events. Personally, I would include in this category terrorist acts as well, which result in multiple deaths caused by criminal actions.

Mass casualty incidents refer to accidental traumatic events which occur at the workplace or are caused by the work performed by the employee and materialized into multiple victims, alive or deceased. The most frequent situations in which mass casualty events appear are mine casualty incidents (gallery collapses, explosions, conflagrations), special traffic accidents (naval), as well as casualty incidents in various factories, companies or other industrial units (possibly with explosions, conflagrations of different intoxications). [1].

¹ *Forensic Pathologist, M.D., Ph.D., Head of SJML Hunedoara,*

² *Resident in Pathology, M.D., IML Cluj-Napoca.*

2. STUDY

When managing mass casualty events, it is necessary to unfold a medical activity based on principles such as the efficient selection of the victims and the rational use of the available medical resources. The particularity of this aspect resides in the necessity of an inter-institutional communication as efficient as possible under the circumstances, because, due to the large number of services involved, for example the first aid teams, the emergency units in the proximity and not only, the pathology services/institutions/offices, respectively, the Police, the local Prosecutor's office, the Territorial Labor Inspectorate and other, the risk of the occurrence of a transmission deficiency of important data may appear. [2]

In the district of Hunedoara and mainly in the Jiu Valley area, numerous such tragic events have occurred along the years, resulting in a variable number of casualties, a vivid example is represented by the deflagrations which occurred in the Livezeni Mine, during which 54 miners and militaries lost their lives; the explosions were caused by the excessive accumulation of methane which, combined with the coal powder, forms the so-called "grizu" that produces explosions similar to the TNT (trinitrotoluen). This event was mainly caused by the neglect of the labor safety rules and also by the technologies used in that period, the increase of „production” representing the most important aim. Certainly, at the time the explanation was that fossil fuels (coal) constituted the main and the cheapest form of energy.

After this unfortunate event, we have witnessed numerous other mass casualty incidents, with a variable number of human casualties but considerably smaller. The causes were mainly the same, deflagrations produced underground due to the neglect of the labor safety rules.

During these incidents, the persons who survive display severe body injuries.

In the case of mass casualty events which result in the death and/or the injury of several persons, involving pathology becomes mandatory. Let us review in short the involvement of the pathology in the cases of the surviving persons who will undergo expertise in order to establish the necessary number of days of medical care, the potential life jeopardy and the possible aesthetic injuries or infirmity. [3]

The investigation of the deaths after the mass casualty incidents is to be performed through a pathological autopsy. [4]

Before, prior to the pathological autopsy, the essential problem is to perform the identification of the victims. This used to be a very difficult task not long ago in the case of mass casualty incidents in the mining sector because the intensity of the deflagration was followed by collapses and sometimes almost complete damage of the deceased.

In this context, a tight cooperation with the criminal officers and prosecutors, with whom the forensic pathologist would gather the most conclusive data in order to identify every victim.

In the 1980s, when the DNA test was not performed on a large scale, besides the forensic photographs which could not be conclusive, blood was collected to determine

the blood type and subtypes and hair to make comparative tests and, if possible, the fingerprinting of the victims.

As the victims' clothing didn't offer useful clues, very often the clothes had been burnt or destroyed, the miner's lamp was particularly useful as it possessed a serial number, the same as nowadays, every miner using only his own lamp.

Only after this identification activity, after having completed the forensic identification chart, often extremely laborious, would the pathologist proceed with the forensic autopsy of the corpses, the collection of biological samples (histopathological and, compulsory, toxicological to determine the carboxihemoglobin).

At the end of the autopsy, a report will be drafted to show the mechanism and cause of death, along with other aspects which would be useful in the investigation. [5]

With these methods of identification, an essential aspect in these cases, often errors can occur for two reasons, as it is possible for the victims to have lost or borrowed certain objects. [6]

Other elements which are useful in establishing the victims' identities are the tattoos.

The most recent and efficient technique used in the identification of the corpses with variable degrees of damage is the DNA analysis. DNA can be collected both from soft tissues and bone fragments. After specific processing of the biological samples, the DNA is extracted and compared with samples from the presumed biological relatives. Also, the samples can be compared with a sample from the person in question, for instance the genetic material extracted from the hair remains on the comb. The disadvantages of this method reside in the high costs and relatively small number of laboratories which perform these tests in our country, translating into a long period of expectation for the results.[7]

We have mentioned above the imperative necessity of identifying the victims of mass casualty incidents from two perspectives, namely:

1. A humanitarian reason which aims at returning the lifeless body to the rightful owners in order to perform the Christian tradition of inhumation.
2. By corroborating the elements determined after the pathological necropsy like causes of death and the place where the victim was found, genuine "maps" are created, death maps, which offer valuable and accurate clues regarding the cause and the place where the unfortunate event took place.

Within the cooperation between the forensic pathologist and the criminal prosecutor, another element of great importance is the on-site investigation, an activity which must be performed as soon as possible, it is irreplaceable and almost impossible to repeat under the same circumstances and with the same results. We mention the fact that the way in which the investigation is performed, the search and collection of evidence or samples as well as establishing the results influences to a great extent the solutioning process and the identification of the causes or the possible active participants in the casualty events. [8].

3. CONCLUSSION

A theoretical study of all these tragic elements with a highly emotional impact displays a practical value. Under similar circumstances which can occur for various reasons, the determined elements are extremely important for the ulterior actions, the activity unfolded by the rescue teams immediately after the event. During the rescue of the victims who may still be alive, it is necessary to take into account all the elements determined through previous analyses, thus avoiding the occurrence of other tragedies with victims.

In my current practice as a forensic pathologist, I have participated in numerous events, for instance, repeated explosions, cascade explosions, when the team consisting of specialists in the field of mining, labor safety and criminal prosecutors were caught by surprise by a new deflagration with fatal results, causing the death of many persons, due to the fact that they didn't follow a set of strict rules which cannot be ignored under any circumstances and reasons, man's life being above all..

REFERENCES

- [1] http://ec.europa.eu/eurostat/statisticsexplained/index.php/Accidents_at_work_statistics
- [2] **Ramesh AC, Kumar S.**, *Triage, monitoring, and treatment of mass casualty events involving chemical, biological, radiological, or nuclear agents*. J Pharm Bioallied Sci. 2010 Jul-Sep; 2(3): 239 – 247.
- [3] **Dermengiu D.** *Evaluarea gravității leziunilor traumatice. Repere axiologice, criteriologice și metodologice*. Editura Gemma. 2015.
- [4] **Belis V.** *Tratat de medicină legală*. Editura Medicală. București. 1995.
- [5] **Dermengiu, D., Alexandrescu, G.**, *Medicina legală prosecturală*. Editura Viața Medicală Românească. 2012.
- [6] <https://www.crimemuseum.org/crime-library/forensic-investigation/postmortem-identification/>
- [7] **Schwark, T., Heinrich, A., Preusse-Prange, A., Wurmb-Schwark, N.**, *Reliable genetic identification of burnt human remains*. Forensic Sci Int Genet, 2011 Nov, 5(5):393-9.
- [8] **Ciobanu, P., Stancu, E.**, *Tactica Criminalistică*, Ed. Universul Juridic, București 2017, pg. 10

RESEARCH REGARDING THE USE OF DRONES IN MONITORING AND CONTROLLING MINING PROCESSES AND ENVIRONMENT PROTECTION

**CĂTĂLIN PLOTOGEA¹, MARIN SILVIU NAN²,
ALIN SULTAN³, BOGDAN VLADU⁴**

Abstract: Unmanned Ariel Vehicles (UAVs) or drones provide real-time information. This kind of systems have advantages of being able to replace humans working in dangerous and unreachable environments in order to reduce working accidents and avoid casualties. Other benefits of UAVs in mining industry are safety and security, productivity and data field collection. The use of drones in mining has proved to be an ideal way of discovering new areas of interest being a vital tool in the extraction process. Vast areas can now be covered in a short space of time and new data can be available, both of them being more vital now than ever taking into account that raw materials are in short supply and high demand.

Keywords: unmanned aerial vehicle, types, safety, risks, mining

1. INTRODUCTION

Drones or UAVs (unmanned aerial vehicles), are defined as aerial vehicles that do not carry a human operator, but uses aerodynamic forces to provide lifting. They can fly autonomously or be piloted remotely and can be expendable or recoverable. The first domain of usage for these devices was within military missions gaining over time their permanent position in the military arsenal. Other applications of these devices are: damage investigations during/after disaster (e.g. hurricane, flood, earthquake), locating forest fires or frost conditions in farmlands, border patrol, search, rescue and, monitor criminal activities, mining, advertising, scientific surveys and secure pipelines and offshore oil platforms.

¹ *Ph. D. Student, Eng., University of Petroșani,*

² *Professor, Ph.D. Eng., University of Petroșani, nan.marins@gmail.com*

³ *Ph. D. Student, Eng., University of Petroșani*

⁴ *Ph. D. Student, Eng., University of Petroșani*

Nowadays, drones are frequently used in mining and they have proved to be the excellent method to discover new areas of interest and an indispensable tool in the extraction process. Because it can take days or even weeks for human workers to cover the full area of a mine, and even then there is the chance for human error or inability to reach some areas, drones can replace human workers in many situations like those listed above. Vast areas can nowadays be covered in a short amount of time and new data can be available, both of which is essential now than ever when raw materials are in short supply, but requested in high demand. In addition, drones can also be used for surveillance or medical aids. The drone can carry medical supplies before first aid is provided and also supervise the whereabouts of workers, equipment, animals, disaster or outsiders.

2. TYPES OF UAVS

Drones are usually made of a control station represented by the human intelligence and one or more Unmanned Aerial Vehicles (UAVs). The UAVs can be equipped with sensors, such as: thermal, gas detecting sensors, motion, pressure, GPS sensors; still cameras or video cameras, including far and near infrared, radar or laser based range finders, or specialized communication devices. The control stations utilized by the human operators can vary from portable computer systems to fixed installations in vehicles or dedicated control rooms.











































There are many types of UAVs designed for different purposes. Some examples include: micro UAVS (small, extremely portable devices), low altitude and long endurance UAVs, high altitude and long endurance UAVs employing a conventional design, high altitude and long endurance UAVs using a low observable design. Table 1 below represents types of UAV with mass, range, altitude and endurance.

Table 1 Different Types of UAVs


Type of UAV	Mass [kg]	Range [km]	Flight altitude [m]	Endurance [hours]
Micro	< 5	< 10	< 250	1
Mini	< 25/30/150	< 10	150/250/300	< 2
Close Range	25 – 150	10-30	3000	2 - 4
Medium Range	50 – 250	30-70	3000	3 – 6
High Altitude Long Endurance	>250	> 70	> 3000	> 6


Some commercial models seen on the online market and frequently purchased are summarized below. (Table 2)


Table 2 Common commercial drones (* - official release photos)

Type	Product	Picture	Characteristics
Best Budget Drone	Holy Stone F181 RC Quadcopter Drone with HD Camera RTF 4 Channel 2.4GHz 6-Gyro	 *	 8 min  24 km/h  90 m  Yes  Remote  Yes
Drone for beginners	UDI U818A HD+ Drone with Camera and Headless Mode 2.4Ghz RC Drone Quadcopter	 *	 9 min  16 km/h  33 m  Yes  Remote  No
Micro Drone	Cheerson Cx-10 Mini 2.4g 4ch 6 Axis LED Rc Quadcopter Airplane Blue	 *	 8 min  13 km/h  30 m  No  Remote  No
Drone with Camera	DJI Phantom 4 Quadcopter	 *	 30 min  72 km/h  4800 m  Yes  Remote  Yes
Drone with Camera	Parrot (PF726203) Bebop 2 with Skycontroller 2 & FPV	 *	 25 min  56 km/h  300 m  Yes  App  Yes
Professional Drone	DJI Phantom 3 Professional Quadcopter 4K UHD Video Camera Drone	 *	 25 min  60 km/h  1500 m  Yes  Remote  Yes

Legend:

 This is the average time your drone will stay in the air on a single charge. Longer is better.

 This is the maximum speed your drone can fly (kilometers per hour)

 The range shows you how far your drone can fly without losing contact to the controller.

 Many drones include an on-board camera or a mount to attach your own camera.

 Controllers can come in the form of a hardware controller or an RC app.

 Return home tells the drone to automatically come back to you using GPS.

3. UAVS BENEFITS IN MINING INDUSTRY

The mining industry is intricate if we consider the extent and nature of work. There are many challenges for the mining and exploration industry to be able to access remote and unsafe topography. The inability to access different areas leads to no information regarding those areas, unavailability of data and finally those remain unexplored.

Currently, mining companies have started to change strategies and to adopt new operating models that include other technologies. Specifically, due to the overwhelming digital revolution, it has become necessary, and significantly more cost effective, to integrate and develop modern technologies into the mining field. The traditional methods of mine surveying are conducted on the ground. Unfortunately, the ground mining methods are unsafe due to the danger to which operators are exposed. Besides, they are slow and provide uncertain and late results which often do not meet the needs of the operators. Considering these reasons, it is easy to understand why mining operators are turning to new technologies in order to improve results. Therefore, the potential usages of drones in mining are endless.

One of the most important application of drones in mining industry is that they can access areas that otherwise are hard and/or dangerous to reach, such as flood or fire areas, thick forests, cliffs or hills, unstable volcanic areas and even historical war zones with unexploded bombs. Another usage of drones is that they can survey disaster areas during and after events in mining operations. The potential usage of drones can be enhanced by developing or modifying applications to collect data such as geological and topographical data, weather conditions data, thermal imaging, sample collection, risk hazard data etc. This technology makes possible the surveillance and monitoring of mining machines and pipelines, conveyor belts, and fleet management in mine. Besides it can also be very useful in search and rescue, in the assessment of landslide zone, analysis incident cause and investigation in an operational environment. Drones can also be able to take photos from multiple angles, permitting the development of a 3D model from the photos. This way, drones can provide an extensive coverage of the whole area. Drones can be equipped with different equipment on board, being able to map out key areas in order to get a visual representation of the area. Topographical mapping provides a surface model for developers with more details than ever, being also a high cost-effective solution. Another essential advantage of drones is that they can even collect soil samples for further analysis. As the demand for new deposits grows, so is the demand of this sort of technology.

Accidents in mining industry can be prevented if drones are included in their operating management. Generally speaking, the main causes for accidents are: unsafe site conditions, unsafe equipment, unsafe working methods or lack of proper training, poor attitude or carelessness regarding safety, isolated, sudden deviation from prescribed behavior, natural disasters (landslides, fire, floods, explosions), bad weather conditions. The safety manager has the responsibility to observe employees, actual methods and sequencing, and actual site condition on frequent daily basis. Therefore, the task of safety

managers' task concerning observation and surveillance can be defined as getting real time data through direct observation and interaction with workers. One of the main responsibilities of safety managers is to provide workers with safety at working place. In order to do this, they must observe the whole construction jobsite. They should walk around to check workers, material, and equipment based on safety criteria. But this can take a lot of time, which could be saved by using drones instead. A drone can be used to fly over the construction jobsite and provide the safety managers with real time information about what is happening on the jobsite (frequent and direct observation). In addition, it can also provide interaction through the communication tools (video and voice transmitters) embedded in the drone; this way, safety managers would be able to interact directly with workers (direct interaction). (Figure 1)

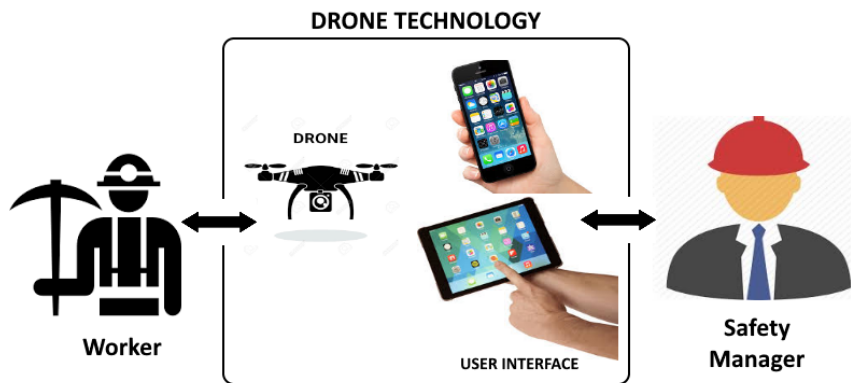


Fig. 1. Worker and safety manager indirect interaction through drone technology

Safety is another primordial concern which is being aided by the use of UAVs. With specific applications drones can be used in identifying potential risks and dangerous zones in an operational mine (misfire, wall damage etc.), exploration and drilling sites, and processing plants. There is no need to physically carry out an exploration mission in a new territory when a drone can go out and survey it. If the data is promising, then the team can proceed. This approach is safer and less invasive for workers and cheaper for the industry.

One of the biggest benefits of using UAV's is the cost. Compared to traditional helicopters, drones are cheaper and currently are restructuring the way mining companies explore new areas, providing better results. Therefore, drones have a great potential of reducing costs and increase productivity.

Regarding limitations of UAVs we must say that due to the legal situation and safety aspects, an autonomous flight system is possible but sometimes not applicable and need more research especially in complex environment. Therefore, a "Pilot" is still necessary for practical implementation.

4. CONCLUSIONS

The use of drones in mining industry clearly has a lot of potentials and, because technology continues to develop, this potential can only grow.

Drones are an appropriate technology to be used in different sectors of the mining industry by providing real time information, being able to fly to different areas and to provide voice interaction. UAVs can make a major impact in the mining industry in terms of productivity, cost and efficiency in coming years. There are many different uses for UAVs in the exploration, extraction, and maintenance of mines. Some companies may use them only to locate points of interest and map out terrain, but they can be used in many other ways. They can act as air support for sample generation, first aid, mapping, maintenance, surveillance. Drones have proved to be invaluable tools.

REFERENCES

- [1]. **Ahmad, A.**, *Digital Mapping Using Low Altitude UAV*. Pertanika J. Sci. & Technol. 19 (S): 51 - 58 (2011).
- [2]. **Indresh, R., Kumar, N.P.**, *Unlocking the potentiality of UAVs in Mining Industry and its Implications*. International Journal of Innovative Research in Science, Engineering and Technology. Vol. 4, Issue 3, March 2015.
- [3]. **Irizarry, J., Gheisari, M., Walker, B.N.**, *Electronic Journal of Information Technology in Construction*, Vol 17 pag 194-212, September 2012.
- [4]. **Irizarry, J., Johnson, E.N.**, *Feasibility Study to Determine the Economic and Operational Benefits of Utilizing Unmanned Aerial Vehicles (UAVs)*. Georgia Institute of Technology Contract with Georgia Department of Transportation May 6, 2014 (<http://docplayer.net/7556639-Feasibility-study-to-determine-the-economic-and-operational-benefits-of-utilizingunmanned-aerial-vehicles-uavs-by.html>)
- [5]. **Krauss, R.**, *Where Automation and the Digital Mining Environment Meet: Automated Drones*. October 26, 2016 (<http://www.expouav.com/news/latest/automation-digital-mining-environment-meet-automated-drones/>)
- [6]. <https://www.gim-international.com/content/article/uavs-in-the-mining-industry>
- [7]. <http://carpentersequip.com/category/drones-in-mining/>
- [8]. <http://www.miningglobal.com/technology/1167/The-Mining-Sector-Puts-Drones-to-Work>
- [9]. <https://www.geekwrapped.com/rc-drones>

TECHNICAL SOLUTIONS FOR MINING TUNNELS EXCAVATION TECHNOLOGY

GABRIEL PRAPORGESCU¹, SORIN MIHĂILESCU²

Abstract: Romania's current economic conditions require the use of locally made machines that have a purchase price and lower operating costs compared to those imported. In Romania, the mining cross section of galleries varies between 3.6 and 20 m² and the length goes up to 10 km, so that a key feature of horizontal underground works is high ratio between length and cross section; subsequently, the work place – i.e. the working face - shall move continuously. The mining process, equipment, personnel and generally, the organization have to continually adapt to new working and sometimes unpredictable conditions (very soft or super hard rock, water inflows, heavy pressure, gas, etc.) so, these aspects imply flexibility of the system and the need for rigorous monitoring. It is said that the cross section of galleries and shafts give permission to introduce in underground large equipment that should comprise parts limited in size and weight.

The paper presents a technology for mining underground working of gentle incline by drilling - blasting method. The proposed technology uses IMP-2 drilling installation, VSAH type self-unloading hydraulic silo car, MIC-4E type loading machine and LDM-45 mine locomotive; all these machines can travel on the railway system.

Key-words: excavation technology, mining tunnel, mining equipment

1. INTRODUCTION

The technologies used for mining these types of excavations include drilling - blasting operations. In this case, mining is done cyclically, usually by repetition of successive operations, of which the most important ones are drilling, blasting, loading, transfer, transport and support. Mechanization of low and medium tilt underground sections raises problems requiring powerful and sometimes highly complex machines, which is one of the main drawbacks to cutting, loading, discharge operations of the material and for support purposes.

¹ *Assoc Prof. Eng.PhD. at University of Petroșani, gpraporgescu@gmail.com*

² *Assoc Prof. Eng.PhD. at University of Petroșani, mihailescus@gmail.com*

2. THE MINING EQUIPMENT USED

The complex of equipment used in this technology comprises: IMP-2 type mobile drilling facility (UMIROM Petroșani), MIC-4E type loading equipment (UNIO Satu Mare), VSAH type silo cars (UMIROM Petroșani), LDM-45 type mine locomotive (UNIO Satu-Mare). The technical parameters of all these equipments are shown in Tables 1, 2, 3, 4.

Table 1. The IMP-2 drilling equipment technical parameters

No.	Technical parameters	M.U.	Value
1	Section of the road-way profile in which can drill	m ²	5...22
2	Maximum width of the fireplace gallery	mm	5980
3	Depth of the bore holes made	m	2; 2.6
4	Maximum diameter of the bore holes	mm	45
5	Drilling speed	m/min	0.8...1
6	Number of the borers	pieces	2
7	Blast air consumption	Nm ³ /min	10
8	Nominal pressure in the hydraulic system	MPa	15
9	Track width	mm	600; 630; 750
10	Strength of the electric motor	kW	5.5
11	Mass	kg	6000

Table 2. The MIC-4E type loading machine technical parameters

No.	Technical parameters	M.U.	Value
1	Technical production	m ³ /h	48
2	Bowl capacity	m ³	0.32
3	Width of the face which loads	m	4 m
4	Total power installed	kW	22.5
5	Overall dimensions: length/width/height	mm	7535/1700/1600
6	Track width	mm	750; 900
7	Mass	kg	9000

Table 3. The VSAH type self-discharging silo-wagon technical parameters

No.	Technical parameters	M.U.	Value
1	Minimum section of gallery	m ²	4.8
2	Minimum working radius of curvature	m	10
3	Overall dimensions: length/width/height	m	10/12.5/1.6
4	Useful volume of the wagon	m ³	7.5...16.5
5	Maximum weight of the charge	t	28
6	Wagon design	-	sectional
7	Scraper conveyer driving	-	electro-hydraulic
8	Power conveyer	kW	15
9	Track width,	mm	600; 630; 750; 900
10	Net mass	kg	11000

Table 4. Mine diesel locomotive LDM-45 technical parameters

No.	Technical parameters	M.U.	Value
1	Working mass	kg	6300
2	Power of engine	kW	33
3	Maximum traction force	kN	15
4	Overall dimensions: length/width/height	mm	4150/1060/1570
5	Track width	mm	570; 630; 700; 750
6	Minimum working radius of curvature	m	10

3. DIGGING TECHNOLOGY

Using perforated IMP-2 facility to carry out the task of drilling has significantly improved the working conditions, it provides a noticeable simplification of how to control it and it improves the comfort of work.

Figure 1 shows how IMP-2 accommodates in the profile of a gallery of average section from which one can notice the work surface covered in one position (the operating range of each arm for drilling horizontal holes is 2650 mm), while Figure 2 shows the operation of the silo car with a MIC-4E loading machine.

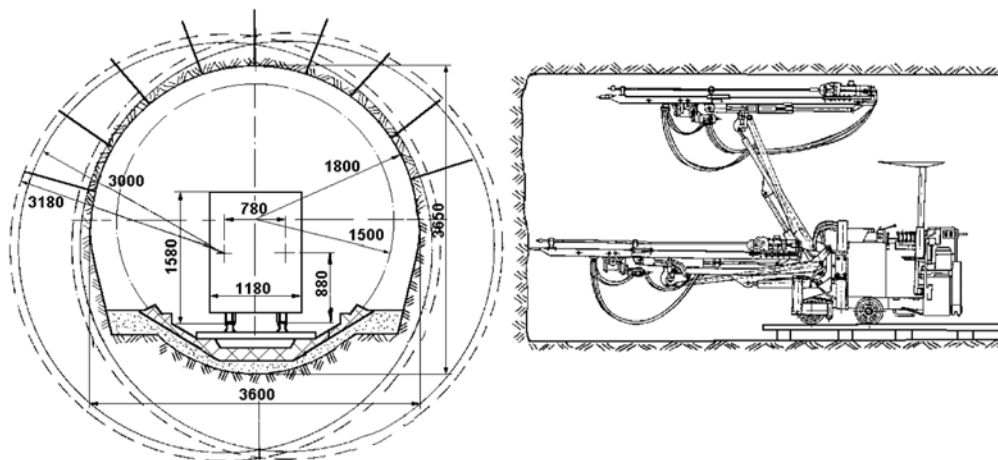


Fig. 1. The framing of the IMP-2 drilling equipment in the profile of the tunnel.

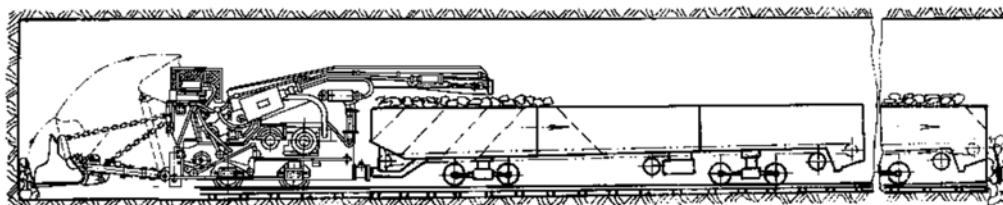


Fig. 2. How to load the VSAH silo-wagon the loading machine MIC-4E.

Complex machines can work as technological scheme shown in Figure 3.

In order to start the drilling process, the drilling equipment (1) is brought in face by the railway engine (3), while the loading machine (2) is shunted on the main line from the first double line from the face situated at maximum 800 m from it (fig. 3.a).

After starting the drilling process, the railway engine (3) goes to the second double line from the face in order to bring the hopper (4) behind the loading machine (2), (fig.3.b). At the end of the drilling, the railway engine (3) will withdraw the drilling equipment (1) from the face on the first double line from the face, on the main line being the loading machine (2) and the hopper (4), (fig.3.c). The railway engine (3) will bring in face, by pushing, the loading machine (2) and the hopper (4), (fig. 3.d).

Meantime the wagon (4) is loaded, a railway engine (6) brings at the first double line from the face a silo-wagon (5), which is shunted behind the drilling equipment (1), waiting for the exit from the face of the loaded hopper (4), (fig. 3.e and fig. 3.f). After the exhaustion of face with a last hopper (7) by the railway engine (6), the railway engine (3) will push in the face the drilling equipment (1), the heading cycle being repeated (fig. 3.g).

At the removal of the materials with the VSAH self-discharging silo-wagons, each hopper will be trailed by a railway engine LDM-45 type, which is permanently connected with this wagon without a brake assembly of its own. 3 hoppers discharged in the waste dump from the gallery entrance have made the removal of the rock from the face during the heading of the gallery.

Double lines of 50m length are used in order to change the wagons in the face. There are placed at a distance of 800 m on the entire headed gallery. Due to the high length of the roadway there are necessary three hoppers in order to obtain a high mining output of the loading machine.

4. DETERMINING THE DURATION OF A DIGGING CYCLE

When digging galleries by drilling-blasting technology, the blastholes drilling operation is accomplished according to the blasting draft. When mining a gallery with

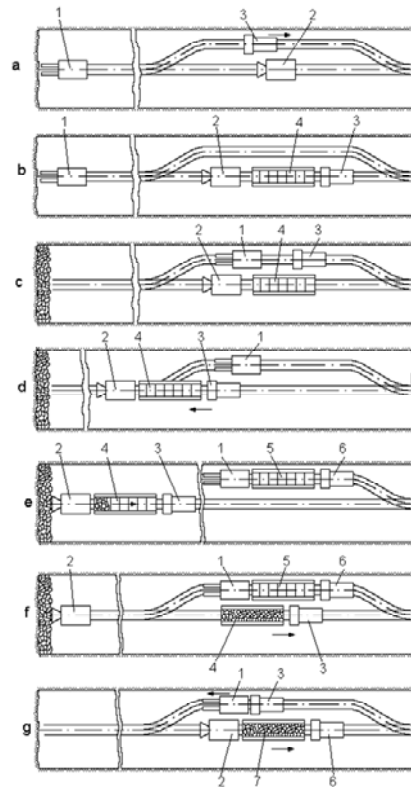


Fig. 3. The digging technology by drilling-blasting.

an average profile (with the cutting section of 13.4 m²) in rocks of average strength ($f = 6-7$, according to Prof. Protodiakonov scale), the periods of time necessary for manipulation for the polar shift are relatively small, resulting a consumed time to raise the maximum manipulator of 14.31 s, and for lowering it to its minimum height of 9.58.

Figure 4 presents the diagram of variation times for drilling installation rotation to the left (t_1), and to the right (t_2), respectively. For the considered situation, it resulted that for the distance travelled by the manipulator situated on the left side on the drilling machine, a period of 94.6 s is necessary and 142.5 s for the manipulator on the right side.

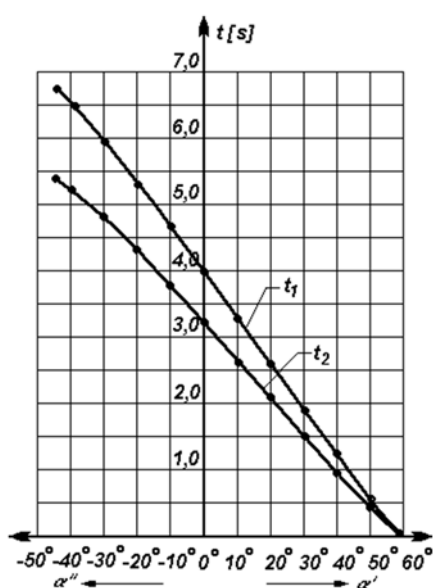


Fig. 4. The variation time for left, respectively right rotation of the drilling installation.

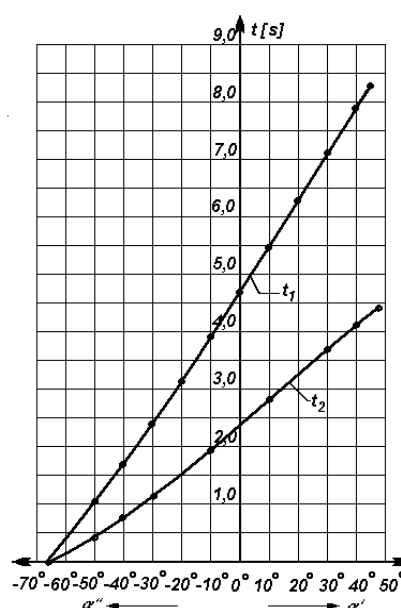


Fig. 5. The time variation for diverging, respectively converging sloping.

Figure 5 determines the time required for diverged sloping of the drilling installation, when drilling shaping blastholes, and represents the time variation graph: t_1 for diverging sloping, and t_2 for converging sloping according to sloping angle α .

Considering preparation – finishing periods of the drilling operation and the period of time necessary to bring the drilling installation in the vicinity of the working face, its connection and preparation, as well its disconnection and withdrawal at the end of drilling of the whole front, we can say that total duration of the drilling operation is 169.85 min, i.e. 2.83 hours.

Knowing the effective operating factor of the loaders depending on the removal equipment used plays an important role in the selecting of the loader and the removal equipments for the rock dislocated during the heading. The factors that influence the effective operating factor of the loaders are the effective period of the rock loading and the auxiliary period determinate by the technological failures for handling the removal

equipment.

The operating period of conveyors at coal face is about 14-15 hours per day, at sectors it reaches 16 to 17 hours/day and along the main transportation routes it may reach up to 18-20 hours per day.

In order to estimate the rational use of the loader, it is used the effective operation factor of the loader. This is expressed by the formula:

$$k = \frac{t_{ef}}{t_{ef} + t_m + t_{pi}} \quad (1)$$

where: t_{ef} - the effective period of loading during the heading period, in min; t_m – the operation period of the removal equipment, in min; $t_{pi} = 10...20$ min - period of preparation and completion of the loading process.

On the basis of the above mentioned relation, there were drawn the curves of variation of the effective operation factor of the loader, dependent on the operating distance, the technical output of the loader, the capacity of the removal equipment, the volume of rock resulted at a jump (Figures 6, 7, 8, 9).

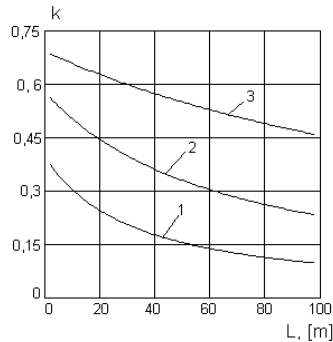


Fig. 6. The curves of variation of the operation factor of the loader, dependent on the operating distance.

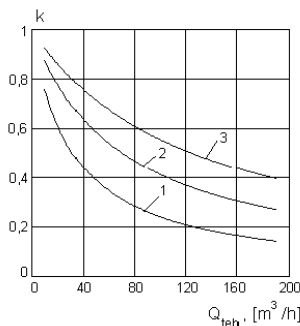


Fig. 7. The curves of variation of the operation factor of the loader, dependent on the technical output of the loader.

In figure 7 there are shown the curves of variation of the operation factor of the loader, dependent on the technical output of the loader, for a volume of rock of 30 m^3 , dislocated at a jump, an operating distance of 5 m for the trucks with 1 m^3 capacity (curve 1), of 20 m for truck with capacity of 3 m^3 (curve 2) and 400 m for silo-wagons with capacity of 10.5 m^3 (curve 3).

In figure 8 there are presented the curves of variation of the working output and the operating factor of the loader, dependent on the capacity of the trucks, for an operating distance of 5 m, a volume of rock of 30 m^3 , dislocated at a jump and for loaders with technical output of $20 \text{ m}^3/\text{h}$ (curve 1), $45 \text{ m}^3/\text{h}$ (curve 2), $70 \text{ m}^3/\text{h}$ (curve 3), $95 \text{ m}^3/\text{h}$ (curve 4).

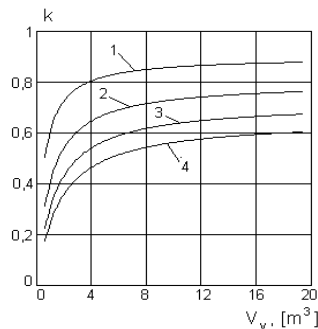


Fig. 8. The curves of variation of the working output and the operating factor of the loader.

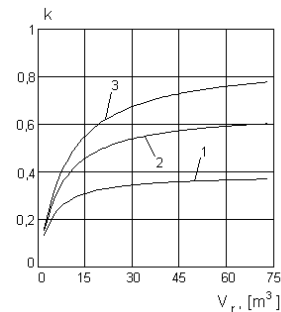


Fig. 9. The curves of variation of the operating factor of the loader, dependent on the volume of dislocated rock.

In figure 9 there are shown the curves of variation of the operating factor of the loader, dependent on the volume of dislocated rock, for a technical output of the loader of $60 \text{ m}^3/\text{h}$ and for an operating distance of 5 m for the trucks having a capacity of 1 m^3 (curve 1), of 20 m for trucks with a capacity of 3 m^3 (curve 2) and 400 m for silo-wagons with capacity of 10.5 m^3 (curve 3). The determination of the period of the heading cycle of the roadway, using the above mentioned equipment has been made for the case of penetration of 4 type of rocks met along the roadway layout.

4. CONCLUSIONS

The use of this complex of machinery has proven effective during the work on the small and medium sections of relatively small lengths, performed on hard rocks and led to the improvement of the working conditions, a reduced duration of loading and transportation of excavated material, resulting in speeds of mining of up to 100 m/month. In order to increase the technical-economical parameters during the loading, it is recommended to use loaders with high enough technical output. When the removal is carried out with trucks, they should have a high capacity and their operating distance should be as much as low possible. When the removal is carried out by silo-wagons, the highest technical-economical parameters are achieved (up to twice higher parameters than in the case of using of the trucks). In conclusion, the equipment produced in Romania may be successfully used in mining in underground and they gave full satisfaction both in terms of technical performance and operational reliability.

REFERENCES

- [1.] Burloiu, P., *Labour Economy and Ergonomically Organization*. Bucharest: Didactical and Pedagogical Publishing House. (Romanian language), 1990
- [2.] Dinescu, S., Andraş, A., *Environmental Friendly Equipment and Technology for Underground Civil Excavations*, Annals Of The University Of Petrosani, Mechanical Engineering, Vol. 10 (XXXVII) 2008, pag. 47-52; ISSN: 1454-9166

- [3.] **Florea V.A.**, *Reliability analysis equipment for cutting and transportation in case of a mining flux technology*, 16th International Multidisciplinary Scientific Geoconference SGEM 2016, Albena Co., Bulgaria, Science and Technologies in Geology, Exploration and Mining, conference proceedings volume II, ISBN 978-619-7105-56-8, ISSN 1314-2704, pg. 719÷725;
- [4.] **Mihăilescu, S.**, *Rail transport equipment for underground*, Petrosani: Universitas Publishing House. (Romanian language), 2006
- [5.] **Mihăilescu S.**, *The Increase of the Mechanization Extent of the Rock Loading-Removal Operation at the Galleries Driving*, Petrosani: Doctoral Thesis. (Romanian language), 1998
- [6.] **Praporgescu, G.**, *Researches to increase performances of drilling installations of Romanian construction used for mining of galleries*, Petrosani: Doctoral Thesis. (Romanian language), 1998
- [7.] ***, *Catalogue of products UMIROM Petrosani*. Romania: Petrosani. (Romanian language), 2000
- [8.] ***, *Catalogue of products UNIO Satu Mare*. Romania: Satu-Mare. (Romanian language), 2006

**IMPROVING SECURITY AND HEALTH
THROUGH PROPER IMPLEMENTATION
OF THE INSPECTION AND MAINTENANCE
PROGRAMME OF ELECTRIC POWER
EX EQUIPMENT DESIGNED IN FLAMEPROOF
ENCLOSURE "D" AND INCREASED
SAFETY "E" TYPE OF PROTECTION**

**RAD MARCEL DANIEL¹, MARIN SILVIU NAN²,
DĂNUȚ GRECEA³, MIHAI MAGYARI⁴,
DIANA SĂLĂȘAN⁵**

Abstract: Inspection is an action that comprises the examination of electrical equipment to be performed without dismantling or with partial removal, where applicable, supplemented by means such as measurements to reach a certain conclusion regarding the state of the equipment in question.

Maintenance is a combination of all actions taken in order to maintain or restore an object given that it is able to meet the relevant specifications and requirements to perform its set functions.

The paper presents the most important aspects to be taken into account when carrying out inspection and maintenance of electrical equipment used in explosive atmosphere with type of protection flameproof enclosure "d" and increased safety "e" to ensure functionality and the type of protection equipment for safe operation.

Keywords: Inspection, maintenance, security and occupational health, electrical equipment used in explosive atmospheres.

¹ *Ph. D. Student, Eng., University of Petroșani,*

² *Professor, Ph.D. Eng., University of Petroșani, nan.marins@gmail.com*

³ *Ph. D. Student, Eng., University of Petroșani*

⁴ *Scientific Researcher, Ph.D. Eng., INCD INSEMEX Petroșani*

⁵ *Scientific Researcher, Ph.D. Eng., INCD INSEMEX Petroșani*

1. INTRODUCTION

Use of electricity for the operation of facilities, equipment, electrical machinery in a potentially explosive atmosphere is of increasingly more interest for the design, erection and the correct selection of the proper type of protection required to ensure safe operation, their approach requiring particular attention in view of the many technical, economic and operational safety and health aspects.

Modern technology tends to fully use materials, labor and safety and health at work, in order to obtain maximum efficiency in production at the desired outcome. This trend which is controlled by designers, is very delicate in itself, because production efficiency can be obtained only from the economy obtained from the manufacturer. Efficiency on site at the end user is based on the safe operation at low power consumption and zero events as regards the health and safety at work, taking into account the investment made for the purchase of equipment used in explosive atmospheres. There is a wide field of action for the reconciliation of the three types of efficiency categories in order to achieve optimal results.:

2. RESEARCH

Electrical systems in hazardous areas have certain features specifically designed for operating in such atmospheres. For security reasons it is essential that in these areas, for the entire lifetime of the plant facility, to be preserved the integrity of these special features.

The main requirements are well established in this direction by the standards, but many technical - administrative issues which require that the operators of installations, appliances, electrical machines operating in potentially explosive environments to be authorized in conformity with Articles 7 of NEx 01 – 06 and to carry out an inspection and maintenance plan in accordance with SR -EN 60079-17, remain unresolved.

Maintenance means a combination of all actions carried out in order to maintain or restore an object while it is able to meet the requirements of the relevant specification and perform its functions.

Inspection is an action which comprises a detailed examination of an object, be carried out either without dismantling or with partially dismantling, as appropriate, supplemented by such means as measurements, to reach a certain conclusion on the state of the object in question.

In order to carry out a correct inspection and maintenance of electrical installations in optimal conditions the following updated documents must be available:

- a) classification of hazardous areas;
- b) the gas group and temperature class classification of the equipment;
- c) sufficient records to allow explosion-proof equipment to be maintained in accordance with the types of protection (list and location of equipment, spare parts,

technical information);

d) the cable runs for underground cables.

Inspection and maintenance of electrical installations must be carried out only by experienced personnel whose training included instruction on the various types of protection and practical ways to install, all relevant rules and regulations, and general principles for the classification of hazardous areas.

The main factors which are likely to cause the alteration of equipment are:

- susceptibility to corrosion;
- exposure to chemicals and solvents;
- the possibility of accumulation of dust and dirt;
- the possibility of water ingress;
- exposure to excessive ambient temperatures;
- risk of mechanical damage;
- exposure to abnormal vibration;
- staff training and experience;
- the possibility of unauthorized changes and adjustments;
- the possibility of improper maintenance, is not in accordance with the manufacturer's recommendations.

Inspections are classified in degrees and types of inspection. A certain type of inspection is carried out with a certain degree of inspection.

The types of inspection are: initial and periodical.

The grades of inspection are: visual, rigorous, detailed.

Visual inspection is the inspection that identifies without the use of auxiliary equipment and tools, those alterations of the equipment that can be identified visually.

In an electrical installation which operates in an explosive atmosphere, during the visual inspection apparatus is checked if it corresponds to the area classification, identification of the circuits is available, the enclosure, windows and the gaskets and / or sealing materials are suitable, there are no authorized visible modifications, screws, cable entries (direct and indirect) and the closing elements, if any, are of the correct type and are complete and tight, no apparent damage to the cable, the sealing columns, tubes, pipes and / or ducts is satisfactory, connections to ground, including any additional connections linking the equipotential to the earth is satisfactory (for example connections are tight and conductors are sectional sufficient, the apparatus is suitably protected from corrosion, weathering, vibration and other harmful factors, there is no abnormal accumulation of dust and dirt.

Rigorous inspection is the inspection that includes aspects covered by visual inspection and, in addition, identifies those defects, such as loose screws, which can be distinguished only by the use of access equipment (where required) and tools.

Detailed inspection is the inspection that includes the aspects covered by rigorous inspection and in addition identifies those defects that can be revealed only by opening the enclosure and / or when necessary using tools and test equipment.

All visual and rigorous inspections can be carried out with the equipment being energized. Detailed inspections generally requires the equipment to be de-energized.

Before the installation or equipment to join the service, it must be subjected to an initial inspection on a regular basis and then re-inspected to ensure that the installation is maintained in a satisfactory condition for further use in a hazardous area.

The initial inspection is the inspection provided for all devices, systems and electrical installations before commissioning, in order to verify the type of protection chosen and the conditions of installation to be appropriate. Initial inspection must be carried out with a detailed degree grade of inspection.

The results of the initial inspections must be recorded for all equipment.

A periodic visual inspection or rigorous inspection can show the need for a detailed inspection. It may not be easy to accurately predict a periodic inspection at an appropriate range.

The interval between inspections and the degree of the inspection should be determined taking into account a number of factors which exert an influence on the electrical apparatus, such as the type of equipment, the factors likely to cause damage to the equipment, the results of previous inspections carried out.

The time interval between inspections shall not exceed three years without requiring the consultation of an expert. However, if the equipment is supposed to be permanently supervised by experienced staff, the time intervals between inspections can be increased or inspections can be removed if this is explicitly allowed by the rules and relevant regulations.

The results of all periodical inspections must be recorded in inspection records, table 1. Inspection survey is applied to a certain fraction of installed equipment. These can be visual, rigorous and detailed. The size and composition of all the samples shall be determined depending on the purpose of the inspection.

Survey inspections should aim to finding defects of random nature (eg. Loose connections), and should be used for monitoring the effects of environmental conditions, vibration, inherent design deficiencies, etc.

Survey results of inspections must also be recorded.

When an electrical apparatus is installed in areas where there may be an atmosphere caused by flammable gas, vapor or mist concentration and dangerous quantities protective measures have to be applied in order to reduce the likelihood of explosion due to the ignition by sparks, arcs or hot surfaces in normal operation or specified fault conditions.

The general condition of all appliances must be established periodically by the application of inspection specified and if necessary appropriate remedial measures shall be taken. Current actions taken to preserve the functionality status of fully installed equipment is called maintenance. It should be considered, in particular, maintaining the integrity of type of protection required for equipment.

Spare parts must comply with documentation for safety.

Electrical equipment located in a hazardous area can be adversely influenced by ambient conditions in which it is used. Some of the key elements to be considered are: corrosion, ambient temperature, ultraviolet radiation, water penetration, accumulation of dust or sand, mechanical effects and chemical aggression.

Corrosion of metals or the influence of chemicals (especially solvents) of the components of plastics or elastomers, can affect the type and degree of protection protections device.

Table 1. Inspection records table

Check if:	Ex d			Ex e			Ex n		
	Degree of inspection								
	D	A	S	D	A	S	D	A	S
0	1	2	3	4	5	6	7	8	9
A. equipment									
The apparatus corresponds to the area classification	x	x	x	x	x	x	x	x	x
2. The appliance group is correct	x	x		x	x		x	x	
3. The temperature class of the appliance is correct	x	x		x	x		x	x	
4. The identification of the circuitry of the appliance is correct	x			x			x		
5. Device circuit identification is available	x	x	x	x	x	x	x	x	x
6 The casing, the glasses of the visors and the gaskets and / or the glazing materials on the metal are adequate	x	x	x	x	x	x	x	x	x
7. There are no unauthorized changes	x			x			x		
8. There are no visible unauthorized changes		x	x		x	x		x	x
9. The screws, the cable entries (direct and indirect) and the closing elements are correct and are complete and tight:									
- Physical verification;	x	x		x	x		x	x	
- visual inspection			x			x			x
10. The surfaces of the flanges (coupling) are clean and non-degraded and the liners, if any, are satisfactory	x								
11. The dimensions of the flame proof between the flanges are within the permissible limits	x	x							
12. he nominal characteristics, the type and position of the lamps are correct	x			x			x		
13. The electrical connections are tight				x			x		
14. The condition of the carcass gaskets is satisfactory				x			x		
15. Capsule and hermetically sealed breakers are not damaged							x		
16. The restricted breathing casing is satisfactory							x		

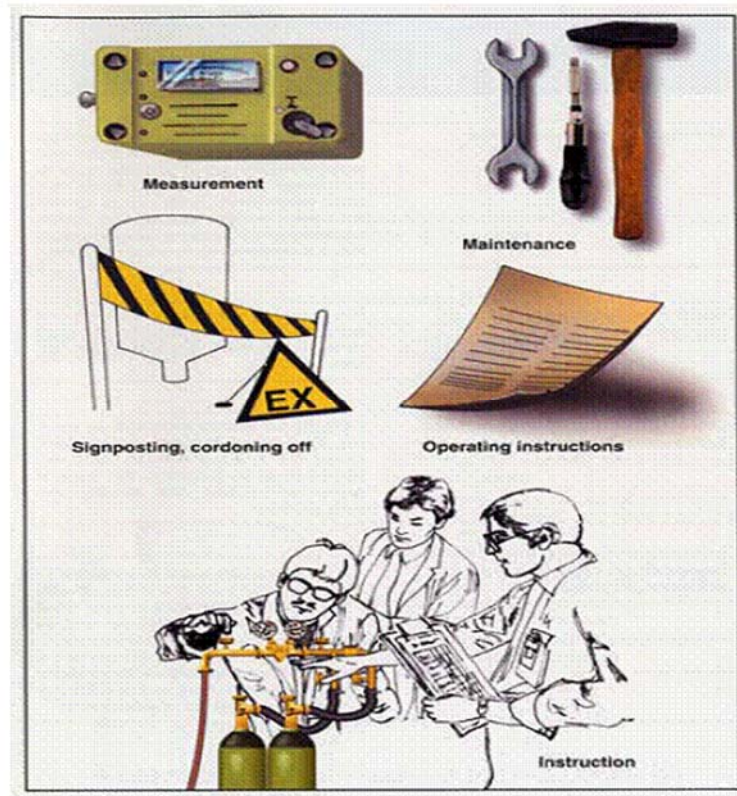


Fig. 1. Conditions for potentially explosive areas

If the enclosure or component is severely corroded, the affected part has to be treated by a suitable protective coating against corrosion, frequency and nature of such treatment being determined by the ambient conditions.

Screws, bolts and similar parts on which the type of protection, only to be replaced with similar parts in accordance with manufacturer's project.

Damaged gaskets must be replaced.

If maintenance is required for the purpose of removal from service of the equipment, exposed conductors must be fixed in a certified enclosure. Alternatively the cable can be adequately protected by isolation and separation of the ends of the cable conductors from all supply sources. If the equipment has to be permanently withdrawn from service, associated wiring must be removed or alternatively, properly fixed otherwise, in an enclosure.

Where screws or other fasteners or special tools have been provided, they must be available and should be used.

It has to checked that the electrical equipment has been designed to withstand the effects of ambient temperatures, of the highest and the lowest values that can be encountered in service.

Personnel in charge with the operation of these facilities operating in explosive atmospheres must be familiar with the requirements of all applicable standards, recommendations of all codes of practice, have access to all information necessary for the examination, if necessary, to use equipment and test procedures similar to those used by authorized bodies.

It is the responsibility of the user of the plant facility, to properly install, use and maintain the integrity of the equipment used in explosive atmospheres during its lifetime. Neglecting the following issues may cancel the type of protection and although this can't be controlled by the manufacturer of the equipment, they are reported to the user as being crucial: to install the equipment correctly, taking into account the manufacturer's instructions to use equipment only in atmospheres for which it was certified, to operate the equipment only within the technical parameters with which it was designed, to limit the uncontrolled increase in temperature of the components of the equipment that may be heated excessively.

3. CONCLUSIONS

Explosion proof equipment, unlike ordinary industrial equipment, is designed having in mind two categories of technical features, which are incorporated:

- One category of technical features, which are strictly related to the proper functioning of the equipment, from the technical point of view (for example, in the case of an electric motor, particular characteristics such as: torque, power, number of revolutions, etc., are of interest), the maintenance of which affects the way in which the equipment carries out its designed role in the technological installation in which it performs. Generally speaking, this category of technical features is well taken care of by the user of the equipment, although they are not directly related to the explosion protection provided by the equipment, but with the proper functioning of the equipment in the installation, from the technical / technological point of view.

The user reacts very quickly when one of these technical features is altered and takes immediate action to restore it to the innitial values, taking into account that the alteration of these features affects the proper functioning of the technological installation directly.

- A second category of technical features, which are specific only in the case of explosion protected technical equipment, and which are related only to the explosion protection provided by the equipment. The alteration of these features (parameters) is not as obvious to the user, as in the previous case, since these parameters are not related to the proper functioning of the equipment from the technological point of view, but only from the explosion protection point of view.

That is the reason why, in many cases, the user leaves the maintenance of these parameters on a secondary level, and in some circumstances tries to restore them to a proper level when it is already too late.

Having in mind these conclusions, it is of paramount importance for the users of explosion protected technical equipment to subscribe to the importance of ensuring a

proper maintenance, especially of these technical characteristics which are related to the explosion protection provided by the equipment.

This is achieved by having in mind the provisions underlined in the specific standards that deal with inspection and maintenance of Ex-proof equipment SR EN 60079-17 and SR EN 60079-14, as well as during the trainings organized on a regular basis by the National Authority in this field INSEMEX Petrosani, with the companies that operate with technical instalations in potentially explosive atmospheres..

REFERENCES

- [1]. SR EN 60079-17: 2014 - Inspection and maintenance of electrical equipment
- [2]. Directive 2014/34 / EU of the European Parliament and Council in 2014 on the assessment of the laws of the Member States concerning equipment and protective systems intended for use in potentially explosive atmospheres.
- [3]. SR EN 60079-0 / 2013 - Explosive atmospheres. Equipment. General requirements
- [4]. NEx 01-06 2007 - Standard on Explosion prevention for the design, installation, commissioning, operation, repair and maintenance of technical installations operating in potentially explosive atmospheres.

RELIABILITY ANALYSIS OF THE BRAKING SYSTEM OF THE INDUSTRIAL LOADER/TRANSPORTER MACHINES

**OVIDIU-BOGDAN TOMUȘ¹, DUMITRU JULA²,
ANDREI CRISTIAN RADA³**

ABSTRACT: The purpose of this study is to estimate the reliability features for the brake pads used in the braking systems of the industrial loader/transporter machines, with focus on machines used in the Romanian mining industry. The input data was taken from five such machines used over a period of four years. The conclusions were used by the operating companies in order to improve the maintenance strategy based on reliability.

Keywords: brake pads, estimation, analysis, reliability, defects.

1. INTRODUCTION

Loading, transport and storage machines are complex equipments used to load the material resulting from the drilling-blasting process, transport it over relatively small distances, and deposit it. They are used both for the removal of material from the front, for the exploitation of useful minerals and for the digging of galleries, including underground and surface hydrotechnical constructions. For the reliability study carried out, the mechanical drive model used in underground and surface hydrotechnical constructions was considered. Tables 1 and 2 show the main technical characteristics for two categories of loading and transport machines produced by Sandvik.

Operational reliability studies were conducted on data regarding the average use of brake pads for five loading machines over four operating years. Figure 1 shows the model TORO 151 produced by Sandvik with a capacity of 3500 kg.

¹ Lecturer Eng. Ph.D., University of Petroșani, tobogdan2002@yahoo.com,

² Assoc. Professor Eng. Ph.D., University of Petroșani, juladumitru@yahoo.com

³ Ph.D. Student, Eng., University of Petroșani

Table 1. The main technical characteristics of the Sandvik loading, transporting and storing machines with mechanical drive

Model	Name	Bucket capacity, kg	Mass, kg	Lenght, mm	Width, mm
LH201	Microscoop 100	1000	3650	4650	1055
LH203	TORO 151	3500	8700	7040	1480
LH307	TORO 6	6700	18020-19600	8631	2236
LH410	TORO 7	10000	26200	9591	2647
LH514	TORO 9	14000	38100	10870	2920
LH517	TORO 0010	17200	44000	11120	3000
LH621	TORO 11	21000	56800	11993	3100

Table 2. The main technical characteristics of the Sandvik loading, transporting and storing machines with electric drive

Model	Name	Bucket capacity, kg	Mass, kg	Lenght, mm	Width, mm
LH203E	TORO 151E	3500	9400	6995	1480
LH306E	EJC 145E	6600	17237	8407	2159
LH409E	TORO 400E	9600	24500	9736	2525
LH514E	TORO 1400E	14000	38500	10950	2880
LH625E	TORO 2500E	25000	77500	14011	3900



Fig. 1. Overall view of the loading, transporting and storing machine, model TORO 151 produced by Sandvik

2. ESTIMATING THE AVERAGE USAGE OF BRAKE PADS IN THE BRAKING SYSTEM

The main defect of the brake pads of the loading and storing machines is their intensive wear due to their repeated use and to the high forces acting on them.

The available database indicates the best running times (BRT, t_i), in h, of the brake pads. The values in the order of their reception in time are shown in Table 3.

The values of the best running times, t_i , represent a statistical series of the form (S1), which comprises $n = 25$ disjoint values, ordered as following: 1180; 1189; 1225; 1242; 1251; 1279; 1301; 1319; 1321; 1345; 1353; 1399; 1442; 1504; 1533; 1621; 1673; 1692; 1710; 1723; 1860; 1870; 1883; 1923; 1976.

The empirical distribution function values $\hat{F}(t_i)$, are shown in Table 4 and the values of the distribution functions parameters that characterize the reliability of the brake pads are shown in Table 5.

Table 3. Values of the best running times of the brake pads

Nr. crt.	BRT, t_i , h	Nr. crt.	BRT, t_i , h	Nr. crt.	BRT, t_i , h	Nr. crt.	BRT, t_i , h	Nr. crt.	BRT, t_i , h
1	1353	6	1442	11	1189	16	1399	21	1923
2	1321	7	1673	12	1533	17	1870	22	1504
3	1251	8	1180	13	1860	18	1242	23	1710
4	1621	9	1345	14	1225	19	1723	24	1692
5	1319	10	1301	15	1976	20	1279	25	1883

Table 4. The values of the empirical distribution function $\hat{F}(t_i)$

1	0.027559	6	0.224409	11	0.421260	16	0.618110	21	0.814961
2	0.066929	7	0.263780	12	0.460630	17	0.657480	22	0.854331
3	0.106299	8	0.303150	13	0.500000	18	0.696850	23	0.893701
4	0.145669	9	0.342520	14	0.539370	19	0.736220	24	0.933071
5	0.185039	10	0.381890	15	0.578740	20	0.775591	25	0.972441

Table 5. The values of the distribution functions parameters that characterize the reliability of the brake pads

Distribution	λ , 1/h	m_n , h	σ_n , h	β_1	η_1 , h	β_2	η_2 , h	γ
Exponential	0.000907							
Normal		1512.56	258.753					
Weibull biparametric, W_p				6.543	1622.593			
Weibull triparametric, W_m						6.866	1618.598	-0.0066

Table 6 shows that the normal distribution and the two variants of the Weibull distribution are valid, but the normal distribution approximates best the experimental (empirical) function with the lowest maximum distance between them.

Table 6. Reliability characteristic functions of the brake pads and their comparison

Theoretical distribution	Expression of reliability function, R (t)	Maxim deviation, Dmax	Risk, α	Critical value, $D_{\alpha,20}$	Validation
Exponential	$e^{-0,000907 \cdot t}$	0.657117	0.005	0.336512	No
Normal	$\frac{1}{2} - \Phi\left(\frac{t-1512,56}{258,753}\right)$ sau $1 - \frac{1}{258,753} \frac{1}{\sqrt{2\pi}} \int_0^t e^{-\frac{1}{2}\left(\frac{x-1512,56}{258,753}\right)^2} dx$	0.152527	0.20	0.207902	Yes
Weibull biparametric, W_p	$e^{-\left(\frac{t}{1622,593}\right)^{6,543}}$	0.158704	0.20	0.207902	Yes
Weibull triparametric W_m	$e^{-\left(\frac{t+0,0066}{1618,599}\right)^{6,866}}$	0.167930	0.20	0.207902	Yes

However, this value of the maximum distance between the two distributions is very close to that characteristic to the two Weibull bi and triparametric distributions, so that any of the three theoretical distribution functions can very well model the experimental function.

The exponential model is not valid.

With the help of the parameters determined for the four distribution laws, including the invalid model, in order to observe the differences, the main quantitative indicators characterizing the reliability of the brake pads were calculated and plotted.

The graphical representations in Figures 2, 3, 4 and 5 show the variations, according to the actual operating time, of the main reliability indicators.

The graphical representations in Figures 2 and 3 show the tendency of grouping, even superposition, of the reliability and non-reliability curves for normal and Weibull distribution laws, in the two forms, which confirm the very close values of the maximum distances between the experimental distribution and the theoretical distributions

It is also confirmed once more that any of these distributions expresses with sufficient precision the closest reliability indicators to the real situation. However, the great difference from the exponential distribution can not be taken into account to

characterize the failure of the brake pads, and in fact has not been validated.

From these representations, it also follows that, for 1000 hours of operating, the reliability of the brake pads is 95%, which would correspond, in analogy to the operating hours of the hydraulic pump in the brake circuit, for five months of functioning.

Essentially, however, in the next 500 hours of effective operation, brake pad reliability drops by half, about 50%, which indicates that the velocity is extremely high, as indicated by the high slope of the reliability and non-reliability functions. This is also confirmed by the high values indicated by the graphs showing the density of the probability of failure and failure intensity (Figures 4 and 5), especially the very rapid increase of the failure intensity.

The calculations show that after about seven months of operation of the braking system, its reliability drops to 50%, which is very low, especially as it concerns the safety of the machine, meaning that the brake pads have to be changed.

All of the above considerations may be clear arguments that the brake pads are totally inadequate, being necessary to reconsider their functionality, especially with regard to their technology and, in particular, the material used.

Table 7 lists the values for a series of quantitative indicators that characterize the reliability of the brake pads.

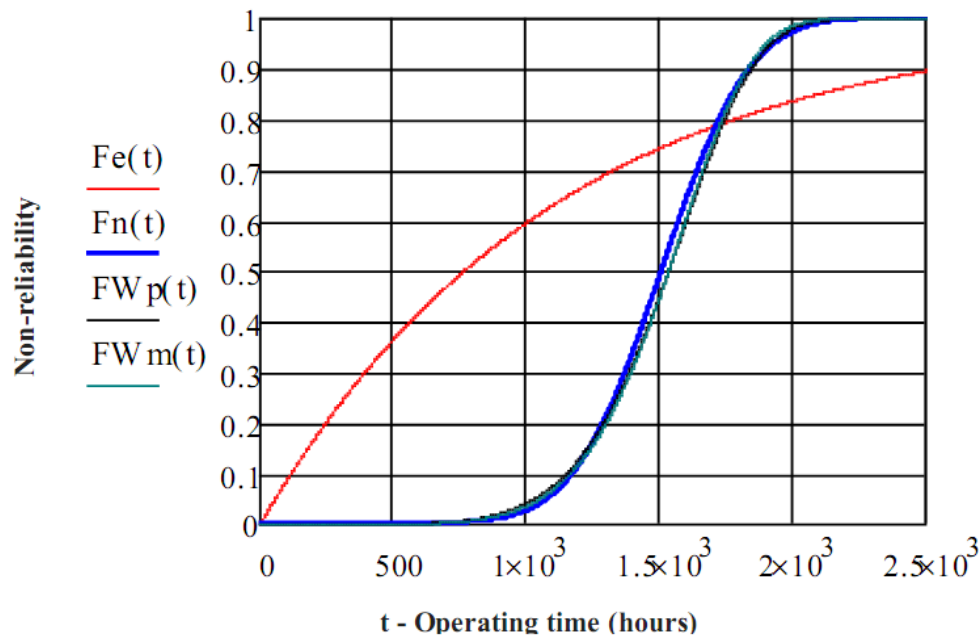


Fig. 2. Graphic representations of reliability functions for brake pads

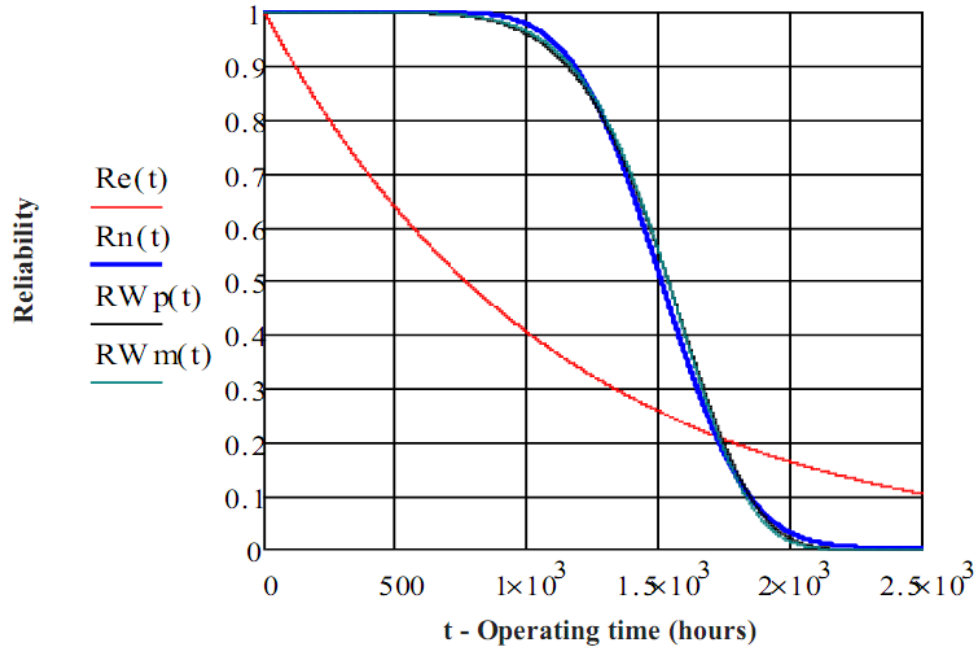


Fig. 3. Graphic representations of the probability of failure of brake pad

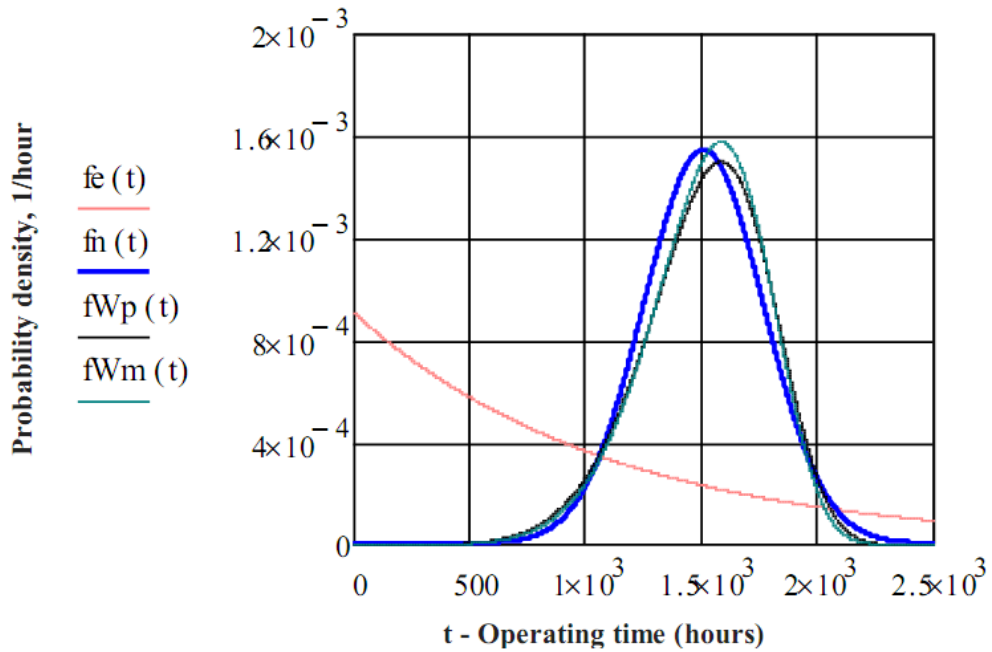


Fig. 4. Graphic representations of the density of the probability failure of brake pad

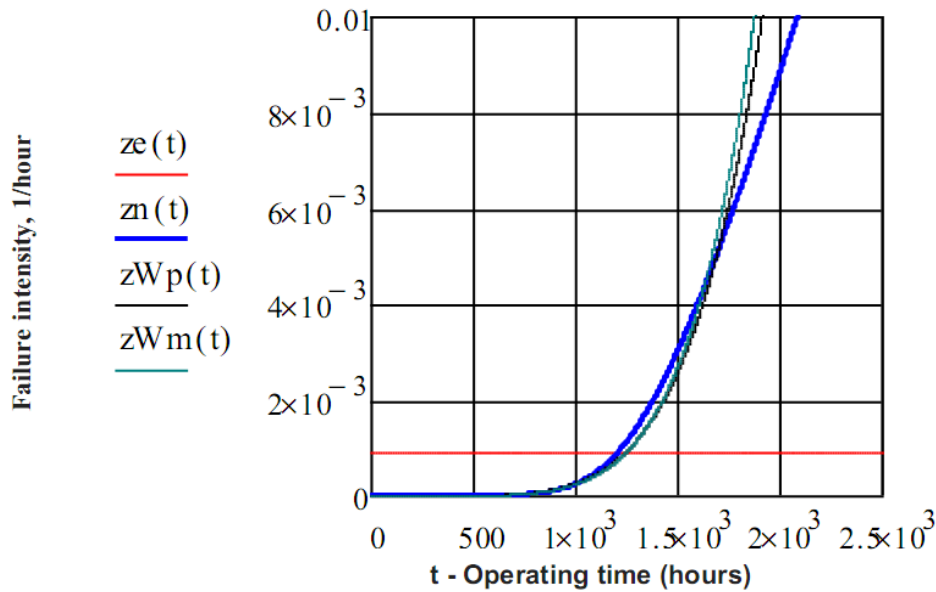


Fig. 5. Graphic representations of brake pad failure intensity

Table 7. Reliability indicators regarding the running time until brake pads failure

No.	Parameter		Parameter value for distribution:		
	Denomination	MU	Normal	Weibull biparametric, Wp	Weibull triparametric, Wm
1	Main Average, m , $MTTF$	h	1512	1512	1512
2	Median, t_{med}	h	1512	1534	1534
3	Module, t_{mod}	h	1512	1582	1582
4	Dispersion, D	h ²	66953	73189	66953
5	Standard deviation, σ	h	259	271	259
6	Variation coefficient, CV	-	0.171	0.179	0.171

Analyzing the indicators presented in Table 7, it is once again confirmed that the normal distributions and Weibull in the two forms also allow the calculation of the most appropriate reliability indicators for the characterization of the brake pads, having almost equal values for all the indicators presented.

It can also be appreciated that the values of the presented indicators demonstrate the low reliability of the brake pads.

3. CONCLUSIONS

Reliability indicator values calculated for the brake pads of loading, transporting and storing machines are used to estimate the need for spare parts by applying specific

methodologies based on the results of reliability studies as part of the maintenance strategy based on reliability.

The main conclusions of the reliability study on the brake pads of the braking system of the loading, transporting and storing machines are:

- The Weibull and normal distributions best characterize the phenomenon of wear and tear which appears very strongly in the operating of the brake pads, the maximum distance between the experimental and the theoretical distributions for the two distributions being virtually identical, especially since the literature indicates the use of the normal distribution to characterize aging phenomena;

- If after 1000 hours of operating, corresponding to five months, the reliability of the plates is 95%, after another 500 hours of operation it reaches 50%, which shows that the speed of failure (wear) is very high, confirmed by the slope of the reliability and non-reliability functions as well as the density curves of the probability of failure and the failure intensity (failure rate);

- The above considerations may be clear arguments that the brake pads are totally inappropriate and that their functionality, especially with regard to their technology, and the material used, must be reconsidered.

REFERENCES

- [1] Balosin, N., Magyari, A., Jula, D., *Aspects Regarding the Functionality of the transmission of Overweight Vehicles Used in Lime Pits*, Annals of the University of Petroşani, Mechanical Engineering. Vol. 11 (XXXVIII), 2009.
- [2] Jula, D., Praporgescu, G., Mihăilescu, S., Tomuş, O.B., Deaconu, I., *Aspecte privind determinarea fiabilităţii utilajelor din carierele de lignit*, Lucrările ştiinţifice ale simpozionului internaţional multidisciplinar “Universitaria SIMPRO”, Volumul: Maşini şi echipamente tehnologice. Editura UNIVERSITAS, Petroşani, 2006.
- [3] Jula, D., Dumitrescu, I.– *Fiabilitatea sistemelor de transport*, Editura Focus, Petroşani, 2009.
- [4] Kovacs I, Nan M.S., Andras I., Urdea G.B., *Research Regarding the Operation of Continuous Transportation Systems in Valea Jiului Colliery's Conditions*, Microcad 2013.
- [5] Kovacs I, Andras I, Nan M.S, Popescu F.D. *Theoretical and experimental research regarding the determination of non-homogeneous materials mechanical cutting characteristics*, Proceedings of the 8th WSEAS International Conference on SIMULATION, MODELLING and OPTIMIZATION (SMO '08).
- [6] Ladányi G., Nagy E., Virág Z., *Study on dynamics of caterpillar track bodies*, VII. International Conference on Mining Techniques, TUR 2011, on CD: TUR 2011 Książka.pdf. , 2011 szeptember 20-23.
- [7] Radu S.M., Chmielarz W., Andras A., *Mining Technological System's Performance Analysis*, Annals of the University of Craiova for Journalism, Communication and Management, Volume 2, 2016, ISSN 2501-3513.
- [8] Urdea Ghe.B., Cozma B.Z., Tomuş O.B. – *Analysis of systematic transport to E.M.Uricani*. „Universitaria Simpro” Petroşani, Ed. Universitas, - Octombrie 2008.

STUDY OF THE CUTTING FORCES AND SPECIFIC CUTTING RESISTANCE FROM THE POINT OF VIEW OF THE CUTTING DIRECTION RELATIVE TO STRATIFICATION OF THE COAL SEAM

OVIDIU-BOGDAN TOMUȘ¹, ANDREI CRISTIAN RADA²

ABSTRACT: The study is a practical and theoretical approach of the influences acting on the digging forces of the wheel in regards to the cutting direction of the BWE. Comparison of perpendicular cutting along stratification and parallel with stratification cutting allow is used, in order to better assess the dislocation phenomenon at the level chips cut by the BWE.

Keywords: the cutting; stratification; lignite; comparative analysis;

1. INTRODUCTION

Based on the determinations made on the parameters of the lignite cutting regime throughout the Oltenia basin, a comparative analysis was performed on quarries and lignite layers. This analysis highlights the cutting forces, the specific resistance to cutting, the penetrating forces, the angle of breaking of the massive chip, the specific consumption of energy for cutting on lignite quarries and studied lignite layers.

Comparative analysis is useful, on one hand, to highlight the lignite cutting behavior of quarries and studied layers and to improve the constructional parameters of teeth, cups and rotor as a whole on the other hand.

This comparative analysis is at the same time the scientific basis for the selection of new extraction equipment in the Oltenia basin.

Comparisons of perpendicular cutting along stratification and parallel with stratification cutting allow a better assessment of the dislocation phenomenon at the level of a chip cut by the excavator's rotor.

¹ *Lecturer Eng. Ph.D., University of Petrosani, tobogdan2002@yahoo.com,*

² *Ph.D.Student, Eng., University of Petrosani*

2. COMPARATIVE ANALYSIS OF PARALLEL LIGNITE CUTTING AND PERPENDICULAR TO STRATIFICATION LIGNITE CUTTING

The rotor excavator mainly cuts "vertical chips", where the perpendicular cutting is predominant on the stratification, so the laboratory tests were carried out mainly with the perpendicular on the stratification cutting. Because in the case of cutting with horizontal chip (mainly excavating at the level of the tracks), the cutting is predominantly parallel to the stratification, as in the case of the entry of the cup in the massive when cutting "vertical chips", there were made 31 experimental trials cutting in parallel with the stratification. These trials were carried out on a properly taken sample from the lignite quarries in Oltenia. The comparison was performed with the results obtained by cutting perpendicular to the stratification of the samples taken from the same layer and quarry.

Figures 1 and 2 show the dependence of the cutting force F_{xm} and the dynamic coefficient k_d in relation to h_0 in the case of parallel cutting, respectively perpendicular to the stratification. It is noted that the force F_{xm} is 2.16 times larger at the perpendicular cutting compared to the parallel cutting and the dynamic coefficient k_d has higher values at perpendicular cutting on an average by 40%.

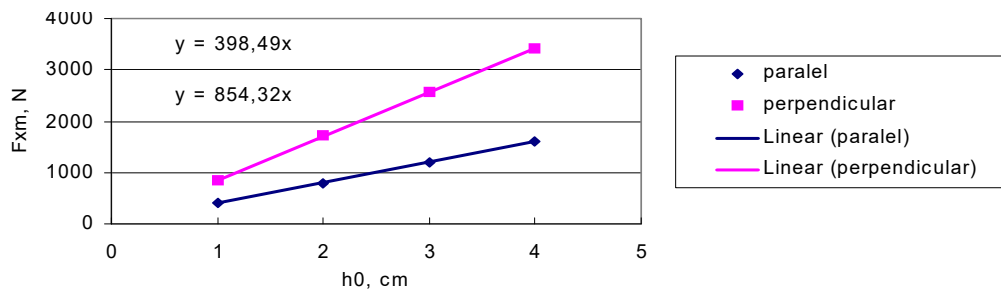


Fig. 1. Effective medium cutting force F_{xm} depending on the cutting depth h_0

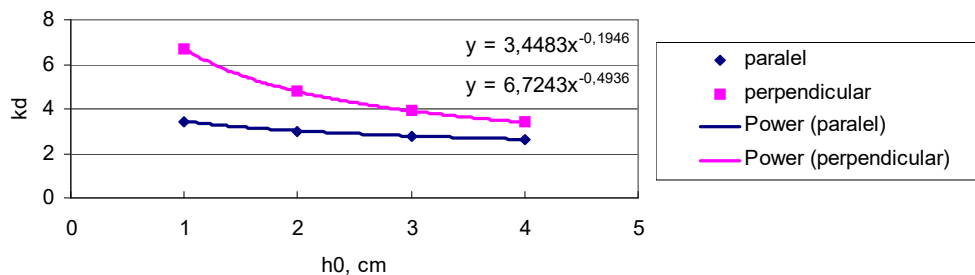


Fig. 2. The dynamic coefficient k_d , depending on the cutting depth h_0

As for the specific cutting resistances, the dependencies $A = f(h_0)$, $A_1 = f(h_0)$ and $K_e = f(S_0)$ are shown in Figures 3, 4 and 5. It can be seen that A and K_e are approximately constant in relation to h_0 , respectively S_0 , and A_1 has a linear variation according to h_0 , analogous to the case of F_{xm} .

The higher values of the specific resistance to cutting are found in the case of perpendicular cutting with the stratification. Thus, for A , the ratio is 2.1 and for K_c of 2.3 between perpendicular and parallel cutting. The same ratio of 2.1 as A is also found in A_1 . It can be concluded that on average the resistance and the specific resistance specific to the perpendicular cutting on the lignite stratification is at least double to the parallel cutting with the stratification.

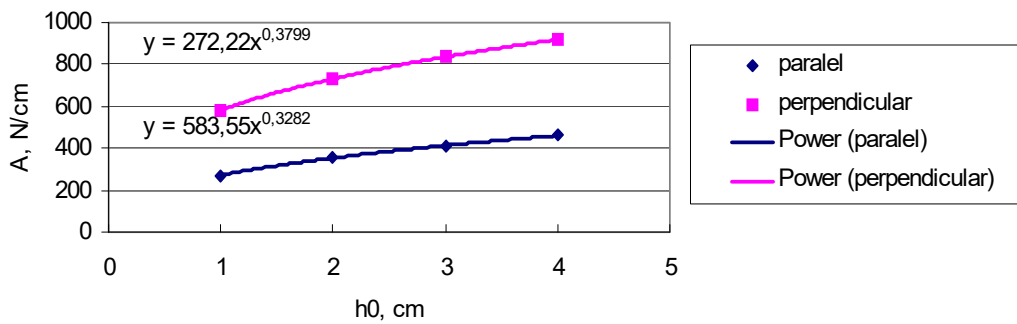


Fig. 3. The specific cutting resistance A , depending on the cutting depth h_0

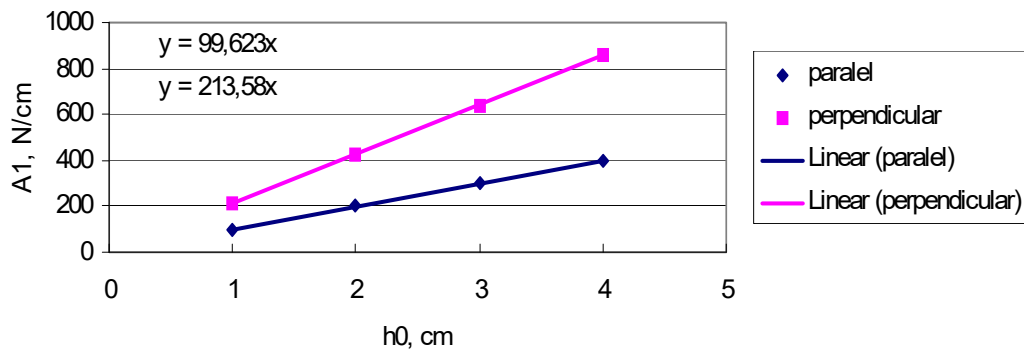


Fig. 4. The specific cutting resistance A_1 , depending on the cutting depth, h_0

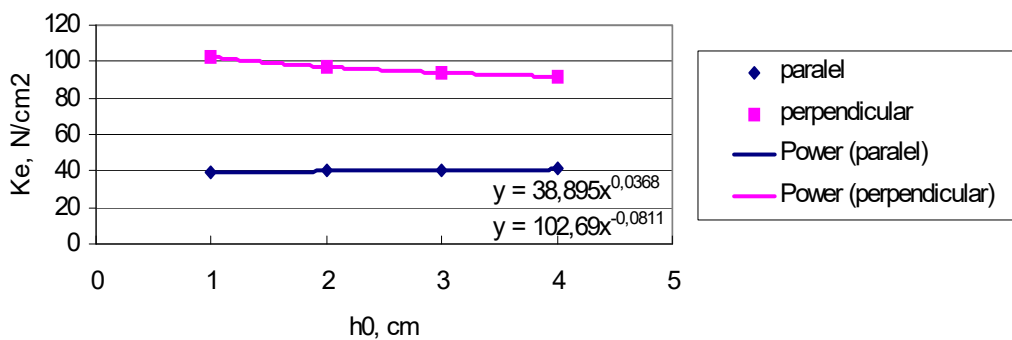


Fig. 5. The specific cutting resistance K_c depending on the transversal section surface of the chip, S_0

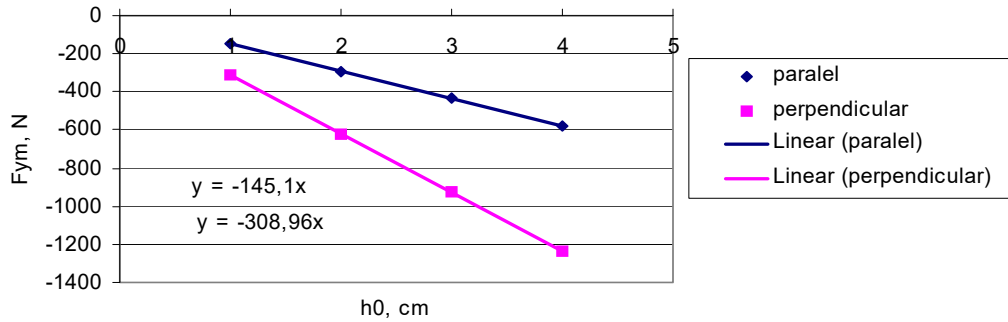


Fig. 6. Effective medium penetration force F_{ym} , depending on the cutting depth, h_0

For F_{ym} penetration force and F_{zm} lateral force according to h_0 , the corresponding curves are shown in Figures 6 and 7. From their analysis it follows that the F_{ym} force has only negative values (to massive) which in absolute value are at least two times higher in the case of perpendicular cutting than the parallel one.

The F_{zm} lateral forces have conventional positive values for the perpendicular cutting and negative in the case of parallel cutting, the absolute values being at least 6 times higher at the perpendicular cutting.

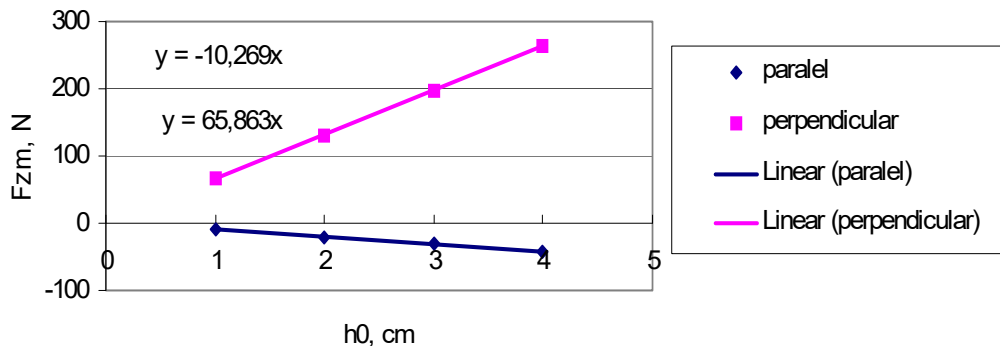


Fig. 7. Effective medium lateral force F_{zm} , depending on the cutting depth, h_0

Comparisons of the breaking angles ψ were made on the basis of the curves represented in Figure 8, from which it follows that both curves tend to flatten. Thus ψ is 60° for parallel cutting and 67° for perpendicular cutting. From this point of view, the perpendicular cutting is more advantageous.

From an energetic point of view, the comparison was made using the curves represented in Figure 9. It can be noticed the tendency of flattening of the both curves with respect to h_0 , with a specific energy consumption E_s that is doubled in the case of perpendicular cutting, in comparison to the parallel cutting, $E_s = 0.22 \text{ kWh} / \text{m}^3$ versus $E_s = 0.11 \text{ kWh} / \text{m}^3$

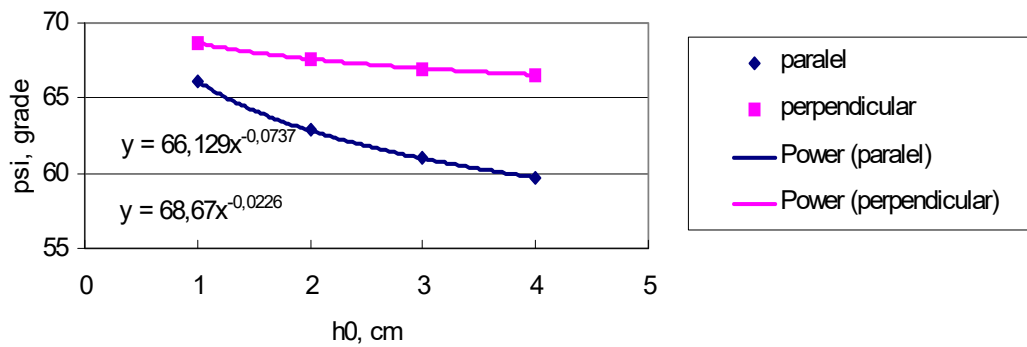


Fig. 8. The breaking angle of the chip ψ , depending on the cutting depth, h_0

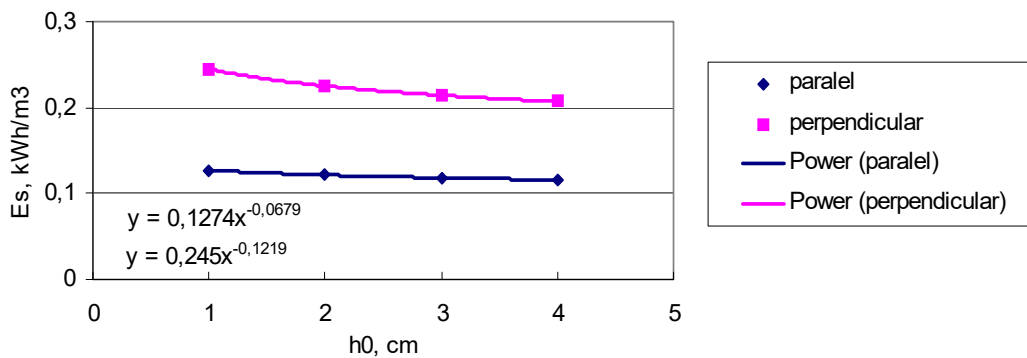


Fig. 9. Specific energy consumption E_s , depending on the cutting depth, h_0

3. CONCLUSIONS

In the comparative analysis of the parallel and perpendicular cutting on lignite stratification, the same aspects were followed as in the comparisons between quarries and layers.

Comparisons of perpendicular cutting along stratification and parallel cutting with stratification allow for a better assessment of the dislocation phenomenon at the level of a chip cut by the rotor of the bucket wheel excavator.

It is emphasized that in almost all the compared aspects, perpendicular cutting is more disadvantageous than parallel cutting, except for the angle of breaking of the massive chips.

As for the forces, the specific resistances to the cutting and the specific energy consumption, the cutting of the lignite perpendicular to the stratification involves roughly double values compared to the parallel cutting with the stratification.

REFERENCES

- [1] **Kovacs, I., Iliăș, N., Nan, M.S.**, *Regimul de lucru al combinelor miniere*, Editura Universitat, Petroșani, (2000).
- [2] **Kovacs, I., Andraș, I., Andraș, A., Tomuș, O.B.** – *Overview Of The Results Obtained In The Field Of Rock Cutting In Underground And Open Pit Conditions.* - Monografia Nowoczesne Metody Eksploatacji Węgla I Skal Zwięzłych. pag. 9 – 16, Akademia Gorniczo-Hutnicza. Krakow 2013
- [3] **Kovacs I., Nan M.S., Jula D., Tomus O.B.** - *New Buckets Mounted on Rotor Excavators, as a Result of Dislocation Tested Process –*, International Conference on Applied Computer Science, Malta September 15-17, 2010, ISSN: 1792-4863; ISBN: 978-960-474-225-7;
- [4] **Kovacs I., Nan M.S., Jula D., Tomus O.B.**, *New Buckets Mounted on Rotor Excavators, as a Result of Dislocation Tested Process –*, International Conference on Applied Computer Science, Malta September 15-17, 2010.
- [5] **Nan M.S., Kovacs I., Popescu F.D.**, *Research regarding the improvement of the methodology and means used for the balancing by weighting of bucket wheel excavators*, Proceedings of the 8th WSEAS International Conference on Simulation, Modelling And Optimization (SMO '08).
- [6] **Radu S.M.**, *The Mechanized Face as a System.* Proceedings of the 8th WSEAS International Conference on Simulation, Modelling And Optimization (SMO '08), Santander, Cantabria, Spain, September 23-25, 2008, ISSN: 1790-2769, ISBN: 978-960-474-007-9.
- [7] **Tomuș O.B.**, *Studiul posibilităților de creștere a performanțelor rotorului excavatoarelor utilizate în carierele de lignit.* Teză de doctorat, Petroșani, 2009.
- [8] **Tomuș O.B., Voicu G.V., Grigorie P., Poiana L.**, *Research Regarding The Use of CAD Methods on the design of Bucket Wheel and Excavator Teeth and Bucket Based on real Working Conditions.* – microCAD 2010, International Scientific Conference Miskolc, 18-20 march 2010.

RESEARCHES ON THE MODERNIZATION OF THE EXECUTION TECHNOLOGIES OF DIGGING, ARRANGING AND FITTING WORKS IN HYDROTECHNICAL CONSTRUCTIONS

**GABRIEL ȚUȚUIANU¹, DORINA BĂDIȚĂ (POPESCU)², MARIN
SILVIU NAN³, DĂNUȚ GRECEA⁴, BOGDAN VLADU⁵, ALIN SULTAN⁶**

Abstract: The purpose of these papers is to minimize the importance of technology, ignoring its basic role in constructing technical products can lead to a substantial increase in the workload and the consumption of material necessary for their manufacture and consequently to the increase in the costs for their manufacture.

As regards the design activity, it is necessary to automate the main stages, which are: conceptual design, analysis and technological design. It is noteworthy that the analysis part is an integral part of the design process. Even if the analysis cannot fully replace the prototype experimental test, it can help the designer develop an optimized prototype.

Keywords: hydrotechnical works, design, software.

1. INTRODUCTION

Hydrotechnical works differ from other engineering constructions in that they are subject to water action, which is manifested in the following aspects:

- mechanical action - is exercised in the form of hydrostatic pressure and dynamic pressure. The first is the main demand that generally determines the shape and dimensions of the hydrotechnical construction, the second is exercised by the moving water on the elements in contact with, the waves, the ram, the seismic waves or the water

¹ *Ph. D. Student, Eng., University of Petroșani,*

² *Ph. D. Student, Eng., University of Petroșani,*

³ *Professor, Ph.D. Eng., University of Petroșani, nan.marins@gmail.com*

⁴ *Ph. D. Student, Eng., University of Petroșani*

⁵ *Ph. D. Student, Eng., University of Petroșani,*

⁶ *Ph. D. Student, Eng., University of Petroșani,*

which infiltrate through porous media;

- physicochemical action - is exerted by erosion of the contact surfaces with moving water, by washing and degradation of concrete or foundation ground, corrosion of metallic elements and degradation of materials in contact with aggressive waters;

- biological action - is exercised by bodies living in water on wood, stone and concrete, degrading them over time.

Minimize the importance of technology, ignoring its basic role in constructing technical products can lead to a substantial increase in the workload and the consumption of material necessary for their manufacture and consequently to the increase in the costs for their manufacture.

As regards the design activity, it is necessary to automate the main stages, which are: conceptual design, analysis and technological design. It is noteworthy that the analysis part is an integral part of the design process. Even if the analysis can not fully replace the prototype experimental test, it can help the designer develop an optimized prototype.

As far as the design activity is concerned, it is necessary to automate the main stages, which are: conceptual design, analysis and technological design. It is noteworthy that the analysis part is an integral part of the design process. Even if the analysis cannot fully replace the prototype experimental test, it can help the designer develop an optimized prototype.

A revolutionary CAD program designed to design the mechanical and detail assemblies (landmarks) is Solid Edge. By implementing the most advanced solid state 3D modeling technology, Solid Edge delivers outstanding performance for interactive mechanical engineering, shortening the design cycle and enhancing its quality, helping manufacturers to market high-quality products at small prices.

Developed specifically for generating technical drawings, Solid Edge provides excellent representation, detailing, annotation and quotations automatically corresponding standard rating used. It also visibly improves design productivity through special media for sheet metal, welding and pipe construction.

Based on the technologies of execution of armored galleries and forced pipelines, an important problem on the site was the slope transport and the centering of the pipe sections. To solve this problem, the Solid Edge software was used for 3D modeling and pipeline transport piping design and pipeline sectioning, and a dimensional calculation program was performed in the MathCAD software.

Figure 1 show the 3D model of the helmet construction solution, which is provided with four screw jacks for centering the pipe section.

For the sizing and checking of the transport and centering moulders, 3D section of the $\Phi 2550 \times 25$ pipe length of 6 m has been modeled, on which the support was positioned one meter from the end of the section. The Solid Edge software determined the mass and position of the center of gravity of this assembly, with the mass of 10793 kg and the center of mass at 2770.6 mm end and 34.6 mm below the axis of the section (green dot), which are shown in Figure 2.

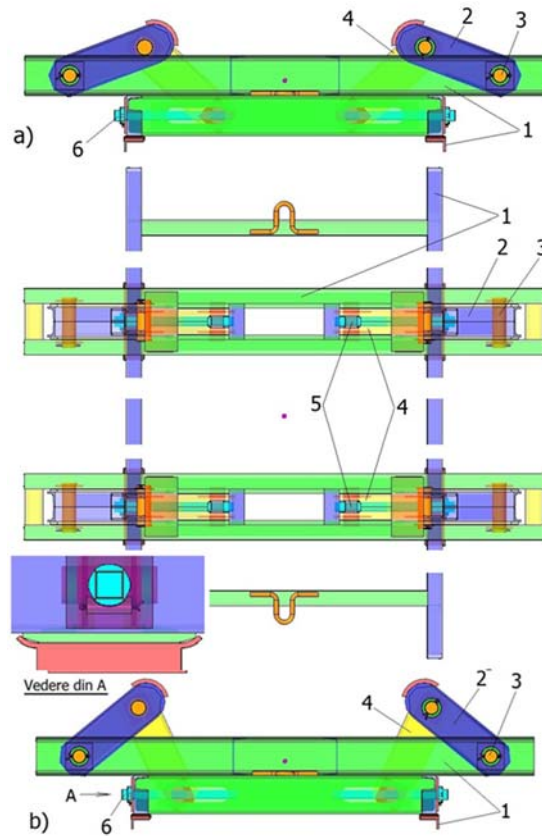


Fig. 1. The construction solution for the transport and centering of the pipe section
 a - the support arms are lowered to a minimum; b - Support arms raised to the maximum.
 1 - the frame of the sledge; 2 - supporting arm; 3 - $\Phi 60$ bolt; 4 - lifting arm; 5 - $\Phi 80$ bolt; 6 -
 M48 threaded rod.

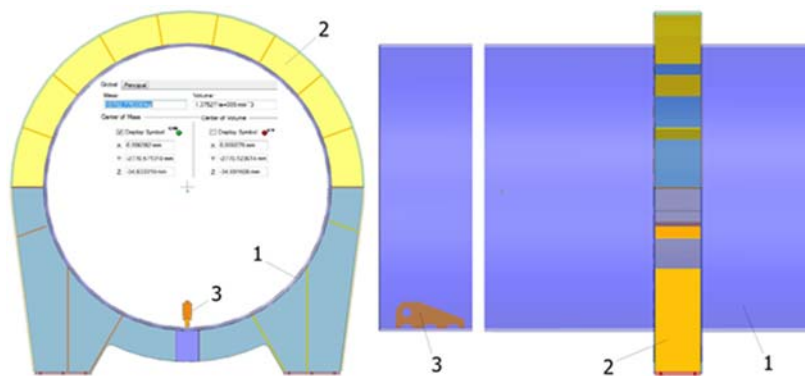


Fig. 2. The 3D model of the pipe section with its support bracket
 1 - $\Phi 2550 \times 25$ pipe section 6 mm and length m; 2 - the metal structure of the section support; 3 -
 towing eye.

Another problem facing work efficiency and quality of welded joints, Air Liquide Welding proposes a mechanized welding solution for the MIG / MAG welding process. This mechanized welding system runs on a rolling path that serves as a guide and support for a MIG / MAG welding torch in order to make welding easier. The entire system is powered by a 14V battery, which makes it easier to use. This mechanized welding equipment can be equipped with magnetic traction paths or via suction cups. The two variants were designed to accommodate the whole range of materials (magnetic, non-magnetic). Thus, magnetic gripping paths have been designed for use on magnetic materials (carbon steel, low alloy, etc.), and those with slotted cups for use in welding aluminum or stainless steel austenitic steels.

To achieve long-lasting welds, the treads can be easily interconnected. Two types of trolleys can be configured:

- Simple mechanized carts, Figure 3;
- Linear oscillator driven carts, Figure 4

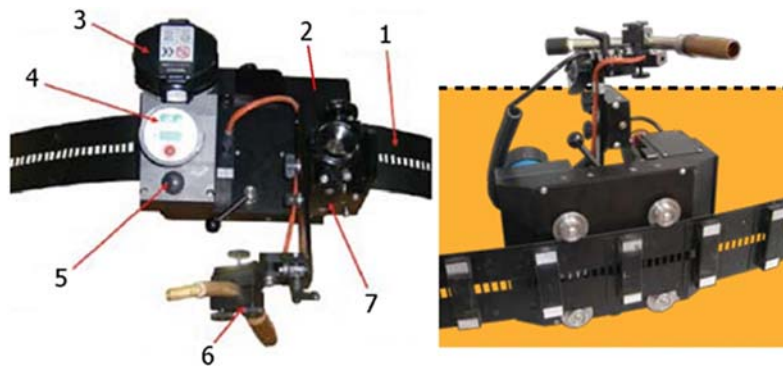


Fig. 3. Simple mechanized carts

- 1 - flexible runway; 2 - stroller; 3 - Battery; 4 - trolley control panel; 5 - trolley start / stop button; 6 - MIG welding torch with detector; 7 - hand slides.

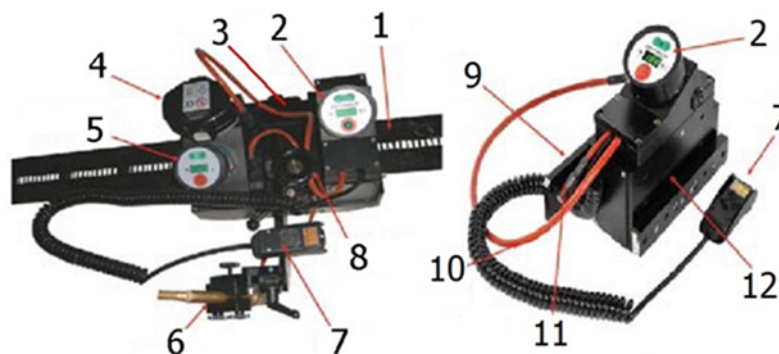


Fig. 4. Linear oscillator driven carts

- 1 - flexible runway; 2 - oscillator control panel; 3 - trolley; 4 - battery; 5 - trolley control panel; 6 - MIG welding torch with detector; 7 - remote oscillator control; 8 - OSCI-WELDY Oscillator; 9 - the oscillator mounting plate on the trolley; 10 - electric cable; 11 - torch trigger connection; 12 - Tube holder mounting plate.

2. ESTABLISH THE OPTIMAL DIMENSIONS OF THE FORCED PIPELINES

Based on the calculation relationships developed in MathCAD software for determining optimal dimensions of forced pipelines that are the main element of a hydroelectric arrangement, the first stage has determined the available hydraulic power of the hydroelectric arrangement for installed flow rates between 2 and 140 m³/s and gross falls between 50 and 300 m. The gross fall is considered to be the difference in the level between equilibrium castle and spillway or the level of runway from turbine. For a flow rate of 5 m/s in a laminar duct at a 32 degree horizontal angle of inclination of duct and existence of two elbows and two butterfly traces along the trail, hydraulic systems shown in Figure 5.

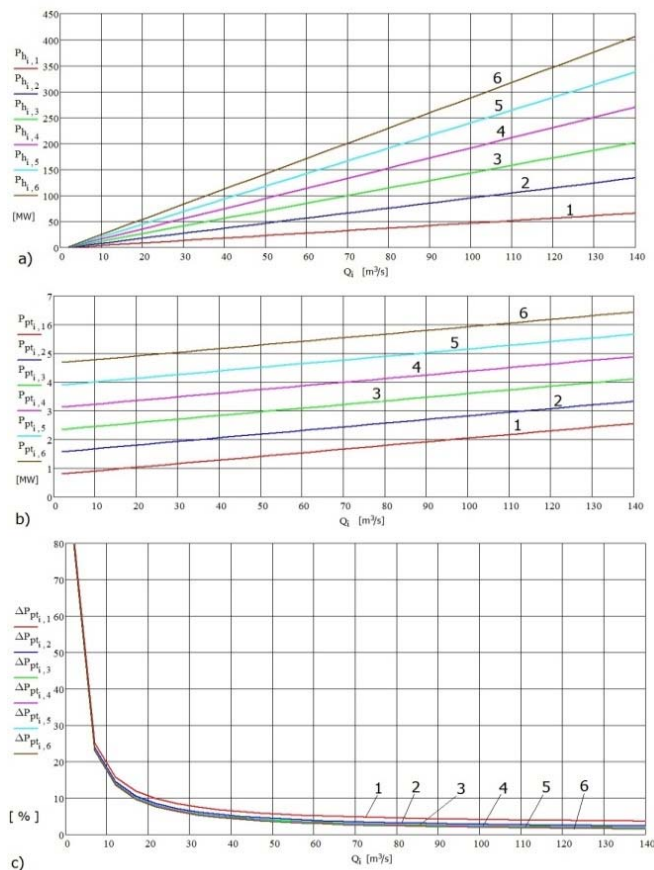


Fig. 5. The mode of variation of the hydraulic power according to installed flow and gross fall, at a flow rate of $v = 5$ m/s
 a - hydraulic power;
 b - total hydraulic losses;
 c - percentage of hydraulic losses in total power
 where:
 1 – gross fall of 50 m;
 2 - gross fall of 100 m;
 3 - gross fall of 150 m;
 4 - gross fall of 200 m;
 5 - gross fall of 250 m;
 6 - gross fall of 300 m.

To see the influence of the flow velocity on the hydraulic losses in the pipe, the same graphs were made for a water flow rate of 2.5 m/s, which are represented in Figure 6.

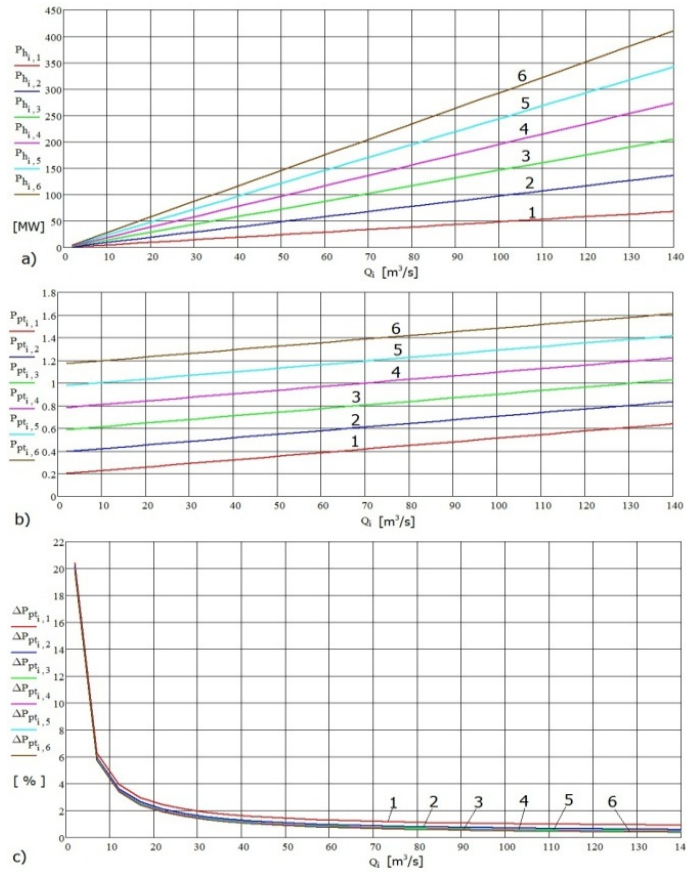


Fig. 6. The mode of variation of the hydraulic power according to installed flow and gross fall, at a flow rate of $v = 2,5$ m/s

a - hydraulic power;
 b - total hydraulic losses;
 c - percentage of hydraulic losses in total power

where:

- 1 – gross fall of 50 m;
- 2 - gross fall of 100 m;
- 3 - gross fall of 150 m;
- 4 - gross fall of 200 m;
- 5 - gross fall of 250 m;

These graphs allow the rapid determination of the hydraulic power at the turbine and of the total hydraulic losses on the forced duct depending on the installed flow and the gross fall of the hydroelectric arrangement, which increases in steps from 50 to 50 m. For intermediate rough fall, the rule of three simple.

It is noted that for installed flows below $10 m^3/s$ the hydraulic losses on the pipeline are very high, over 20% and reach 80% for a flow rate of $2 m^3/s$, regardless of the size of the hydroelectric discharge. It results that for flow rates lower than $20 m^3/s$, it is necessary to reduce the flow rate by increasing the diameter of the pipe. At a half flow rate reduction of 2.5 m/s, an increase in pipe diameter from 0.7 m to 1.0 m, hydraulic losses below 20% are reduced even at a flow rate of 2 m/s, which makes hydroelectric power efficient.

In the next step, the internal diameter of the pipeline was analyzed economically, based on the minimum cost of the construction investment, and the results are shown in Figure 7.

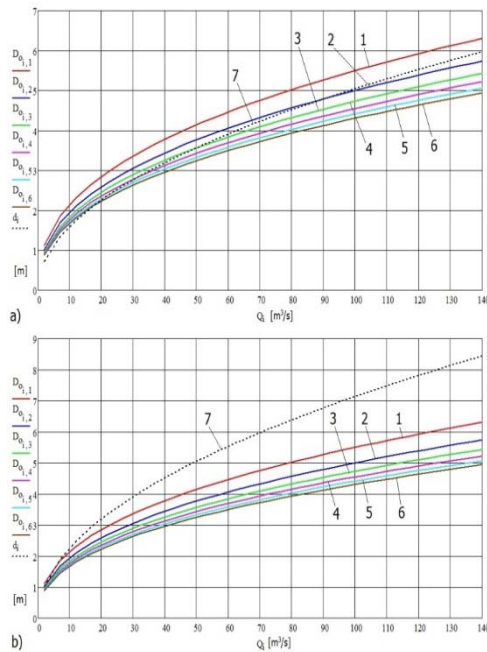


Fig. 7. The mode of variation the inside diameter of the pipe according to flow and drop

a – for a flow velocity of 5 m/s;
b – for a flow velocity of 2,5 m

where:

- 1 – gross fall of 50 m;
- 2 - gross fall of 100 m;
- 3 - gross fall of 150 m;
- 4 - gross fall of 200 m;
- 5 - gross fall of 250 m;
- 6 - gross fall of 300 m.
- 7 - for a flow velocity of 5 m/s.

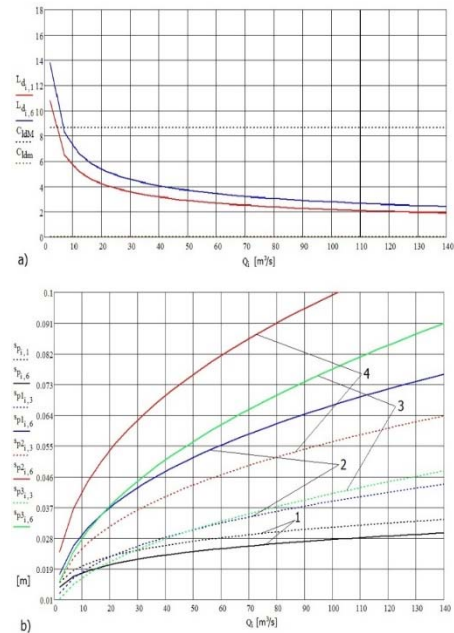


Fig. 8. Modulation of the thickness of the pipe wall according to flow and drop
a - the limits of application of the relationship of calculation of the wall thickness of the pipe;

b - wall thickness variation line of the pipe.

where:

- 1 - the wall thickness of the wall according to the external pressure stability criterion;
- 2 - the wall thickness after the internal pressure for the R510 steel and the optimum diameter according to the economic criterion;
- 3 - the wall thickness after the internal pressure for the R510 steel and the optimum diameter according to the flow velocity of 5 m / s in laminar mode;
- 4 - the wall thickness after the internal pressure for R360 steel and the optimal diameter according to the economic criterion.

For the determination of the wall thickness of the pipe, the conditions for the stability of the virolets at atmospheric pressure given by the technical prescriptions PT C4 / 2-2003 - Guide for the design, construction, mounting, and repair of stable pressure vessels. In the first stage, the length-diameter ratio, Figure 8a, was determined for a distance between the supports of the 12 m sections. It should be noted that only for flows lower than $7 \text{ m}^3/\text{s}$, another calculation relation must be applied or reduces the distance between the supports at 6 m. From the calculation program it was found that for the calculation relation for L/D higher than LdM we obtain values of thickness smaller than with the first relationship, which allowed its use on the whole debts beach.

The following are the variations of the wall thickness of the pipe, Figure 8b, for the external pressure stability criterion and the internal pressure check criterion for the welding cords applied to the pressure receptacle plates R510 and R360, STAS 2883 / 2-91 for diameters determined by the economic criterion and the flow rate criterion of $5 \text{ m} / \text{s}$ in laminar mode.

Based on the values of the internal diameter and the thickness of the wall of the forced pipe, the geometrical characteristics of its cross-section (area, strength mode) were determined. With the help of these, the forced duct was tested for stresses due to the own weight and the water inside the pipe and the axial force given by the friction between the water and the pipe wall, and the safety coefficients for the R510 steel are shown in Figure 9.

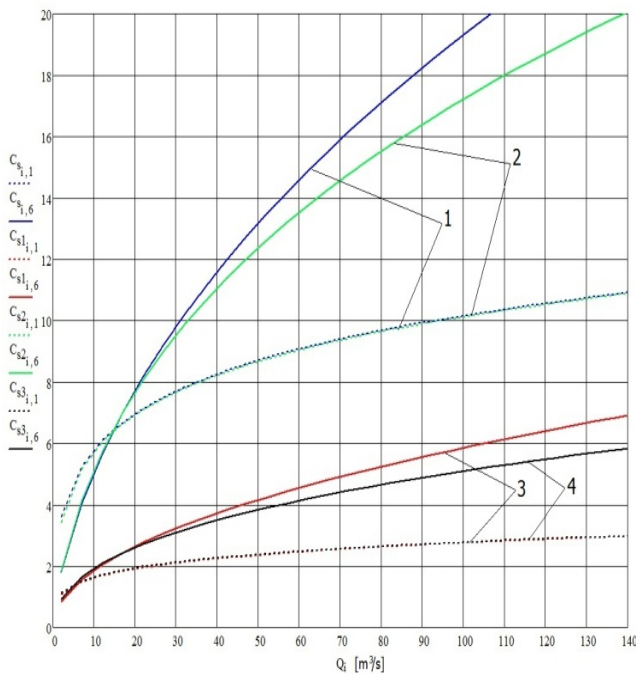


Fig. 9. Variation of the forced-pipe safety coefficients to the stresses
 1 - for the diameter given by flow velocity of $5 \text{ m} / \text{s}$ in laminar regime;
 2 - for diameter determined by economic criterion;
 3 - for the diameter given by the flow velocity of $5 \text{ m} / \text{s}$ in laminar regime at increasing the distance between supports at 24 m ;
 4 - for the diameter determined by the economic criterion to increase the distance between supports at 24 m .

3. CONCLUSIONS

From the comparison of the internal diameters determined by the economic criterion and the flow velocity of 5 m / s in laminar regime, Figure 7a, it was found that according to the criterion of the minimum investment cost it is recommended to reduce the inner diameter of the pipe by up to 15% of 140 m³ / s and 300 m fall. In the case of the flow velocity of 2.5 m/s, figure 7b, it was found that according to the economic criterion it is recommended to reduce the inner diameter of the pipe by up to 42% m³/s and 300 m fall.

It can be noticed that even according to the economic criterion it is recommended to reduce the flow rate of the water through the forced duct for installed flow rates of less than 10 m³ / s, and for flows higher than 10 m³ / s to increase the flow rate up to the maximum values of 5 ... 6 m / s. It is also noted that from an economic point of view it is recommended to reduce the diameter of the pipe to the increase of the fall, of the inner pressure, which in practice is solved by the stepwise execution of the large diameter pipe at the top.

From these variations of the thickness of the wall of the pipeline due to flow and fall, the following observations are made:

- The thickness of the pipe wall determined by the condition of external pressure stability is greater than the thickness determined by the internal pressure for gross falls less than 150 m;

- The thickness of the pipe diameter determined for the economically optimized diameter for a R510 steel (blue) is within the diameter range determined by the flow velocity of 5 m / s in laminar (green);

- It is recommended that for drops of less than 150 m, determine the thickness of the wall to be made under the condition of external pressure stability, and for larger falls use the sizing according to the internal pressure.

From the variation of the safety coefficients for the two criteria for determining the inner diameter of the pipe and the pipe support mode, the following observations are made:

- The safety factors for the loads due to the weight and water inside the pipe and the axial force given by the friction between the water and the wall of the pipe have values greater than 2 for an opening between the 12 m supports;

- For flows smaller than 10 m³/s, it is recommended to reduce the distance between supports at 6 m, and for flows higher than 50 m³/s and large falls, the distance between the sections of the sections up to 24 m can be increased.

REFERENCES

- [1]. **Băduț, M., Iosip, M.**, *Bazele proiectării cu Solid Edge*, Editura Albastră, Cluj-Napoca, 2003.
- [2]. **Blumfeld, M.**, *Introducere în metoda elementelor finite*, Editura Tehnică, București, 1995.
- [3]. **Buzdugan, Gh.**, *Rezistența materialelor*, Editura Didactică și Pedagogică, București, 1986.

- [4]. **Chișiu, A., Matieșan, D., Mădărășan, T., Pop, D.,** *Organe de mașini*, Editura Didactică și Pedagogică, București, 1976.
- [5]. **Constantinescu, V.P.,** *Prescripții de calcul pentru instalații de extracție mono și multicablu, vol. I.*, ODPT, București, 1972.
- [6]. **Constantinescu, V.P.,** *Prescripții de calcul pentru instalații de extracție mono și multicablu, vol. II.*, ODPT, București, 1973.
- [7]. **Tutuianu, G., ș.a.,** *Contract Nr. 8/2008, titlul: Cercetări teoretice și aplicative privind creșterea gradului de mecanizare a săpării galeriilor în cadrul amenajărilor hidrotehnice realizate de către S.C Hidroconstrucția S.A. Caransebeș- Sucursala Poiana Mărului, Autoritatea contractantă: S.C. Hidroconstrucția S.A. prin S.C TAPEDO S.R.L Petrila, Responsabil temă: Nan Marin Silviu, Valoare: 45.000 lei.*
- [8]. **Tutuianu, G.,** *Stadiul actual și tendințe moderne în domeniul tehnologiilor de execuție a lucrărilor de săpare, de amenajare și montaj în construcțiile hidrotehnice*, Raport de cercetare științifică nr. 1, Universitatea Petroșani, 22.12.2011.
- [9]. **Tutuianu, G.,** *Cercetări teoretice și experimentale privind îmbunătățirea parametrilor constructiv și funcționali a mașinilor și instalațiilor destinate lucrărilor de săpare, amenajare și montaj în construcțiile hidrotehnice*, Raport de cercetare științifică nr. 2, Universitatea Petroșani, 30.04.2012.
- [10]. **Tutuianu G.,** *Contribuții teoretice și aplicative la modernizarea tehnologiilor de execuție la lucrările de săpare, amenajare și montaj în construcțiile hidrotehnice*, Raport de cercetare științifică nr. 3, Universitatea Petroșani, 15.07.2012.

INDEX OF AUTHORS

A ndraș, A.,	71	N an, M. S.,	5, 49, 113, 127, 149
B ădiță (Popescu), D.,	5, 149	Nicolescu, C.,	49
C ozma, B. Z.,	15, 23	P ăun, A.-P.,	103
D umitrescu, I.,	15, 23, 55	Plotogea, C.,	5, 113
G ireadă, A. L.,	49	Popescu, F. D.,	71, 81
Gilma, I.,	31, 39, 63	Popescu-Stelea, M.,	103
Grecea, D.,	5, 49, 127	Praporgescu, G.,	119
I lioni, C.,	39, 81	R ad, M.D.,	49, 127
Itu, R. B.,	55	Rada, A.C.,	135, 143
Itu, V.,	55	Radu, S. M.,	81
J ula, D.,	63, 135, 143	S ălășan, D.,	127
K ertész, (B.) I.,	71, 81	Sultan, A.,	5, 113, 149
Kovacs, I.,	49	Stănilă, S.,	113
L adányi, G.,	91, 97	T omuș O. B.,	135, 143
Lazăr, G.,	109	Ț utuianu, G.,	5, 149
M agyari, M.,	127	U rdea, G.-B.,	15, 23
Mareș, R.,	103	V ladu, B.,	113, 149
Mărculescu, D. O.,	109		
Mihăilescu, S.,	119		

INSTRUCTIONS FOR AUTHORS¹

THE TITLE OF THE PAPER WILL BE WRITTEN WITH CAPITAL LETTERS, CENTERED, AT 7.0 cm FROM THE UPPER EDGE OF A4 FORMAT, ALONG THE ENTIRE WIDTH, TIMES NEW ROMAN, 14 POINTS, BOLD.

↓ (14 points)

↑ (14 points)

The first name and the family name will be written with CAPITAL LETTERS, BOLD, CENTERED, 130 mm width, Times New Roman, 12 points, each name being followed by number, and in the footnote the didactic and scientific degree, the position and place of work of the authors (possibly fax, E-mail) are indicated, with italics, 130 mm width, Times New Roman, 11 points.

↓ (12 points)

↑ (12 points)

<Tab> **Abstract: (Times New Roman, 10 points, bold)** The Abstract will only be in English and will have between 50 and 100 words, arranged all over the entire width, single, left – right alignment, all over the width of the printed space, Times New Roman, 10 points.

↓ (10 points)

↑ (10 points)

<Tab> **Key words: (Times New Roman, 10 points, bold)** 5 – 10 words, in English, along the entire width, Times New Roman, 10 points.

↓ (10 points)

↑ (10 points)

↓ (10 points)

<Tab> **1. THE TITLE OF THE CHAPTER IS WRITTEN WITH CAPITAL LETTERS, BOLD, TIMES NEW ROMAN, 11 POINTS AND WILL BE NUMBERED WITH ARABIC NUMBERS.**

↓ (11 points)

<Tab> The paper text paragraphs will be left – right aligned. The lines of the entire text will be single spaced with Times New Roman fonts, size 11 points.

The paper will be edited in a language of international circulation (English, French, German) on A4 format (210 x 297), page setup: top 5.6 cm, bottom 4.6 cm, left 3.7 cm, right 3.7 cm, in WORD and the number of pages must be even between 4 and 16. The size of the symbol is given next and is written in the instructions used to assist in editing the text. It indicates a blank line and does not show in the text of the paper, being obtained by pressing <ENTER>. The size of a <Tab> is 1.27 cm. No blank line is left between the paragraphs. Between the last line before the title and the title of the chapter and between the title and the first next line a blank line is left for each.

¹ Professor Eng., Ph.D. at the University of Petroşani, email adress

<Tab> **1.1 Subchapter. Subchapters can be used in the text, numbered with the number of the chapter and a number showing the number of the subtitle within the chapter. The subchapters and the numbers are Times New Roman, 11 points, bold.**

↑ (11 points)

The text is written in new paragraph and not continuing the subtitle, an 11 point blank line being left between the subtitle and the following text.

↑ (11 points)

2. PRESENTATION OF THE FIGURES

↑ (11 points)

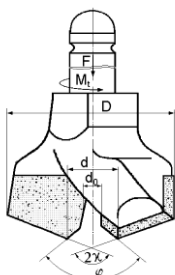


Fig. 1. Detachable bit

↑ (11 points)

3. PRESENTATION OF THE TABLES

↑ (11 points)

The tables will be enclosed in the text, a 10 points blank line being left above and under the table, and will be numbered with Arabic numbers. Both the number and the explanations to the table are written with Times New Roman, 10 points, italic, for the number and bold for the explanation to the table, centered in the space of the table and above it. The table entries will be Times New Roman, 10 points, bold, and the data in the table will be Times New Roman, 10 points. The thin lines of the table will be ½ points (0.02 cm), and the thick ones will be ¾ ... 1 points (0.03 ... 0.04 cm).

↑ (11 points)

4. PRESENTATION OF THE MATHEMATICAL EQUATIONS

↑ (11 points)

The mathematical equations will be with times New Roman, 11 points, center of the page and numbered on the right with Arabic numbers between round brackets.

↑ (8 points) <Blank line 8 point high>

$$X^2 + Y^2 = Z^2 \quad (1)$$

↑ (8 points) <Blank line 8 point high>

An 8 point high blank line is left between the last line before the relation and the relation and between the latter and the next first line.

The last page will be at least 2/3 full.

The pages of the paper will only be numbered by a pencil outside the printing space.

↑ (11 points)

REFERENCES (will be written according to the model, Times New Roman 10 points).

↑ (10 points)

[1]. **Marian I.**, *Mining mechanization*, Technical Publishing House, Bucharest, 1969 (Romanian language)